

Electronic Thesis and Dissertation Repository

---

3-15-2021 4:00 PM

## Assessment of the impacts of climate change, land cover transition, and internal climate variability on the hydrology of a forested watershed

Vahid Mehdipour, *The University of Western Ontario*

Supervisor: Najafi, M. Reza, *The University of Western Ontario*

A thesis submitted in partial fulfillment of the requirements for the Master of Engineering Science degree in Civil and Environmental Engineering

© Vahid Mehdipour 2021

Follow this and additional works at: <https://ir.lib.uwo.ca/etd>



Part of the [Environmental Engineering Commons](#)

---

### Recommended Citation

Mehdipour, Vahid, "Assessment of the impacts of climate change, land cover transition, and internal climate variability on the hydrology of a forested watershed" (2021). *Electronic Thesis and Dissertation Repository*. 7698.

<https://ir.lib.uwo.ca/etd/7698>

This Dissertation/Thesis is brought to you for free and open access by Scholarship@Western. It has been accepted for inclusion in Electronic Thesis and Dissertation Repository by an authorized administrator of Scholarship@Western. For more information, please contact [wlsadmin@uwo.ca](mailto:wlsadmin@uwo.ca).

## Abstract

In this study, the impacts of climate and land cover (LC) changes on the hydrologic processes of the Batchawana watershed in Central Ontario are assessed. Batchawana is a snow-dominated forested watershed with coniferous, deciduous and mixed trees and numerous small lakes. A semi-distributed hydrological model, based on the Raven hydrological framework, is calibrated and validated using ground-based observations for 1981-2001 and 2002-2011, respectively. Eight downscaled General Circulation Models (GCMs) that participated in the Coupled Model Intercomparison Project Phase 5 (CMIP5) and three large ensembles (50 members) of Regional Climate Model (RCM) simulations, under the Representative Concentration Pathway (RCP) 8.5, are used to characterize the role of anthropogenic forcing and internal climate variability in projected changes of watershed runoff. Analyses are performed in the historical and future time frames corresponding to global mean temperature increases of 1.5, 2, 2.5, 3, 3.5 and 4 °C compared to the preindustrial (1851-1900) level. The historical trends of land cover changes are extended to develop future LC scenarios including changes from coniferous to deciduous and mixed forests. Besides, to assess the influence of lakes four scenarios are investigated considering 25% lake shrinkage increments. Deciduous and mixed tree cover result in higher flow rates during fall compared to the base model with partial coniferous tree cover. A decrease in the area of lakes can decrease the streamflow in all seasons. Responding to climate change, the snowpack is projected to decline in the future indicating a shift from nival to a rainfall-dominated hydrological regime in a warmer climate. Further, the mean annual streamflow is projected to increase while the annual maximum flow is expected to decline. Analysis of Internal Variability indicates that human-induced climate change, compared with natural variability, will dominate the hydrological changes in the region during the last decade of the 21st century. Overall, the results show significant changes in the hydrological processes of this forested watershed associated with both climate and land cover changes. This will affect the flood and drought hazards and consequently endanger the agriculture, wood industry and lives of indigenous residents of Batchawana.

## Keywords

Hydrological Modeling; Raven; Batchawana Watershed; Climate Change; Forest Hydrology; Land Cover; Satellite Imagery; Internal Climate Variability

## Summary for Lay Audience

To manage water resources, it is essential to understand the variability and changes of components of the hydrological processes associated with natural factors and (in)direct influence of human activities. These components include freshwater storage in the region such as surface water, groundwater, snowpack among others. The Batchawana watershed, located in Central Ontario, is mainly covered by three forest types: deciduous, coniferous and mixed trees and include numerous lakes. Snow is one of the main hydrological variables in this region as it constitutes ~34% of the total precipitation. Ground-based surveys and satellite imagery show that the forest types have changed in this watershed during the past decades. Besides, the total lake area has declined. In addition, increases in temperature associated with climate change are projected to be more tangible over Canada (similar to other countries with higher latitudes and vast lands) compared to the global average and its effects on the hydrologic components can be dramatic. To assess the hydrological effects of forest type change, lakes shrinkage and climate change on the Batchawana hydrology, a hydrological model is set up and verified. Two land cover and four lakes scenarios are developed based on the historical trends. Further, the outputs of eight global climate models and three regional climate models are used to drive the model to assess the future streamflow changes corresponding to global mean temperature increases of 1.5, 2, 2.5, 3, 3.5 and 4 °C. Results show that changes in the forest type from deciduous to coniferous tree cover can result in higher streamflow rates in fall. The presence of lakes is essential for low flow generation in this forested watershed. Under climate change, the hydrologic regime of the basin is expected to shift to rain-dominated flows with lower annual maximum and higher annual mean streamflow rates compared to the historical period. Snowfall and snowpack are expected to decline to result in lower spring snowmelt. In the last decades of the 21<sup>st</sup> century, the impacts of human activities on streamflow will be more pronounced compared to the effects of internal variability.

## Acknowledgments

I would like to thank my thesis supervisor, Dr. Mohammad Reza Najafi who patiently guided me not only as a scrupulous advisor but also as a compassionate friend. His extraordinary personality has taught me more than science. I would like to express my thankfulness to Dr. Jason Leach for his invaluable comments throughout my research and this thesis would not be completed without his help. I would like to thank my research group and the experts who provided passionate support throughout my study. I thank Saber, Jason, Harry and Farshad for their precious help and advice. The help of the support team of Raven, Mr. Robert Chlumsky, is acknowledged and appreciated. I thank NRCan for providing data and maps. Setting up a model with limited data and turning the data into a text-based model could not be achievable without the help of the Raven support team (<http://raven.uwaterloo.ca>). Funding for this project was provided by the NSERC Discovery grant.

Finally, I must express my very profound gratitude to my parents, to my beloved wife, Dr. Farnaz Ghadimi, to my lovely siblings (Solmaz, Babak, David and Saeed) and my friends for providing me with nonstop encouragement throughout my studies in Canada. This would not be possible without their unfailing supports.

# Table of Contents

Abstract .....	i
Keywords .....	i
Summary for Lay Audience.....	ii
Acknowledgments .....	iii
Table of Contents.....	iv
List of Tables .....	vii
List of Figures .....	viii
Chapter 1: Thesis Overview .....	1
1.1 Research Objectives.....	2
1.2 Research Questions.....	3
1.3 Summary of Chapters .....	3
1.4 References.....	5
2 Chapter 2: Background Literature.....	9
2.1 The Batchawana Watershed.....	9
2.2 Hydrological Modeling.....	9
2.3 Raven, A Hydrological Modelling Framework .....	10
2.4 Land Cover Scenarios .....	13
2.5 Climate Change Scenarios .....	14
2.6 Internal Climate Variability and Anthropogenic Impacts.....	18
2.7 References.....	19
3 Chapter 3: Hydrological Modelling of the Batchawana Watershed .....	39
3.1 Introduction.....	39
3.2 Study Area .....	40

3.3 Hydrological Modelling.....	44
3.3.1 Model Setup.....	45
3.3.2 Data.....	49
3.3.3 Basin Information .....	51
3.3.4 Calibration and Validation of the Model .....	52
3.3.5 Modelling Workflow and Evaluation .....	55
3.4 Results.....	55
3.5 Conclusions.....	61
3.6 References.....	62
4 Chapter 4: Impacts of Land Cover, External Forcings and Internal Climate Variability	69
4.1 Introduction.....	69
4.2 Land cover scenarios .....	69
4.2.1 Lake changes Scenarios .....	71
4.3 Climate Change Scenarios.....	73
4.3.1 General Circulation Models (GCMs).....	73
4.3.2 Large Ensembles of Regional Climate Models .....	74
4.4 Methodology.....	75
4.4.1 GCM Selection.....	75
4.4.2 Assessing the Hydrologic Impacts of Climate Change using Raven.....	78
4.5 Results and discussion .....	78
4.5.1 Land cover change scenarios .....	78
4.5.2 Lake change scenarios .....	79

4.5.3	Climate change scenarios.....	80
4.5.4	The role of internal climate variability & external forcings .....	92
4.6	Conclusions.....	94
4.7	References.....	97
5	Chapter 5: Concluding Remarks and future works.....	103
5.1	References.....	105
	Curriculum Vitae .....	108

## List of Tables

Table 3-1: Hydrologic processes represented by Raven for the Batchawana watershed. ....	45
Table 3-2: Storages, classes and parameters for Raven’s model for the Batchawana watershed. ....	50
Table 3-3: Delineated HRUs based on land cover, DEM, soil and slope maps using ArcSWAT. .....	52
Table 3-4: Calibrated parameters of Raven’s hydrological modelling framework for the Batchawana watershed. 16 parameters from different storages are calibrated. Their calibration range and the final estimated values are provided. ....	54
Table 3-5: Performance evaluation of the Raven hydrological model simulations at daily time steps for the calibration and validation periods .....	56
Table 4- 1: Selected global climate models for Batchawana Watershed hydrological modelling. .....	73
Table 4- 2: Anticipated 9-year period for each GCM to reach a specific global mean temperature change. The period represents the average temperature 4.5 years before or after the given year. Data provided by Jiang et. al (2016).....	77
Table 4- 3: Global mean temperature change (GMTC) for the 8 selected GCMs of the study area. .....	81



## List of Figures

Figure 1- 1: Six major steps of the thesis	16
Figure 3- 1: The Batchawana Watershed in Central Ontario.	40
Figure 3- 2: Batchawana land cover map. The Eastern part is covered by mixed and coniferous trees while most of the western part is covered by deciduous trees.	41
Figure 3- 3: Elevation distribution of the Batchawana watershed.	42
Figure 3- 4: Blue line is a direct line from the most western point to the most eastern point in the basin. The Redline shows the temperature variation of both points during the winter while the orange one shows the temperature of points for summer in a given year (2019)	42
Figure 3- 5: Boxplot of the spatially averaged daily temperature for 1980-2011.	43
Figure 3- 6: Annual max. and mean streamflow for station # 02FB001 (Batchawana River near Batchawana)	43
Figure 3- 7: Historical annual max. and mean air temperature	44
Figure 3- 8: Annual accumulative max snow over the Batchawana watershed	44
Figure 3- 9: Hydrological processes represented in the Raven hydrological framework. Precipitation can be stored in soil, canopy, ponds or depressions. Each water storage has a specified capacity and water flows after reaching the maximum capacity	45
Figure 3- 10: Simulated and observed streamflow during the validation period	56
Figure 3- 11: Maximum and minimum daily temperature variations at the Batchawana watershed	57
Figure 3- 12: Daily values for rainfall and snow water equivalent (SWE) over the Batchawana watershed	57
Figure 3- 13: Daily potential evapotranspiration based on daily precipitation and temperature.	58

Figure 3- 14: Observed and simulated daily streamflow during the calibration (1981-2001) and validation (2001-2011) periods for Batchawana River Station.	58
Figure 3- 15: Comparison between daily observed and simulated streamflow at the Batchawana station for a three-year period	59
Figure 3- 16: Monthly average observed and simulated streamflow for calibration and validation periods	60
Figure 3- 17: Annual mean (a) and max (b) of observed and simulated streamflow values for 30 years from 1981 to 2011.	61
Figure 4 - 1: Satellite Imagery of the Batchawana Watershed. Coniferous or mixed forests have been replaced with deciduous type trees from 1995 to 2011. All satellite products are captured during summer with a cloud cover of less than 10%. Images are produced by processing the Landsat products ( <a href="https://www.usgs.gov/core-science-systems/nli/landsat">https://www.usgs.gov/core-science-systems/nli/landsat</a> ).....	70
Figure 4-2: Percentage of water bodies in Batchawana. Data are extracted using Landsat products.....	71
Figure 4-3: Global mean temperature changes for different GCMs under RCP8.5 (Jiang et. al, 2016).....	76
Figure 4- 4: Monthly mean streamflow for land cover change scenarios. Coniferous to deciduous (CTD) and mixed forest scenarios (CTM) result in larger flow rates in the fall compared to the base model.....	79
Figure 4- 5: The hydrograph corresponding to the No_Lake scenario. Simulated values for low flows are almost zero most of the time regardless of the season. ....	79
Figure 4- 6: Monthly mean streamflow corresponding to the lake scenarios. Lower lake areas result in lower monthly mean streamflow rates with the No_Lake scenario showing almost zero values during winter.....	80

Figure 4- 7: The projected annual mean temperature corresponding to the global mean temperature increases. Darker colours indicate more GMTCs. ....	83
Figure 4- 8: Projected annual precipitation rates corresponding to the global mean temperature increases. The darker colour represents higher global mean temperature change.....	84
Figure 4- 9: Projected changes in the annual streamflow rates of the Batchawana watershed corresponding to the global mean temperature increases. The boxplots show the variation ranges of projected streamflow by GCMs.....	85
Figure 4- 10: Projected annual maximum streamflow corresponding to the global mean temperature increases. The generated results are showing boxplots which are covering the variation bound of 8 GCMs. ....	86
Figure 4- 11: Projected annual snow corresponding to the global mean temperature increases.	87
Figure 4- 12: Projected annual mean temperature based on the three large ensembles corresponding to the global mean temperature increases .....	88
Figure 4- 13: Projected annual precipitation based on the large ensembles corresponding to the global mean temperature increases. ....	89
Figure 4- 14: Projected annual mean streamflow for large ensembles corresponding to the global mean temperature increases. ....	90
Figure 4- 15: Projected annual maximum streamflow for large ensembles corresponding to the global mean temperature increases. ....	91
Figure 4- 16: Projected annual snow for three large ensembles for corresponding to the global mean temperature increases .....	92
Figure 4- 17: Signal to noise ratio (SNR) anomalies for the large ensembles.....	93
Figure 4- 18: Projected mean and standard deviation of the large ensembles.....	94

## Chapter 1: Thesis Overview

Forested watersheds are covered by relatively tall and condensed trees (Kurt-Karakus et al. 2011). Forests and specially concentrated forests play a major role in the hydrology of a region in many ways such as intercepting precipitation, changing wind direction and speed, retaining humidity in the region, affecting the infiltration rate and altering the evaporation rates (K. Wu and A. Johnston 2008). Forested watersheds are also important for downstream regions. Studies show that deforestation can lead to increasing flood risks (Haigh et al. 2004). Further, lakes are important components of a hydrological system (Smith 2005). Depending on the morphology of regions and type and size of the lakes, they can retain precipitations or humidity, release or maintain groundwater and surface water (Selmes et al. 2011). Therefore, changes in land cover factors (including forest cover and lakes) can affect the hydrology of forested watersheds. Besides, there is strong evidence that climate change can alter the hydrologic components of small and large river basins including precipitation (K. Trenberth 2011), snowpack and snowmelt (Adam, Hamlet, and Lettenmaier 2009), evaporation, and runoff (Chattopadhyay and Hulme 1997). Recent studies showed significant impacts of climate change on Canadian regions including increases in temperature, snowpack decline, reduction in summer runoff, and more intense extreme precipitation events (Bush et al. 2019). Understanding the individual and combined impacts of climate and land cover change can help develop effective mitigation and adaptation plans (Shooshtari and Gholamalifard 2015; Carlson and Traci Arthur 2000; L. Zhang et al. 2018).

Batchawana, located in central Ontario, is a snow-dominated watershed covered by three main forest types including coniferous, deciduous, and mixed trees. There are numerous large and small lakes covering the surface of the region (Sanford et al. 2007). The Turkey Lake, a small subwatershed in Batchawana, is heavily instrumented and is studied extensively to analyze the water quality, biodiversity and fishery industry (Kelso 1988; D. S. Jeffries et al. 1986, 2002, 1988; Morris and Kwain 1988). There have been limited studies on the hydrology and water quantity of this basin (Sanford et al. 2007; Creed et al. 2003; Sanford et al. 2007). Understanding the

hydrology of the region is essential to estimate the water budget components, analyze extreme flow conditions, the volume of streamflow, seasonality, and the corresponding future changes. This will lead to efficient water resources planning and management, and the development of resilient infrastructure systems, safe urban/rural areas and help the economy to blossom (Forsythe et al. 2019).

Previous studies have focused on the impacts of distinct land cover/land use types such as urban versus agricultural land. In this study, we analyze the impacts of different tree covers on the hydrological processes of the Batchawana watershed by setting up and calibrating a process-based model. Leaves, stems, heights and roots of different trees in a forested area can dramatically alter the water cycle in the region (Wei et al. 2005). Lakes are other important factors for the forested areas and changes in their volume, area and shape may cause significant alterations in the basin's hydrology (Buttle, et al 2009; Han et al. 2020). The effects of lakes on flow characteristics are also investigated. Further, we assess the impacts of climate change using eight downscaled General Circulation Models (GCMs) and three large ensembles of Regional Climate Model (RCM) simulations and quantify the influence of internal climate variability. The downscaled data are ingested into the hydrological model to assess the projected streamflow under RCP 8.5 scenario. This comprehensive analysis of the hydrological response is performed for incremental increases in global mean temperature.

## 1.1 Research Objectives

The overall objective of this study is to assess the impacts of climate and land cover changes on the hydrological processes of the snow-dominated, forested watershed of Batchawana. Following are the sub-objectives of this study:

- Set up, calibrate and validate a semi-distributed hydrological model for the Batchawana watershed based on Raven as a novel flexible hydrological modelling framework.
- Apply land cover change scenarios to analyze the response of the hydrological system to forest type changes. Land cover changes scenarios include two main forest type changes from coniferous to mixed and from coniferous to deciduous (McKenney et al. 2011, 2007).
- Assess the influence of lakes by decreasing the lakes' areas considering 25% increments.

- Investigate the hydrological response of the Batchawana watershed to the projected changes in climate factors.
- Assess the distinct role of anthropogenic forcings from internal climate variability's impacts on the projected streamflow changes.

## 1.2 Research Questions

The following questions will be addressed in this study:

1. What are the hydrological attributes and characteristics of the Batchawana watershed?
2. How does the satellite imagery assist in understanding the morphology of the basin and detect land cover changes?
3. How does the hydrological system respond to changes from coniferous trees to deciduous and mixed trees? What processes are involved?
4. What is the influence of the lakes' on the flow characteristics in Batchawana? How does the hydrological system respond to the lakes' shrinkage?
5. How will climate change affect the hydrological regime of the region?
6. What are the similarities and differences between projections of statically downscaled GCMs and dynamically downscaled RCMs for the Batchawana watershed?
7. How does internal climate variability influence the projected changes of the hydrology of Batchawana?

## 1.3 Summary of Chapters

This thesis is based on three main chapters. Chapter 1 of this thesis includes a brief background about the thesis and the research objectives of the study. Chapter 2 represents the related literature review. It covers the previous studies on the Batchawana watershed and lakes within the Batchawana watershed followed by a comprehensive literature review on the forested basins' hydrology, and prediction of their characteristics. Lakes as one of the most important components of hydrological systems are studied to understand their roles in forested basins. Global climate changes and anticipated consequences of climate change from a hydrological aspect have been considered in the literature review. Global climate models, regional climate models, large ensembles and concepts of internal climate variability and anthropogenic impacts on the projected climate are then discussed in chapter 2.

Chapter 3 presents the hydrological model set up for the Batchawana watershed. It starts with a brief introduction of the importance of the hydrological models and the Raven modelling framework. The area of the study is discussed thoroughly in this section. The economic importance of forests, vegetation type, DEMs and land-use maps are explained. Historical meteorological data and streamflow are illustrated and their trends are deliberated. Data and their sources are presented. The main body of Chapter 3 is dedicated to explaining the details of the Raven and applied methodology for model development and evaluation. Selected hydrological processes within the model and their mathematical representations are explained in detail. The calibration of Raven using the Ostrich tool is described in a sub-section in chapter 3 where the selected parameters for optimization are described. Results of the model based on the validation and calibration periods are demonstrated in the results sub-section. Simulated results for forcing parameters are also represented. The conclusion is the last sub-section for chapter 3

Chapter 4 describes the main body of the thesis where the novelty of the study is presented. An introduction to the land cover changes, lake changes, climate change, climate models and large ensembles, internal variability and anthropogenic forcings impacts on the future climate is presented. Based on the results of the previous chapters and satellite imagery the proposed scenarios of land cover changes are discussed. Satellite imagery of the past few decades showed that the lakes and freshwater availability are depleting in the region. This trend founded another set of proposed lake shrinking scenarios, in which the areas of the lakes are assumed to be decreasing by 25% steps for each scenario. Global climate changes under RCP 8.5  $W/m^2$  from different models are presented in this section. Further, three large ensembles including CanRCM4, CanLEAD-E and CanLEAD-S (Chattopadhyay and Hulme 1997) are used to represent the influence of internal climate variability and external forcings on the projected streamflow changes. The methodology for GCM/RCM and large ensembles selection processes and strategies are described. Results of Raven simulations corresponding to the projection of different climate models are discussed. To illustrate the processes of this thesis and enlighten the major steps following Figure 1-1 is added.

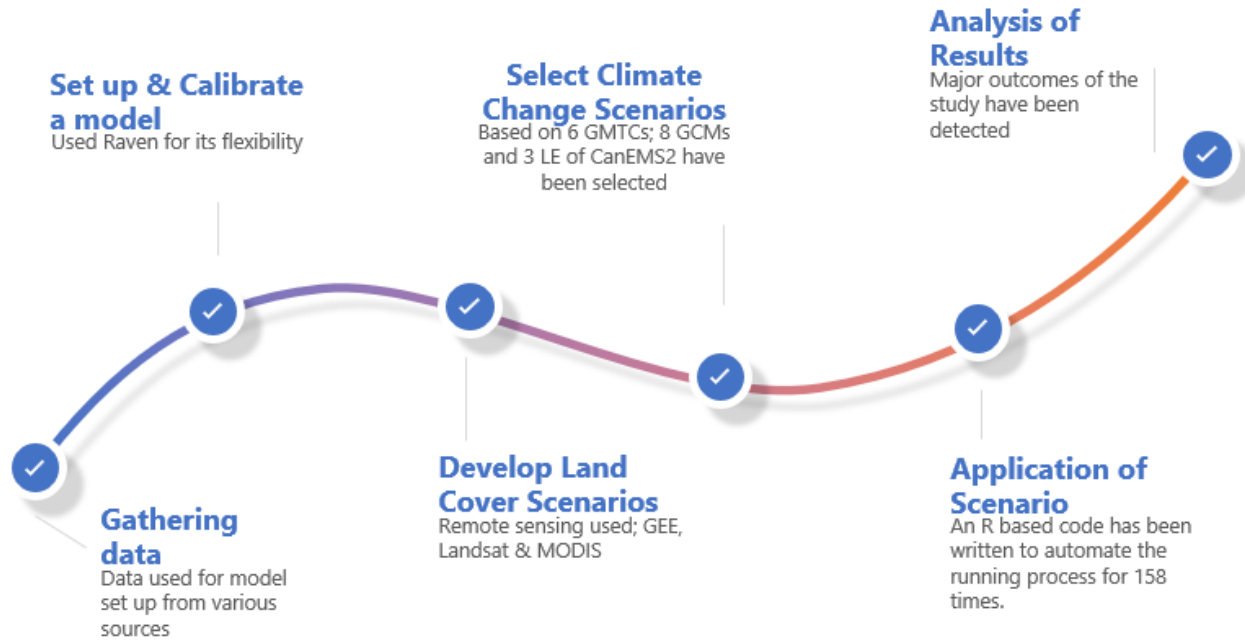


Figure 1-1: Six major steps of thesis

## 1.4 References

Bush, E, N Gillet, E Watson, J Fyfe, F Voge, and N Swart. 2019. “Understanding Observed Global Climate Change, CCCR Chapter 2.” Ottawa, Ontario.

Buttle, J M, I F Creed, and R D Moore. 2009. “Advances in Canadian Forest Hydrology, 2003-2007.” Canadian Water Resources Journal 34 (2): 113–26. <https://doi.org/10.4296/cwrj3402113>.

Carlson, Toby N, and S Traci Arthur. 2000. “The Impact of Land Use — Land Cover Changes Due to Urbanization on Surface Microclimate and Hydrology: A Satellite Perspective.” Global and Planetary Change 25 (1–2): 49–65. [https://doi.org/10.1016/S0921-8181\(00\)00021-7](https://doi.org/10.1016/S0921-8181(00)00021-7).

Creed, I. F., S. E. Sanford, F. D. Beall, L. A. Molot, and P. J. Dillon. 2003. “Cryptic Wetlands: Integrating Hidden Wetlands in Regression Models of the Export of Dissolved Organic Carbon from Forested Landscapes.” Hydrological Processes 17 (18): 3629–48. <https://doi.org/10.1002/hyp.1357>.

Fatichi, S., S. Rimkus, P. Burlando, and R. Bordoy. 2014. “Does Internal Climate Variability Overwhelm Climate Change Signals in Streamflow? The Upper Po and Rhone Basin Case



Studies.” *Science of The Total Environment* 493 (September): 1171–82.

<https://doi.org/10.1016/j.scitotenv.2013.12.014>.

Forsythe, Nathan, David R. Archer, David Pritchard, and Hayley Fowler. 2019. “A Hydrological Perspective on Interpretation of Available Climate Projections for the Upper Indus Basin.” In *Indus River Basin*, 159–79. Elsevier. <https://doi.org/10.1016/B978-0-12-812782-7.00008-4>.

Haigh, Martin J., Libor Jansky, and Jon Hellin. 2004. “Headwater Deforestation: A Challenge for Environmental Management.” *Global Environmental Change* 14 (January): 51–61.

<https://doi.org/10.1016/j.gloenvcha.2003.11.004>.

Jeffries, D. S., R. G. Semkin, R. Neureuther, M. Seymour, and J. A. Nicolson. 1986. “Influence of Atmospheric Deposition on Lake Mass Balances in the Turkey Lakes Watershed, Central Ontario.” In *Acidic Precipitation*, 1033–44. Dordrecht: Springer Netherlands.

[https://doi.org/10.1007/978-94-009-3385-9\\_104](https://doi.org/10.1007/978-94-009-3385-9_104).

Jeffries, D S, R G Semkin, F D Beall, and J Franklyn. 2002. “Temporal Trends in Water Chemistry in the Turkey Lakes Watershed Ontario, Canada, 1982-1999.” *Water, Air and Soil Pollution: Focus* 2 (1): 5–22. <https://doi.org/10.1023/A:1015878106199>.

Jeffries, D. S., J. R. M. Kelso, and I. K. Morrison. 1988. “Physical, Chemical, and Biological Characteristics of the Turkey Lakes Watershed, Central Ontario, Canada.” *Canadian Journal of Fisheries and Aquatic Sciences* 45 (S1): s3–13. <https://doi.org/10.1139/f88-262>.

Johnson, Richard. 1998. “The Forest Cycle and Low River Flows: A Review of UK and International Studies.” *Forest Ecology and Management* 109 (1–3): 1–7.

[https://doi.org/10.1016/S0378-1127\(98\)00231-X](https://doi.org/10.1016/S0378-1127(98)00231-X).

Kelso, J. R. M. 1988. “Fish Community Structure, Biomass, and Production in the Turkey Lakes Watershed, Ontario.” *Canadian Journal of Fisheries and Aquatic Sciences* 45 (S1): s115–20.

<https://doi.org/10.1139/f88-275>.

Kurt-Karakus, Perihan Binnur, Camilla Teixeira, Jeff Small, Derek Muir, and Terry F. Bidleman. 2011. “Current-Use Pesticides in Inland Lake Waters, Precipitation, and Air from Ontario,

Canada.” *Environmental Toxicology and Chemistry* 30 (7): 1539–48.  
<https://doi.org/10.1002/etc.545>.

McKenney, Daniel W., John H. Pedlar, Kevin Lawrence, Kathy Campbell, and Michael F. Hutchinson. 2007. “Potential Impacts of Climate Change on the Distribution of North American Trees.” *BioScience* 57 (11): 939–48. <https://doi.org/10.1641/B571106>.

McKENNEY, DANIEL W., JOHN H. PEDLAR, RICHARD B. ROOD, and DAVID PRICE. 2011. “Revisiting Projected Shifts in the Climate Envelopes of North American Trees Using Updated General Circulation Models.” *Global Change Biology* 17 (8): 2720–30.  
<https://doi.org/10.1111/j.1365-2486.2011.02413.x>.

Morris, J. R., and W. Kwain. 1988. “A Study of Metal Accumulation Trends in Sediment Cores from the Turkey Lakes (Algoma, Ontario).” *Canadian Journal of Fisheries and Aquatic Sciences* 45 (S1): s145–54. <https://doi.org/10.1139/f88-279>.

Muhammad, Ameer, Grey R. Evenson, Fisaha Unduche, and Tricia A. Stadnyk. 2020. “Climate Change Impacts on Reservoir Inflow in the Prairie Pothole Region: A Watershed Model Analysis.” *Water* 12 (1): 271. <https://doi.org/10.3390/w12010271>.

Sanford, S. E., I. F. Creed, C. L. Tague, F. D. Beall, and J. M. Buttle. 2007. “Scale-Dependence of Natural Variability of Flow Regimes in a Forested Landscape.” *Water Resources Research* 43 (8). <https://doi.org/10.1029/2006WR005299>.

Selmes, N., T. Murray, and T. D. James. 2011. “Fast Draining Lakes on the Greenland Ice Sheet.” *Geophysical Research Letters* 38 (15). <https://doi.org/10.1029/2011GL047872>.

Shooshtari, Sharif Joorabian, and Mehdi Gholamalifard. 2015. “Scenario-Based Land Cover Change Modeling and Its Implications for Landscape Pattern Analysis in the Neka Watershed, Iran.” *Remote Sensing Applications: Society and Environment* 1 (July): 1–19.  
<https://doi.org/10.1016/j.rsase.2015.05.001>.

Smakhtin, V.U. 2001. “Low Flow Hydrology: A Review.” *Journal of Hydrology* 240 (3–4): 147–86. [https://doi.org/10.1016/S0022-1694\(00\)00340-1](https://doi.org/10.1016/S0022-1694(00)00340-1).

Smith, L. C. 2005. “Disappearing Arctic Lakes.” *Science* 308 (5727): 1429–1429.  
<https://doi.org/10.1126/science.1108142>.

Wei, X., S. Liu, G. Zhou, and C. Wang. 2005. “Hydrological Processes in Major Types of Chinese Forest.” *Hydrological Processes* 19 (1): 63–75. <https://doi.org/10.1002/hyp.5777>.

Wu, Kangsheng, and Carol A. Johnston. 2008. “Hydrologic Comparison between a Forested and a Wetland/Lake Dominated Watershed Using SWAT.” *Hydrological Processes* 22 (10): 1431–42. <https://doi.org/10.1002/hyp.6695>.

Zhang, Ling, Zhuotong Nan, Wenjun Yu, Yanbo Zhao, and Yi Xu. 2018. “Comparison of Baseline Period Choices for Separating Climate and Land Use/Land Cover Change Impacts on Watershed Hydrology Using Distributed Hydrological Models.” *Science of The Total Environment* 622–623 (May): 1016–28. <https://doi.org/10.1016/j.scitotenv.2017.12.055>.

## Chapter 2: Background Literature

### 2.1 The Batchawana Watershed

Batchawana, in central Ontario, is a forested watershed with many lakes. It contains the Turkey Lake sub-watershed, which has been studied extensively to understand the effects of human activities on water quantity or quality (Creed et al. 2003; Sanford et al. 2007). A study on the fish community, biomass and production in the Turkey lake watershed showed that fish biomass and production per unit surface are inversely associated with the lake's depth. However, the fish biomass and production in this area are related to the water alkalinity and phytoplankton carbon assimilation along with the lake depth (Kelso 1988). The Turkey Lake watershed in Batchawana was selected for an intensive study on acidic depositions of long-range transport of air pollutants. In this experimental study, several water quality parameters such as Calcium, Sulphate, Phosphorous and Nitrogen were assessed and measured for four lakes. Also, the fish community and production were analyzed in those lakes. According to their report for Turkey Lake Watershed, 90% of the area is covered by sugar maple, with 9% of hardwood (usually yellow birch) and the rest is covered by coniferous (Dean S. Jeffries et al, 1988). Results for two years of the experimental study showed that forest harvesting in the area would lead to more flows during the snowmelt season (Murray and Buttle 2005). A study in Batchawana River Watershed was conducted to examine the association between the natural flow regime's variability and the scale of the basin. Results showed that in wet conditions, flow variability is relatively low and during dry conditions, there is higher variability in smaller basins than larger ones. A distributed hydrological model, i.e. Regional Hydro-Ecological Simulation System (RHESys, version 5.9.5), was set up for Batchawana in which 5 different scales were considered to analyze the impacts of basin size on flow variability (Sanford et al. 2007).

### 2.2 Hydrological Modeling

The processes and structures of hydrological models are extensively discussed in review studies conducted by Sood and Smakhtin (2015), Montanari (2011), Tegegne, et al (2017) among others. Hydrological models are divided into two major categories; i. process-based (conceptual or physical models) models, which represent the hydrological unit and water storage processes (Beven 1989; Rodhe 2012) ii. statistical or mathematical models (Jajarmizad and Salarpour 2012)

that search for associations between the outcome (streamflow most of the time) and forcings data (Hamed 2008). These empirical models assess the relationship between the observed variables and can be applied to analyze the trends in historical data (Wallis 1965).

Some of the commonly applied process-based models are discussed in this section. Soil and water assessment tool or SWAT is one the most widely used hydrological models (White and Chaubey 2005). ArcSWAT is the GIS-based interface of the SWAT model that can be used to delineate hydrologic response units based on soil map, land use/land cover map, slope and aspects map etc. (Santra and Das 2013; Ali et al. 2014). SHE and or MIKE-SHE (Abbott et al. 1986), variable infiltration capacity or VIC (Hamman et al. 2018), GR4J (Kunnath-Poovakka and Eldho 2019), Hydrologiska Byråns Vattenbalansavdelning or HBV (Jia and Sun 2012; Bergström and Lindström 2015), precipitation-runoff modelling system or PRMS (F. Teng, et al 2018) are some of the other widely applied hydrological models.

Calibration and validation are essential steps in setting up a reliable hydrological model (Beven 1989). There are some non-measured parameters and unknown coefficients in the mathematical relations between the hydrological storage that need to be estimated based on observable input/output variables (Daggupati et al. 2015). Calibration or optimization of a model is the process of altering unknown coefficients/variables and run the model to find the best match between the observed and simulation results. The process of the optimization can be conducted either manually or automatically (Ahmadisharaf et al. 2019).

### 2.3 Raven, A Hydrological Modelling Framework

Raven (Craig et al. 2020) is a flexible hydrological modelling framework that allows for setting up models with different structures that best suits the modelling objectives. It can blend multiple hydrological models with more than 100 possible configurations and 80 interchangeable options for the routing and estimation of forcing. Therefore, it has been applied to study the hydrological processes of different watersheds across Canada in recent years (Craig et al. 2020; Snowdon 2016; 2010; K. Lee 2018; Sgro 2016). Chernos et al. (2017) studied the Elk River in British Columbia, western Canada to quantify the glaciers' contribution to streamflow and assess the impacts of land cover and climate change. Leach et al. 2020 investigated the impacts of forest harvesting and wetlands on the travel time and linkages to streamflow quality in the snow-dominated Turkey Lake

Watershed in central Ontario. They set up Environment Canada’s version of HVB (HBV-EC) within the Raven framework. Spatial discretization of the model to generate HRUs and sub-basins to form lumped, semi-distributed or distributed models are described in Craig et al. (2020).

Model optimization (i.e. calibration and validation of the hydrological model) can be performed using OSTRICH (Mattot, LS, 2017; Craig et al. 2020). There are multiple algorithms within OSTRICH including dynamically dimensioned search or DDS (Tolson and Shoemaker 2007; Lespinas, Dastoor, and Fortin 2018) and its evolved versions such as DDS-AU (Tolson and Shoemaker 2008), Discrete DDS (Tolson and Shoemaker 2008), Pareto Archived DDS (Tolson and Shoemaker 2008), generalized likelihood uncertainty estimation GLUE (Beven 2014), shuffle complex evolution or SCE (Vrugt et al. 2003; Nezhad et al. 2018) among others. Dynamically dimensioned search algorithms have shown promising performance to optimize a high number of parameters (Tolson and Shoemaker 2007). We consider the split-sampling calibration and validation approach in this study.

Considering the uncertainties in future predictions of land cover and land use changes multiple scenarios are commonly developed to analyze the impacts of land cover changes, urban development and forest harvesting and the corresponding impacts on hydrology to enlighten policymakers for better planning of urban developments and infrastructure improvements (Xiang and Clarke 2003). Developing a scenario for the land cover change is based on the historical trends, infrastructure development plans for the future, possible threats to the vegetation types and many other factors that may vary by region’s characteristics (Rounsevell et al. 2006; Y. Chen, Xu, and Yin 2009; Niehoff, Fritsch, and Bronstert 2002). The future of a region is prone to many unprecedented incidents, hence none of the evolved scenarios can confidently predict the future. Therefore, to conduct a coherent study, all possible land cover change scenarios should be considered (Kepner et al. 2004).

The Kling-Gupta Efficiency (KGE) metric is one of the commonly used criteria in hydrological modelling. KGE assesses the correlation, variability and bias errors (Pechlivanidis and Arheimer 2015). It varies between  $-\infty$  to  $+1$  and the optimal value is  $+1$ . Here is the equation for KGE:

$$KGE = 1 - \sqrt{(r - 1)^2 + (\alpha - 1)^2 + (\beta - 1)^2} \quad \text{Equation 3-9}$$

In Equation 3-9,  $r$ ,  $\alpha$  and  $\beta$  represent the linear regression coefficient, the standard deviation of simulations over the standard deviation of the observations, and the mean of simulations over the mean of observations, respectively (Gupta et al. 2009). In other words, the term  $(r-1)^2$  assesses the timing of the observed and simulated values,  $(\alpha-1)^2$  compares their variability and  $(\beta-1)^2$  assessing the magnitude of values. KGE is the decomposition of means square error (MSE) and Nash-Sutcliff Efficiency (NSE) (Muhammad et al. 2019).

Nash-Sutcliff Efficiency (NSE) is another commonly applied metric for model assessments. It varies between  $-\infty$  and  $+1$  with  $+1$  as the optimal value. The corresponding equation is:

$$NSE = 1 - \frac{\sum_{t=1}^T (Y_m^t - Y_0^t)^2}{\sum_{t=1}^T (Y_m^t - \bar{Y}_0^t)^2} \quad \text{Equation 3-10}$$

$\bar{Y}_0^t$  is the average of observed flow,  $Y_m^t$  is simulated and  $Y_0^t$  is observed flows at time  $t$  (Nash and Sutcliffe 1970). The acceptable range for NSE is highly dependent on data accuracy. But, generally, an NSE greater than 0.5 is considered acceptable for hydrological studies (D. N. Moriasi et al. 2007). However, 0.36 to 0.75 is a satisfactory range for most hydrological models (Motovilov et al. 1999).

To assess whether the model simulations over-estimate or under-estimate the recorded data, the bias percentage or PBIAS is used:

$$PBIAS = \frac{\sum_{t=1}^n (Y_t^{obs} - Y_t^{sim})}{\sum_{t=1}^n (Y_t^{obs})} \times 100 \quad \text{Equation 3-11}$$

PBIAS in Equation 3-11 varies between  $-\infty$  to  $+\infty$ , positive values suggest overestimation while negative values indicate the underestimation of the observed flows.  $Y_t^{obs}$  and  $Y_t^{sim}$  represent observed and simulated values, respectively (Khamis et al. 2015).  $\pm 25\%$  can be an acceptable range (Muhammad et al. 2019) but  $\pm 10$  is commonly accepted as very good results (D. N. Moriasi et al. 2007).

To quantify the linear correlation between observed and modelled data,  $r^2$  or coefficient of determination is considered. R-squared in Equation 3-12 varies between  $-1$  and  $+1$  where  $-1$  shows

a completely negative association and +1 shows a perfectly positive correlation between observed and simulated values (Colin Cameron and Windmeijer 1997).

$$r^2 = 1 - \frac{\Sigma(y^{obs}-y^{sim})^2}{\Sigma(y^{obs}-\bar{y})^2} \quad \text{Equation 3-12}$$

## 2.4 Land Cover Scenarios

Canada is the second-largest country with the 3<sup>rd</sup> largest forests after Russia and Brazil. Based on the data for 2017, 347 million hectares of forests cover the vast lands of Canada. 4.5% of the forest areas are impacted by insects, 0.7% is burned due to wildfires, 0.2% of the trees are harvested and 0.01% or 35385 ha of the Canadian forests have been deforested as of 2017. The Forest industry is crucial for the Canadian economy as more than 210,000 people are contributing to the \$25.8 billion or 1.2% of the GDP based on the 2018 data ( <https://www.nrcan.gc.ca/our-natural-resources/forests-forestry/13497>). Therefore, understanding and predicting the threats and changes in the forest and forestry industry is crucial for different stakeholders across Canada.

Satellite imagery has a very broad application in areas such as air pollution (Canuti et al., 2017), forest management (Ritchie and sdaRango 1996), wetland management and study of the river systems (Mahajan et al. 2014; Jong, Meer), traffic management (Gholizadeh et al. 2016), urban development planning (Clevers 2004), and to understand the trend and possible interactions between the elements of a forest (Shooshtari and Gholamalifard 2015). Landsat satellites are launched by NASA in 1972 (Landsat 8 is the latest satellite) to collect scientifically valuable images to observe the Earth's surface (Irons, Dwyer, and Barsi 2012). Moderate Resolution Imaging Spectroradiometer (MODIS) was launched in 1999 to provide images from the upper surface and surface of the earth (Petus et al. 2014).

There is no specific definition for “lake”, but routinely it is a water body containing water for at least more than few weeks a year and it is refilled for the next time (Downing et al. 2006). Lakes are vital sources of potable water for humankind and natural livelihood. Hence, it is essential to understand the lakes' impacts and analyze how they interactively affect the water quantity and quality.



Canada contains the largest resource of drinkable water (Hammer et al. 1983). 9% of Canada's land area is covered by freshwater resources, mainly lakes (Dean S. Jeffries et al. 2003) but these resources are shrinking in some regions (Smith 2005). Therefore, it is critical to assess their impacts on the hydrologic components of river basins. The presence of a lake in the basin dramatically alters the hydrological characteristics of the region as they can retain the surface water for a relatively long period and release it gradually (Mishra et al., 2010). lakes are a nest for growing biomaterials and animals (Cardille et al. 2007) and affect the quality of the water by adding and removing contaminants (Williams et al. 2004).

## 2.5 Climate Change Scenarios

The climate of the earth has changed dramatically during the past centuries and millenniums (Feulner and Rahmstorf 2010). These changes are partly associated with natural variability and partly due to human activities after industrialization (T. R. Karl 2003). Natural forcing factors such as volcanic eruptions, gas release from lower layers of earth, earth's orbital changes, solar variation, etc. affect the global climate (Halloran et al. 2020). Variations in global climate, and mainly temperature, are not stationary, but a global warming trend is detectable from the mid-20<sup>th</sup> century. There is strong evidence that such changes are attributable to human activities (95% - 100% probability) (Bush et al. 2019). Warmer climate, directly and indirectly, affects the hydrological cycle (Thomas R. Karl et al. 1996). During the past few decades, the snow-melting process has shifted earlier in the year resulting in higher winter and early spring flows (CCCR, 2019). Surface water resources including wetlands and lakes are projected to decline in southern Canada. Droughts are projected to be more severe and frequent in the Canadian Prairies and interior British Columbia. Assessing groundwater resources is complicated and because there is no sufficient reliable data, the magnitude and even direction of changes are not well understood. A study on the historical trends of streamflow in Western Canada was conducted considering nine rivers throughout 1960-2006. Results suggested early spring freshet, reduced summer flows and a delay in the onset of enhanced autumn flows (Déry et al. 2009). Boyer et al. (2010) conducted a study to understand the impact of climate change on the St. Lawrence tributaries in the eastern province of Canada (QC). Results showed that most scenarios are simulating increased streamflow for annual mean and winter while flows for summer are projected to decrease by 2050s. Other related studies are provided in the 6<sup>th</sup> chapter of CCCR.

Greenhouse gases (GHG) either absorb or emit radiant energy within the thermal infrared range and their presence is important for life compatibility on Earth. Without GHGs the average Earth's temperature would drop to  $-18\text{ }^{\circ}\text{C}$  instead of the current  $+15\text{ }^{\circ}\text{C}$  (Ma and Tipping 1998). Water vapour ( $\text{H}_2\text{O}$ ), carbon dioxide ( $\text{C}_2\text{O}$ ), methane ( $\text{CH}_4$ ), nitrous oxide ( $\text{N}_2\text{O}$ ) and stratospheric ozone ( $\text{O}_3$ ), Chlorofluorocarbons (CFCs) and Hydrofluorocarbons (HCFCs and HFCs) are the GHGs (Canadell et al. 2007). Comparing the preindustrial era with the contemporary period, human activities have changed the natural GHG balance by adding a substantial amount of GHG, especially during the past few decades (Feulner and Rahmstorf 2010). GHGs act like a blanket that covers the earth and makes it warm. But excessive amounts of GHGs cause excessive heat traps and make the earth warmer causing other changes in the earth's climate system (EPA, 2020). One major non-GHG atmospheric contributor to climate change is cloud cover which traps the energy and/or emits it in the infrared range (Kiehl and Trenberth 1997).

Studies on GHG contributions to climate change and increases in the earth's temperature show that water vapour contributes to 36% to 72 % of the greenhouse gas effects. It should be noted that water vapour varies drastically between the regions (Kiehl and Trenberth 1997). Carbon dioxide, Methane and ozone contribute to the greenhouse gas effects for 9% to 26%, 4% to 9% and 3 to 7%, respectively. GHGs trap the solar heat reflectance from the earth and resend it to the earth's surface. A few natural factors can reduce the incoming solar radiation leading to a cooler environment such as Sulfur dioxide emitted from volcanic eruptions (Intergovernmental Panel on Climate Change 2013d). Earth's temperature and the environment are in a balance between the incoming and outgoing energy and if this balance is shifted by any means, the earth's environment will be affected (Kiehl and Trenberth 1997).

GHGs presence in the atmosphere of the earth alters the radiative solar forces. The GHG contribution to global warming should be quantified using radiative forces (RF) and by setting up scenarios based on possible carbon and other GHG emissions (Intergovernmental Panel on Climate Change 2013; Najafi et al., 2017). The Intergovernmental Panel on Climate Change (IPCC) in the fifth assessment report (AR5) (Chapter 10, IPCC 2013) introduced four representative concentration pathways (RCP) scenarios based on GHG concentrations in the future. As an instance, RCP 2.6 represents the GHG concentration that leads to a solar radiative force increase equal to  $2.6\text{ Watts per m}^2\text{ (W/m}^2\text{)}$ . Future scenarios for GHG concentration are considerably

uncertain because of numerous effective factors including socio-economic activities (Ward et al. 2012).

Here are the four major RCPs (Granier et al. 2011):

- i. RCP 2.6: is a very stringent scenario where according to the IPCC AR5 (Pachauri and Meyer 2014) carbon dioxide emission will start to decline from 2020 and reach 0 emissions by 2100. Like most of the RCPs, this scenario considers negative CO<sub>2</sub> production which relies on forest carbon absorption and ocean uptake. The RF is assumed to increase 2.6 W/m<sup>2</sup> by the end of the 21<sup>st</sup> century.
- ii. RCP 4.5: Even though that is considered as an intermediate scenario, but many animals and currently living species are unable to adapt to this condition (IPCC, 2013). It is assumed that carbon dioxide emission will peak by 2040 and then starts to decline and by the end of the century, the CO<sub>2</sub> concentration will be half of 2050. It relies on negative emissions of 2 Gigatons of carbon dioxide per year. Sea levels would be 35% higher than RCP 2.6 (Chapter 15 IPCC, 2013)
- iii. RCP 6.0: It is also known as an intermediate scenario. This scenario is asserting that sea levels will be increased up to two times higher than RCP 2.6. GHG concentration peaks in 2060 and then declines (Masui et al. 2011).
- iv. RCP 8.5: This is considered as the worst-case scenario where population spikes, technology improvements are not helpful for less GHG concentration and relatively slow income growth happens (Riahi et al. 2011). Even though initially this scenario was considered as an overestimation for GHGs concentration, the current trend is aligned with this scenario. 8.5 W/m<sup>2</sup> is predicted to be the radiative force increase under this scenario.

To assess projected streamflow changes, we use downscaled General Circulation Models (GCMs). GCMs simulate the complex interactions between the atmosphere, oceans, and lands to represent climate change impacts (Scinocca et al. 2016a). GCMs are complex computer-based models that exploit the mathematical formulas to imitate the physical and chemical cycle of the earth to understand the processes that drive the global climate (Jakob 2014). The first generations of GCMs represented the atmosphere, land surface and vegetation along with oceans' physical and chemical characteristics (Bony et al. 2015) and thereafter they have been improved by adding sea ice, marine ecosystem, ice sheet, sulphate aerosols, biogeochemical cycles and carbon cycle

processes (Jakob 2014). GCMs possess three dimensions to show the location and elevation of each grid cell which build up a global model (Chapter 2 IPCC, 2013). Further details are provided in the IPCC reports as well as Phillips 1956 and Jakob 2014.

GCMs have different spatial resolutions which are not fine enough to study the hydrological processes of small regions (Zhao et al. 2009) and are commonly biased (Cannon 2015). Therefore, downscaling methods are developed to translate GCM results at fine scales suitable for regional assessments (Crosbie et al. 2011; H. Chen et al. 2010). Downscaling methods are categorized into dynamical and statistical downscaling (Sahour et al. 2020; Azmat et al. 2018). Statistical downscaling methods can be divided into three major groups: weather generators, weather typing and transfer function (Meehl et al. 2009). Weather generators are based on the observed weather variables (i.e. temperature, precipitation) and Markov chain approach (Hughes and Guttorp 1994) and the spell-length approach (Wilks 1999). Weather typing finds an association between a group of meteorological data to the atmospheric circulation (Brown and Katz 1995). The transfer function is the most prevalent statistical downscaling method that relies on regression and the direct quantitative association between local meteorological data and global simulated data (Brown and Katz 1995). Dynamical downscaling uses a limited-area, high-resolution model (a regional climate model, or RCM) driven by boundary conditions from a GCM to derive smaller-scale information. RCMs generally have a domain area of 10<sup>6</sup> to 10<sup>7</sup> km<sup>2</sup> and a resolution of 20 (or lower) to 60 km. Regional climate models are the downscaled versions of global climate models where their applicability has been assessed to be more accurate on smaller regions (P. Jiang et al. 2013).

There are considerable uncertainties among different GCMs, which stem from many potential reasons such as; considering different physical and chemical procedures for the earth's hydroclimate system (J. Teng et al. 2012). To validate the newly developed models WCRP adopts several verification steps. The Coupled Model Intercomparison Project (CMIP) is an experimental framework to support national and international assessments of climate change, evaluate the coupled ocean-atmosphere GCM simulations, reveal the weak points and deficiencies to evolve and focus on the development of improved climate models (Taylor et al 2012). CMIPs are released in 5 phases so far. The first phase of CMIP or CMIP1 was based on only 18 coupled ocean-atmosphere global climate models. CMIP5 includes a set of 35 climate models that can be used to

assess how realistically models simulate historical changes and to enlighten key differences in model projections (Meehl et al. 2009).

According to CCCR, the global mean surface temperature (GMST) has significantly increased since 1880 and specifically since 1950. From 1880 to 2012, GMST increased by 0.8 °C with a 90% uncertainty range of 0.65 °C to 1.06 °C (Intergovernmental Panel on Climate Change 2013b). 2016, 2020, 2019, 2015 and 2017 are respectively the 5 warmest years in the earth's history (Arguez et al. 2020). Considering the impacts of climate change on temperature, precipitation and hydrological system of the earth (Abbasian et al., 2021; Creed et al. 2015; Muhammad et al. 2020; Bormann 2011; L. Zhang et al. 2018) it is critical to assess the climate change-induced effects at regional scales for future planning and management of natural resources.

## 2.6 Internal Climate Variability and Anthropogenic Impacts

The uncertainties in global climate models are associated with the initial condition, parameterization and boundary conditions. These uncertainties can propagate into future simulations resulting in different realizations of the hydroclimate projections (Hawkins and Sutton 2009). In recent years, large ensembles of GCM/RCM simulations generated by perturbing the initial conditions of the models are used to characterize the role of internal climate variability (Kirchmeier-Young et al. 2017; Singh et al., 2021). The large ensembles provide the opportunity to distinguish between the uncertainties associated with the model structure and parameterization and assess the external forcing and internal climate variability influence on future projections (Wallach et al. 2016). External forcings include changes in greenhouse gas emissions, anthropogenic aerosols, tropospheric and stratospheric ozone, solar radiation, land-use changes and volcanic eruptions (Dai and Bloecker 2019). Examples of the internal climate variability (ICV) are El Niño, PDO, AMO, etc. that occur in decadal timeframes regardless of humankind presence and activities and can affect regional hydroclimatic parameters (Y. Xu and Hu 2018; Yang et al. 2015).

Human growth is happening with consequences on the climate (K. E. Trenberth 2018). Accurate quantification and separation of the impacts of the natural climate variability and anthropogenic impacts on the future climate are not technically possible because natural climate alterations and

anthropogenic effects sometimes cancel each other out and sometimes amplitude their effects (Thompson et al. 2015). The mean of the large ensemble members (runs) is commonly considered as an estimate of the anthropogenic impact by removing the internal climate variability (ICV) and the standard deviation of the residuals represents the ICV (Dai and Bloecker 2019; Dai et al. 2015). Identifying the role of anthropogenic factors and internal climate variability on future projections provides insights for policymakers and researchers to understand the degree to which human activities can influence future extremes to implement effective climate change adaptation plans (Jalili and Najafi, 2020; Zhang and Najafi, 2020).

Several studies have been conducted to quantify the role of ICV and external forces impacts on climatic extremes including temperature and precipitation anomalies (Wallace et al. 2012; Ting et al. 2009; Z. Wu et al. 2011; DelSole, Tippet, and Shukla 2011; R. Zhang et al. 2013). Only a few studies have analyzed the role of ICV on projected hydrological changes (Champagne et al. 2020; Liu et al. 2020). In this study, the influence of ICV on future projections of temperature, precipitation and streamflow is quantified, assessed and analyzed over the Batchawana watershed.

## 2.7 References

Abbasian MS, Najafi MR, Abrishamchi A. Increasing risk of meteorological drought in the Lake Urmia basin under climate change: Introducing the precipitation–temperature deciles index. *Journal of Hydrology*. 2021 Jan 1;592:125586.

Abbott, M.B., J.C. Bathurst, J.A. Cunge, P.E. O’Connell, and J. Rasmussen. 1986. “An Introduction to the European Hydrological System — Systeme Hydrologique European, ‘SHE’, 1: History and Philosophy of a Physically-Based, Distributed Modelling System.” *Journal of Hydrology* 87 (1–2): 45–59. [https://doi.org/10.1016/0022-1694\(86\)90114-9](https://doi.org/10.1016/0022-1694(86)90114-9).

Ahmadisharaf, Ebrahim, René A. Camacho, Harry X. Zhang, Mohamed M. Hantush, and Yusuf M. Mohamoud. 2019. “Calibration and Validation of Watershed Models and Advances in Uncertainty Analysis in TMDL Studies.” *Journal of Hydrologic Engineering* 24 (7): 03119001. [https://doi.org/10.1061/\(ASCE\)HE.1943-5584.0001794](https://doi.org/10.1061/(ASCE)HE.1943-5584.0001794).

Akhavan, Samira, Jahangir Abedi-Koupai, Sayed-Farhad Mousavi, Majid Afyuni, Sayed-Saeid Eslamian, and Karim C. Abbaspour. 2010. “Application of SWAT Model to Investigate Nitrate

Leaching in Hamadan–Bahar Watershed, Iran.” *Agriculture, Ecosystems & Environment* 139 (4): 675–88. <https://doi.org/10.1016/j.agee.2010.10.015>.

Ali, Mohd Fozi, Nor Faiza Abd Rahman, Khairi Khalid, and Nguyen Duy Liem. 2014. “Langat River Basin Hydrologic Model Using Integrated GIS and ArcSWAT Interface.” *Applied Mechanics and Materials* 567 (June): 86–91. <https://doi.org/10.4028/www.scientific.net/AMM.567.86>.

Almeida, Rafael A., Silvio B. Pereira, and Daniel B. F. Pinto. 2018. “CALIBRATION AND VALIDATION OF THE SWAT HYDROLOGICAL MODEL FOR THE MUCURI RIVER BASIN.” *Engenharia Agrícola* 38 (1): 55–63. <https://doi.org/10.1590/1809-4430-eng.agric.v38n1p55-63/2018>.

Azmat, Muhammad, Muhammad Uzair Qamar, Shakil Ahmed, Muhammad Adnan Shahid, Ejaz Hussain, Sajjad Ahmad, and Rao Arsalan Khushnood. 2018. “Ensembling Downscaling Techniques and Multiple GCMs to Improve Climate Change Predictions in Cryosphere Scarcely-Gauged Catchment.” *Water Resources Management* 32 (9): 3155–74. <https://doi.org/10.1007/s11269-018-1982-9>.

Bergström, Sten, and Göran Lindström. 2015. “Interpretation of Runoff Processes in Hydrological Modelling-Experience from the HBV Approach.” *Hydrological Processes* 29 (16): 3535–45. <https://doi.org/10.1002/hyp.10510>.

Beven, Keith. 1989. “Changing Ideas in Hydrology — The Case of Physically-Based Models.” *Journal of Hydrology* 105 (1–2): 157–72. [https://doi.org/10.1016/0022-1694\(89\)90101-7](https://doi.org/10.1016/0022-1694(89)90101-7).

———. 2014. “The GLUE Methodology for Model Calibration with Uncertainty.” In *Applied Uncertainty Analysis for Flood Risk Management*, 87–97. IMPERIAL COLLEGE PRESS. [https://doi.org/10.1142/9781848162716\\_0006](https://doi.org/10.1142/9781848162716_0006).

Biondi, Daniela, Gabriele Freni, Vito Iacobellis, Giuseppe Mascaro, and Alberto Montanari. 2012. “Validation of Hydrological Models: Conceptual Basis, Methodological Approaches and a Proposal for a Code of Practice.” *Physics and Chemistry of the Earth, Parts A/B/C* 42–44 (January): 70–76. <https://doi.org/10.1016/j.pce.2011.07.037>.

Bittner, Matthias, Hauke Schmidt, Claudia Timmreck, and Frank Sienz. 2016. "Using a Large Ensemble of Simulations to Assess the Northern Hemisphere Stratospheric Dynamical Response to Tropical Volcanic Eruptions and Its Uncertainty." *Geophysical Research Letters* 43 (17): 9324–32. <https://doi.org/10.1002/2016GL070587>.

Bonsal, B.R., D.L. Peters, F. Seglenieks, A. Rivera, and Bergm A. n.d. "Changes in Freshwater Availability across Canada; Chapter 6 in Canada's Changing Climate Report." Ottawa, Ontario.

Bony, Sandrine, Bjorn Stevens, Dargan M. W. Frierson, Christian Jakob, Masa Kageyama, Robert Pincus, Theodore G. Shepherd, et al. 2015. "Clouds, Circulation and Climate Sensitivity." *Nature Geoscience* 8 (4): 261–68. <https://doi.org/10.1038/ngeo2398>.

Bormann, Helge. 2011. "Sensitivity Analysis of 18 Different Potential Evapotranspiration Models to Observed Climatic Change at German Climate Stations." *Climatic Change* 104 (3): 729–53. <https://doi.org/10.1007/s10584-010-9869-7>.

Boyd, D. S., and F. M. Danson. 2005. "Satellite Remote Sensing of Forest Resources: Three Decades of Research Development." *Progress in Physical Geography: Earth and Environment* 29 (1): 1–26. <https://doi.org/10.1191/0309133305pp432ra>.

Boyer, Claudine, Diane Chaumont, Isabelle Chartier, and André G. Roy. 2010. "Impact of Climate Change on the Hydrology of St. Lawrence Tributaries." *Journal of Hydrology* 384 (1–2): 65–83. <https://doi.org/10.1016/j.jhydrol.2010.01.011>.

Brown, Barbara G., and Richard W. Katz. 1995. "Regional Analysis of Temperature Extremes: Spatial Analog for Climate Change?" *Journal of Climate* 8 (1): 108–19. [https://doi.org/10.1175/1520-0442\(1995\)008<0108:RAOTES>2.0.CO;2](https://doi.org/10.1175/1520-0442(1995)008<0108:RAOTES>2.0.CO;2).

Bulygina, Nataliya, Caroline Ballard, Neil McIntyre, Greg O'Donnell, and Howard Wheeler. 2012. "Integrating Different Types of Information into Hydrological Model Parameter Estimation: Application to Ungauged Catchments and Land Use Scenario Analysis." *Water Resources Research* 48 (6). <https://doi.org/10.1029/2011WR011207>.

Bush, E, N Gillet, E Watson, J Fyfe, F Voge, and N Swart. 2019. "Understanding Observed Global Climate Change, CCCR Chapter 2." Ottawa, Ontario.



Canadell, J. G., C. Le Quere, M. R. Raupach, C. B. Field, E. T. Buitenhuis, P. Ciais, T. J. Conway, N. P. Gillett, R. A. Houghton, and G. Marland. 2007. “Contributions to Accelerating Atmospheric CO<sub>2</sub> Growth from Economic Activity, Carbon Intensity, and Efficiency of Natural Sinks.” *Proceedings of the National Academy of Sciences* 104 (47): 18866–70.

<https://doi.org/10.1073/pnas.0702737104>.

Cannon, Alex J. 2015. “Selecting GCM Scenarios That Span the Range of Changes in a Multimodel Ensemble: Application to CMIP5 Climate Extremes Indices\*.” *Journal of Climate* 28 (3): 1260–67. <https://doi.org/10.1175/JCLI-D-14-00636.1>.

Canuti, Paolo, Nicola Casagli, Filippo Catani, Giacomo Falorni, and Paolo Farina. n.d. “Integration of Remote Sensing Techniques in Different Stages of Landslide Response.” In *Progress in Landslide Science*, 251–60. Berlin, Heidelberg: Springer Berlin Heidelberg.

[https://doi.org/10.1007/978-3-540-70965-7\\_18](https://doi.org/10.1007/978-3-540-70965-7_18).

Cardille, Jeffrey A., Stephen R. Carpenter, Michael T. Coe, Jonathan A. Foley, Paul C. Hanson, Monica G. Turner, and Julie A. Vano. 2007. “Carbon and Water Cycling in Lake-Rich Landscapes: Landscape Connections, Lake Hydrology, and Biogeochemistry.” *Journal of Geophysical Research* 112 (G2): G02031. <https://doi.org/10.1029/2006JG000200>.

Champagne, Olivier, M. Altaf Arain, Martin Leduc, Paulin Coulibaly, and Shawn McKenzie. 2020. “Future Shift in Winter Streamflow Modulated by the Internal Variability of Climate in Southern Ontario.” *Hydrology and Earth System Sciences* 24 (6): 3077–96.

<https://doi.org/10.5194/hess-24-3077-2020>.

Chen, Hua, Jing Guo, Wei Xiong, Shenglian Guo, and Chong-Yu Xu. 2010. “Downscaling GCMs Using the Smooth Support Vector Machine Method to Predict Daily Precipitation in the Hanjiang Basin.” *Advances in Atmospheric Sciences* 27 (2): 274–84.

<https://doi.org/10.1007/s00376-009-8071-1>.

Chen, Ying, Youpeng Xu, and Yixing Yin. 2009. “Impacts of Land Use Change Scenarios on Storm-Runoff Generation in Xitiaoxi Basin, China.” *Quaternary International* 208 (1–2): 121–28. <https://doi.org/10.1016/j.quaint.2008.12.014>.

Chernos, Matthew, Ryan MacDonald, and James Craig. 2017. “Efficient Semi-Distributed Hydrological Modelling Workflow for Simulating Streamflow and Characterizing Hydrologic Processes.” *Confluence: Journal of Watershed Science and Management* 1 (3).

<https://doi.org/10.22230/jwsm.2018v1n3a6>.

Churches, Christopher E., Peter J. Wampler, Wanxiao Sun, and Andrew J. Smith. 2014. “Evaluation of Forest Cover Estimates for Haiti Using Supervised Classification of Landsat Data.” *International Journal of Applied Earth Observation and Geoinformation* 30 (August): 203–16. <https://doi.org/10.1016/j.jag.2014.01.020>.

Craig, James R. n.d. “Raven Hydrological Model.” Accessed September 15, 2020.

<http://raven.uwaterloo.ca/>.

Craig, James R., Genevieve Brown, Robert Chlumsky, R. Wayne Jenkinson, Georg Jost, Konhee Lee, Juliane Mai, et al. 2020. “Flexible Watershed Simulation with the Raven Hydrological Modelling Framework.” *Environmental Modelling & Software* 129 (July): 104728.

<https://doi.org/10.1016/j.envsoft.2020.104728>.

Creed, I. F., T. Hwang, B. Lutz, and D. Way. 2015. “Climate Warming Causes Intensification of the Hydrological Cycle, Resulting in Changes to the Vernal and Autumnal Windows in a Northern Temperate Forest.” *Hydrological Processes* 29 (16): 3519–34.

<https://doi.org/10.1002/hyp.10450>.

Creed, I. F., S. E. Sanford, F. D. Beall, L. A. Molot, and P. J. Dillon. 2003. “Cryptic Wetlands: Integrating Hidden Wetlands in Regression Models of the Export of Dissolved Organic Carbon from Forested Landscapes.” *Hydrological Processes* 17 (18): 3629–48.

<https://doi.org/10.1002/hyp.1357>.

Crosbie, Russell S., Warrick R. Dawes, Stephen P. Charles, Freddie S. Mpelasoka, Santosh Aryal, Olga Barron, and Greg K. Summerell. 2011. “Differences in Future Recharge Estimates Due to GCMs, Downscaling Methods and Hydrological Models.” *Geophysical Research Letters* 38 (11): n/a-n/a. <https://doi.org/10.1029/2011GL047657>.

- Daggupati, Prasad, Naresh Pai, Srinivasulu Ale, Kyle R. Douglas-Mankin, Rebecca W. Zeckoski, Jaehak Jeong, Prem B. Parajuli, Dharmendra Saraswat, and Mohamed A. Youssef. 2015. “A Recommended Calibration and Validation Strategy for Hydrologic and Water Quality Models.” *Transactions of the ASABE* 58 (6): 1705–19. <https://doi.org/10.13031/trans.58.10712>.
- Dai, Aiguo, and Christine E. Bloecker. 2019. “Impacts of Internal Variability on Temperature and Precipitation Trends in Large Ensemble Simulations by Two Climate Models.” *Climate Dynamics* 52 (1–2): 289–306. <https://doi.org/10.1007/s00382-018-4132-4>.
- Dai, Aiguo, John C. Fyfe, Shang-Ping Xie, and Xingang Dai. 2015. “Decadal Modulation of Global Surface Temperature by Internal Climate Variability.” *Nature Climate Change* 5 (6): 555–59. <https://doi.org/10.1038/nclimate2605>.
- DelSole, Timothy, Michael K. Tippett, and Jagadish Shukla. 2011. “A Significant Component of Unforced Multidecadal Variability in the Recent Acceleration of Global Warming.” *Journal of Climate* 24 (3): 909–26. <https://doi.org/10.1175/2010JCLI3659.1>.
- Déry, Stephen J., K. Stahl, R. D. Moore, P. H. Whitfield, B. Menounos, and Jason E. Burford. 2009. “Detection of Runoff Timing Changes in Pluvial, Nival, and Glacial Rivers of Western Canada.” *Water Resources Research* 45 (4). <https://doi.org/10.1029/2008WR006975>.
- Deser, C., F. Lehner, K. B. Rodgers, T. Ault, T. L. Delworth, P. N. DiNezio, A. Fiore, et al. 2020. “Insights from Earth System Model Initial-Condition Large Ensembles and Future Prospects.” *Nature Climate Change* 10 (4): 277–86. <https://doi.org/10.1038/s41558-020-0731-2>.
- Downing, J. A., Y. T. Prairie, J. J. Cole, C. M. Duarte, L. J. Tranvik, R. G. Striegl, W. H. McDowell, et al. 2006. “The Global Abundance and Size Distribution of Lakes, Ponds, and Impoundments.” *Limnology and Oceanography* 51 (5): 2388–97. <https://doi.org/10.4319/lo.2006.51.5.2388>.
- EPA. n.d. “Greenhouse Gas Emissions.” Accessed April 10, 2020. <https://www.epa.gov/ghgemissions/overview-greenhouse-gases>.
- Fatichi, S., S. Rimkus, P. Burlando, and R. Bordoy. 2014. “Does Internal Climate Variability Overwhelm Climate Change Signals in Streamflow? The Upper Po and Rhone Basin Case

Studies.” *Science of The Total Environment* 493 (September): 1171–82.

<https://doi.org/10.1016/j.scitotenv.2013.12.014>.

Feulner, Georg, and Stefan Rahmstorf. 2010. “On the Effect of a New Grand Minimum of Solar Activity on the Future Climate on Earth.” *Geophysical Research Letters* 37 (5): n/a-n/a.

<https://doi.org/10.1029/2010GL042710>.

Flückiger, Jacqueline, Eric Monnin, Bernhard Stauffer, Jakob Schwander, Thomas F. Stocker, Jérôme Chappellaz, Dominique Raynaud, and Jean-Marc Barnola. 2002. “High-Resolution Holocene N<sub>2</sub>O Ice Core Record and Its Relationship with CH<sub>4</sub> and CO<sub>2</sub>.” *Global Biogeochemical Cycles* 16 (1): 10-1-10–18. <https://doi.org/10.1029/2001GB001417>.

Franklin, Steven E. 2001. *Remote Sensing for Sustainable Forest Management*. CRC Press.

<https://doi.org/10.1201/9781420032857>.

Geneletti, Davide. 2012. “Environmental Assessment of Spatial Plan Policies through Land Use Scenarios.” *Environmental Impact Assessment Review* 32 (1): 1–10.

<https://doi.org/10.1016/j.eiar.2011.01.015>.

Gholizadeh, Mohammad, Assefa Melesse, and Lakshmi Reddi. 2016. “A Comprehensive Review on Water Quality Parameters Estimation Using Remote Sensing Techniques.” *Sensors* 16 (8): 1298. <https://doi.org/10.3390/s16081298>.

Granier, Claire, Bertrand Bessagnet, Tami Bond, Ariela D’Angiola, Hugo Denier van der Gon, Gregory J. Frost, Angelika Heil, et al. 2011. “Evolution of Anthropogenic and Biomass Burning Emissions of Air Pollutants at Global and Regional Scales during the 1980–2010 Period.” *Climatic Change* 109 (1–2): 163–90. <https://doi.org/10.1007/s10584-011-0154-1>.

Halloran, Paul R., Ian R. Hall, Matthew Menary, David J. Reynolds, James D. Scourse, James A. Screen, Alessio Bozzo, et al. 2020. “Natural Drivers of Multidecadal Arctic Sea Ice Variability over the Last Millennium.” *Scientific Reports* 10 (1): 688. <https://doi.org/10.1038/s41598-020-57472-2>.

Hamed, Khaled H. 2008. "Trend Detection in Hydrologic Data: The Mann–Kendall Trend Test under the Scaling Hypothesis." *Journal of Hydrology* 349 (3–4): 350–63.

<https://doi.org/10.1016/j.jhydrol.2007.11.009>.

Hamman, Joseph J., Bart Nijssen, Theodore J. Bohn, Diana R. Gergel, and Yixin Mao. 2018. "The Variable Infiltration Capacity Model Version 5 (VIC-5): Infrastructure Improvements for New Applications and Reproducibility." *Geoscientific Model Development* 11 (8): 3481–96.

<https://doi.org/10.5194/gmd-11-3481-2018>.

Hammer, U. Theodore, Jennifer Shames, and Robert C. Haynes. 1983. "The Distribution and Abundance of Algae in Saline Lakes of Saskatchewan, Canada." *Hydrobiologia* 105 (1): 1–26.

<https://doi.org/10.1007/BF00025173>.

Han, Ming, Juliane Mai, Bryan A. Tolson, James R. Craig, Étienne Gaborit, Hongli Liu, and Konhee Lee. 2020. "Subwatershed-Based Lake and River Routing Products for Hydrologic and Land Surface Models Applied over Canada." *Canadian Water Resources Journal / Revue Canadienne Des Ressources Hydriques* 45 (3): 237–51.

<https://doi.org/10.1080/07011784.2020.1772116>.

Hawkins, Ed, and Rowan Sutton. 2009. "The Potential to Narrow Uncertainty in Regional Climate Predictions." *Bulletin of the American Meteorological Society* 90 (8): 1095–1108.

<https://doi.org/10.1175/2009BAMS2607.1>.

Hill, Michael J., John FitzSimons, and Craig J. Pearson. 2009. "Creating Land Use Scenarios for City Greenbelts Using A Spatial Multi-Criteria Analysis Shell: Two Case Studies." *Physical Geography* 30 (4): 353–82. <https://doi.org/10.2747/0272-3646.30.4.353>.

Hughes, James P., and Peter Guttorp. 1994. "A Class of Stochastic Models for Relating Synoptic Atmospheric Patterns to Regional Hydrologic Phenomena." *Water Resources Research* 30 (5): 1535–46. <https://doi.org/10.1029/93WR02983>.

Intergovernmental Panel on Climate Change, ed. 2013a. "Anthropogenic and Natural Radiative Forcing." In *Climate Change 2013 - The Physical Science Basis*, 659–740. Cambridge: Cambridge University Press. <https://doi.org/10.1017/CBO9781107415324.018>.

———. , ed. 2013b. *Climate Change 2013 - The Physical Science Basis*. Cambridge: Cambridge University Press. <https://doi.org/10.1017/CBO9781107415324>.

———. , ed. 2013c. “Climate Phenomena and Their Relevance for Future Regional Climate Change.” In *Climate Change 2013 - The Physical Science Basis*, 1217–1308. Cambridge: Cambridge University Press. <https://doi.org/10.1017/CBO9781107415324.028>.

———. , ed. 2013d. “Evaluation of Climate Models.” In *Climate Change 2013 - The Physical Science Basis*, 741–866. Cambridge: Cambridge University Press. <https://doi.org/10.1017/CBO9781107415324.020>.

———. , ed. 2013e. “Introduction.” In *Climate Change 2013 - The Physical Science Basis*, 119–58. Cambridge: Cambridge University Press. <https://doi.org/10.1017/CBO9781107415324.007>.

———. , ed. 2013f. “Sea Level Change.” In *Climate Change 2013 - The Physical Science Basis*, 1137–1216. Cambridge: Cambridge University Press. <https://doi.org/10.1017/CBO9781107415324.026>.

———. , ed. 2013g. “Summary for Policymakers.” In *Climate Change 2013 - The Physical Science Basis*, 1–30. Cambridge: Cambridge University Press. <https://doi.org/10.1017/CBO9781107415324.004>.

———. , ed. 2013h. “Technical Summary.” In *Climate Change 2013 - The Physical Science Basis*, 31–116. Cambridge: Cambridge University Press. <https://doi.org/10.1017/CBO9781107415324.005>.

Irons, James R., John L. Dwyer, and Julia A. Barsi. 2012. “The next Landsat satellite: The Landsat Data Continuity Mission.” *Remote Sensing of Environment* 122 (July): 11–21. <https://doi.org/10.1016/j.rse.2011.08.026>.

J. G. Arnold, D. N. Moriasi, P. W. Gassman, K. C. Abbaspour, M. J. White, R. Srinivasan, C. Santhi, et al. 2012. “SWAT: Model Use, Calibration, and Validation.” *Transactions of the ASABE* 55 (4): 1491–1508. <https://doi.org/10.13031/2013.42256>.

Jajarmizad, Milad, Sobri Harun, and Mohsen Salarpour. 2012. "A Review on Theoretical Consideration and Types of Models in Hydrology." *Journal of Environmental Science and Technology* 5 (5): 249–61. <https://doi.org/10.3923/jest.2012.249.261>.

Jakob, Christian. 2014. "Going Back to Basics." *Nature Climate Change* 4 (12): 1042–45. <https://doi.org/10.1038/nclimate2445>.

Jalili Pirani F, Najafi MR. Recent trends in individual and multivariate compound flood drivers in Canada's coasts. *Water Resources Research*. 2020 Aug;56(8):e2020WR027785.

Jeffries, Dean S., Thomas A. Clair, Suzanne Couture, Peter J. Dillon, Jacques Dupont, Wendel (Bill) Keller, Donald K. McNicol, Michael A. Turner, Robert Vet, and Russell Weeber. 2003. "Assessing the Recovery of Lakes in Southeastern Canada from the Effects of Acidic Deposition." *AMBIO: A Journal of the Human Environment* 32 (3): 176–82. <https://doi.org/10.1579/0044-7447-32.3.176>.

Jeffries, Dean S., John R. M. Kelso, and Ian K. Morrison. 1988. "Physical, Chemical, and Biological Characteristics of the Turkey Lakes Watershed, Central Ontario, Canada." *Canadian Journal of Fisheries and Aquatic Sciences* 45 (S1): s3–13. <https://doi.org/10.1139/f88-262>.

Jia, Q.Y., and F.H. Sun. 2012. "Modeling and Forecasting Process Using the HBV Model in Liao River Delta." *Procedia Environmental Sciences* 13: 122–28. <https://doi.org/10.1016/j.proenv.2012.01.012>.

Jiang, Peng, Mahesh R. Gautam, Jianting Zhu, and Zhongbo Yu. 2013. "How Well Do the GCMs/RCMs Capture the Multi-Scale Temporal Variability of Precipitation in the Southwestern United States?" *Journal of Hydrology* 479 (February): 75–85. <https://doi.org/10.1016/j.jhydrol.2012.11.041>.

Jong, Steven M. de, Freek D. van der Meer, and Jan G.P.W Clevers. 2004. "Basics of Remote Sensing." In , 1–15. [https://doi.org/10.1007/978-1-4020-2560-0\\_1](https://doi.org/10.1007/978-1-4020-2560-0_1).

Kang, Hyunwoo, Jongpil Moon, Yongchul Shin, Jichul Ryu, Dong Hyuk Kum, Chunhwa Jang, Joongdae Choi, Dong Soo Kong, and Kyoung Jae Lim. 2016. "Modification of SWAT Auto-

Calibration for Accurate Flow Estimation at All Flow Regimes.” *Paddy and Water Environment* 14 (4): 499–508. <https://doi.org/10.1007/s10333-015-0519-6>.

Karl, T. R. 2003. “Modern Global Climate Change.” *Science* 302 (5651): 1719–23. <https://doi.org/10.1126/science.1090228>.

Karl, Thomas R., Richard W. Knight, David R. Easterling, and Robert G. Quayle. 1996. “Indices of Climate Change for the United States.” *Bulletin of the American Meteorological Society* 77 (2): 279–92. [https://doi.org/10.1175/1520-0477\(1996\)077<0279:IOCCFT>2.0.CO;2](https://doi.org/10.1175/1520-0477(1996)077<0279:IOCCFT>2.0.CO;2).

Kelso, J. R. M. 1988. “Fish Community Structure, Biomass, and Production in the Turkey Lakes Watershed, Ontario.” *Canadian Journal of Fisheries and Aquatic Sciences* 45 (S1): s115–20. <https://doi.org/10.1139/f88-275>.

Kennedy, Christopher, Julia Steinberger, Barrie Gasson, Yvonne Hansen, Timothy Hillman, Miroslav Havránek, Diane Pataki, Aumnad Phdungsilp, Anu Ramaswami, and Gara Villalba Mendez. 2009. “Greenhouse Gas Emissions from Global Cities.” *Environmental Science & Technology* 43 (19): 7297–7302. <https://doi.org/10.1021/es900213p>.

Kepner, William G., Darius J. Semmens, Scott D. Bassett, David A. Mouat, and David C. Goodrich. 2004. “Scenario Analysis for the San Pedro River, Analyzing Hydrological Consequences of a Future Environment.” *Environmental Monitoring and Assessment* 94 (1–3): 115–27. <https://doi.org/10.1023/B:EMAS.0000016883.10110.15>.

Kiehl, J. T., and Kevin E. Trenberth. 1997. “Earth’s Annual Global Mean Energy Budget.” *Bulletin of the American Meteorological Society* 78 (2): 197–208. [https://doi.org/10.1175/1520-0477\(1997\)078<0197:EAGMEB>2.0.CO;2](https://doi.org/10.1175/1520-0477(1997)078<0197:EAGMEB>2.0.CO;2).

Kirchmeier-Young, Megan C., Francis W. Zwiers, Nathan P. Gillett, and Alex J. Cannon. 2017. “Attributing Extreme Fire Risk in Western Canada to Human Emissions.” *Climatic Change* 144 (2): 365–79. <https://doi.org/10.1007/s10584-017-2030-0>.

Kite, G. W. 1993. “Application of a Land Class Hydrological Model to Climatic Change.” *Water Resources Research* 29 (7): 2377–84. <https://doi.org/10.1029/93WR00582>.



Kunnath-Poovakka, A, and T I Eldho. 2019. “A Comparative Study of Conceptual Rainfall-Runoff Models GR4J, AWBM and Sacramento at Catchments in the Upper Godavari River Basin, India.” *Journal of Earth System Science* 128 (2): 33. <https://doi.org/10.1007/s12040-018-1055-8>.

Leach, Jason A., James M. Buttle, Kara L. Webster, Paul W. Hazlett, and Dean S. Jeffries. 2020. “Travel Times for Snowmelt-dominated Headwater Catchments: Influences of Wetlands and Forest Harvesting, and Linkages to Stream Water Quality.” *Hydrological Processes* 34 (10): 2154–75. <https://doi.org/10.1002/hyp.13746>.

Lee, Konhee. 2018. “Assessing the Utility of Hydrologic Model Diagnostics for Decision Support.” UWSpace. <http://hdl.handle.net/10012/14179>.

Lespinas, Franck, Ashu Dastoor, and Vincent Fortin. 2018. “Performance of the Dynamically Dimensioned Search Algorithm: Influence of Parameter Initialization Strategy When Calibrating a Physically Based Hydrological Model.” *Hydrology Research* 49 (4): 971–88. <https://doi.org/10.2166/nh.2017.139>.

Levine, Aaron F. Z., Michael J. McPhaden, and Dargan M. W. Frierson. 2017. “The Impact of the AMO on Multidecadal ENSO Variability.” *Geophysical Research Letters* 44 (8): 3877–86. <https://doi.org/10.1002/2017GL072524>.

Liu, Yanli, Jianyun Zhang, Guoqing Wang, Gaoxu Wang, Junliang Jin, Cuishan Liu, Sicheng Wan, and Ruimin He. 2020. “How Do Natural Climate Variability, Anthropogenic Climate and Basin Underlying Surface Change Affect Streamflows? A Three-Source Attribution Framework and Application.” *Journal of Hydro-Environment Research* 28 (January): 57–66. <https://doi.org/10.1016/j.jher.2018.08.005>.

Ma, Q., and R. H. Tipping. 1998. “The Distribution of Density Matrices over Potential-Energy Surfaces: Application to the Calculation of the Far-Wing Line Shapes for CO<sub>2</sub>.” *The Journal of Chemical Physics* 108 (9): 3386–99. <https://doi.org/10.1063/1.475774>.

Mahajan, G. R., R. N. Sahoo, R. N. Pandey, V. K. Gupta, and Dinesh Kumar. 2014. “Using Hyperspectral Remote Sensing Techniques to Monitor Nitrogen, Phosphorus, Sulphur and

Potassium in Wheat (*Triticum Aestivum* L.).” *Precision Agriculture* 15 (5): 499–522.

<https://doi.org/10.1007/s11119-014-9348-7>.

Martinez del Castillo, Edurne, Alberto García-Martin, Luis Alberto Longares Aladrén, and Martin de Luis. 2015. “Evaluation of Forest Cover Change Using Remote Sensing Techniques and Landscape Metrics in Moncayo Natural Park (Spain).” *Applied Geography* 62 (August): 247–55. <https://doi.org/10.1016/j.apgeog.2015.05.002>.

Masui, Toshihiko, Kenichi Matsumoto, Yasuaki Hijioka, Tsuguki Kinoshita, Toru Nozawa, Sawako Ishiwatari, Etsushi Kato, P. R. Shukla, Yoshiki Yamagata, and Mikiko Kainuma. 2011. “An Emission Pathway for Stabilization at 6 Wm<sup>-2</sup> Radiative Forcing.” *Climatic Change* 109 (1–2): 59–76. <https://doi.org/10.1007/s10584-011-0150-5>.

Mattot, L.S. 2017. “Optimization Software Tool, Documentation and User’s Guide.” University at Buffalo Center for Computational Research.

[www.eng.buffalo.edu/~lsmatott/Ostrich/OstrichMain.html](http://www.eng.buffalo.edu/~lsmatott/Ostrich/OstrichMain.html).

Meehl, Gerald A., Lisa Goddard, James Murphy, Ronald J. Stouffer, George Boer, Gokhan Danabasoglu, Keith Dixon, et al. 2009. “Decadal Prediction.” *Bulletin of the American Meteorological Society* 90 (10): 1467–86. <https://doi.org/10.1175/2009BAMS2778.1>.

Mishra, Vimal, Keith A. Cherkauer, and Laura C. Bowling. 2010. “Parameterization of Lakes and Wetlands for Energy and Water Balance Studies in the Great Lakes Region\*.” *Journal of Hydrometeorology* 11 (5): 1057–82. <https://doi.org/10.1175/2010JHM1207.1>.

Montanari, A. 2011. “Uncertainty of Hydrological Predictions.” In *Treatise on Water Science*, 459–78. Elsevier. <https://doi.org/10.1016/B978-0-444-53199-5.00045-2>.

Muhammad, Ameer, Grey R. Evenson, Fisaha Unduche, and Tricia A. Stadnyk. 2020. “Climate Change Impacts on Reservoir Inflow in the Prairie Pothole Region: A Watershed Model Analysis.” *Water* 12 (1): 271. <https://doi.org/10.3390/w12010271>.

Murray, C.D., and J.M. Buttle. 2005. “Infiltration and Soil Water Mixing on Forested and Harvested Slopes during Spring Snowmelt, Turkey Lakes Watershed, Central Ontario.” *Journal of Hydrology* 306 (1–4): 1–20. <https://doi.org/10.1016/j.jhydrol.2004.08.032>.

Najafi MR, Zwiers FW, Gillett NP. Attribution of observed streamflow changes in key British Columbia drainage basins. *Geophysical Research Letters*. 2017 Nov 16;44(21):11-012.

Nezhad, Omid Bakhtiari, Mohsen Najarchi, Mohammad Mahdi NajafiZadeh, and S. Mohammad Mirhosseini Hezaveh. 2018. “Developing a Shuffled Complex Evolution Algorithm Using a Differential Evolution Algorithm for Optimizing Hydropower Reservoir Systems.” *Water Supply* 18 (3): 1081–92. <https://doi.org/10.2166/ws.2017.179>.

Niehoff, Daniel, Uta Fritsch, and Axel Bronstert. 2002. “Land-Use Impacts on Storm-Runoff Generation: Scenarios of Land-Use Change and Simulation of Hydrological Response in a Meso-Scale Catchment in SW-Germany.” *Journal of Hydrology* 267 (1–2): 80–93. [https://doi.org/10.1016/S0022-1694\(02\)00142-7](https://doi.org/10.1016/S0022-1694(02)00142-7).

NRCAN. n.d. “Forest and Forestry.” Accessed October 12, 2020. <https://www.nrcan.gc.ca/our-natural-resources/forests-forestry/13497>.

Pachauri, R.K., and L.A. Meyer. 2014. “Climate Change 2014: Synthesis Report. Contribution of Working Groups I, II and III to the Fifth Assessment Report of the Intergovernmental Panel on Climate Change.” Geneva, Switzerland.

Petus, Caroline, Catherine Collier, Michelle Devlin, Michael Rasheed, and Skye McKenna. 2014. “Using MODIS Data for Understanding Changes in Seagrass Meadow Health: A Case Study in the Great Barrier Reef (Australia).” *Marine Environmental Research* 98 (July): 68–85. <https://doi.org/10.1016/j.marenvres.2014.03.006>.

Phillips, Norman A. 1956. “The General Circulation of the Atmosphere: A Numerical Experiment.” *Quarterly Journal of the Royal Meteorological Society* 82 (352): 123–64. <https://doi.org/10.1002/qj.49708235202>.

Pradhanang, Soni M., Aavudai Anandhi, Rajith Mukundan, Mark S. Zion, Donald C. Pierson, Eliot M. Schneiderman, Adao Matonse, and Allan Frei. 2011. “Application of SWAT Model to Assess Snowpack Development and Streamflow in the Cannonsville Watershed, New York, USA.” *Hydrological Processes* 25 (21): 3268–77. <https://doi.org/10.1002/hyp.8171>.

Riahi, Keywan, Shilpa Rao, Volker Krey, Cheolhung Cho, Vadim Chirkov, Guenther Fischer, Georg Kindermann, Nebojsa Nakicenovic, and Peter Rafaj. 2011. “RCP 8.5—A Scenario of Comparatively High Greenhouse Gas Emissions.” *Climatic Change* 109 (1–2): 33–57.

<https://doi.org/10.1007/s10584-011-0149-y>.

Ritchie, J. C., and A. Rango. 1996. “Remote Sensing Applications to Hydrology: Introduction.” *Hydrological Sciences Journal* 41 (4): 429–31. <https://doi.org/10.1080/02626669609491518>.

Rodhe, A. 2012. “Physical Models for Classroom Teaching in Hydrology.” *Hydrology and Earth System Sciences* 16 (9): 3075–82. <https://doi.org/10.5194/hess-16-3075-2012>.

Rounsevell, M.D.A., I. Reginster, M.B. Araújo, T.R. Carter, N. Dendoncker, F. Ewert, J.I. House, et al. 2006. “A Coherent Set of Future Land Use Change Scenarios for Europe.” *Agriculture, Ecosystems & Environment* 114 (1): 57–68.

<https://doi.org/10.1016/j.agee.2005.11.027>.

Sahour, Hossein, Mohamed Sultan, Mehdi Vazifedan, Karem Abdelmohsen, Sita Karki, John A. Yellich, Esayas Gebremichael, Fahad Alshehri, and Tamer M. Elbayoumi. 2020. “Statistical Applications to Downscale GRACE-Derived Terrestrial Water Storage Data and to Fill Temporal Gaps.” *Remote Sensing* 12 (3): 533. <https://doi.org/10.3390/rs12030533>.

Sahraei, Shahram, Masoud Asadzadeh, and Fisaha Unduche. 2020. “Signature-Based Multi-Modelling and Multi-Objective Calibration of Hydrologic Models: Application in Flood Forecasting for Canadian Prairies.” *Journal of Hydrology* 588 (September): 125095.

<https://doi.org/10.1016/j.jhydrol.2020.125095>.

Salathe, Eric P., Philip W. Mote, and Matthew W. Wiley. 2007. “Review of Scenario Selection and Downscaling Methods for the Assessment of Climate Change Impacts on Hydrology in the United States Pacific Northwest.” *International Journal of Climatology* 27 (12): 1611–21.

<https://doi.org/10.1002/joc.1540>.

Saleh, J. G. Arnold, P. W. Gassman, L. M. Hauck, W. D. Rosenthal, J. R. Williams, and A. M. S. McFarland. 2000. “Application of swat for the upper north bosque River watershed.”

*Transactions of the ASAE* 43 (5): 1077–87. <https://doi.org/10.13031/2013.3000>.

Sanford, S. E., I. F. Creed, C. L. Tague, F. D. Beall, and J. M. Buttle. 2007. "Scale-Dependence of Natural Variability of Flow Regimes in a Forested Landscape." *Water Resources Research* 43 (8). <https://doi.org/10.1029/2006WR005299>.

Santra, Priyabrata, and Bhabani Sankar Das. 2013. "Modeling Runoff from an Agricultural Watershed of Western Catchment of Chilika Lake through ArcSWAT." *Journal of Hydro-Environment Research* 7 (4): 261–69. <https://doi.org/10.1016/j.jher.2013.04.005>.

Scinocca, J. F., V. V. Kharin, Y. Jiao, M. W. Qian, M. Lazare, L. Solheim, G. M. Flato, S. Biner, M. Desgagne, and B. Dugas. 2016. "Coordinated Global and Regional Climate Modeling\*." *Journal of Climate* 29 (1): 17–35. <https://doi.org/10.1175/JCLI-D-15-0161.1>.

Setegn, Shimelis G., Ragahavan Srinivasan, and Bijan Dargahi. 2008. "Hydrological Modelling in the Lake Tana Basin, Ethiopia Using SWAT Model." *The Open Hydrology Journal* 2 (1): 49–62. <https://doi.org/10.2174/1874378100802010049>.

Sgro, Nicholas. 2016. "Formal Hypothesis Testing for Prospective Hydrological Model Improvements." UWSpace. <http://hdl.handle.net/10012/11042>.

Shooshtari, Sharif Joorabian, and Mehdi Gholamalifard. 2015. "Scenario-Based Land Cover Change Modeling and Its Implications for Landscape Pattern Analysis in the Neka Watershed, Iran." *Remote Sensing Applications: Society and Environment* 1 (July): 1–19. <https://doi.org/10.1016/j.rsase.2015.05.001>.

Smith, L. C. 2005. "Disappearing Arctic Lakes." *Science* 308 (5727): 1429–1429. <https://doi.org/10.1126/science.1108142>.

Snowdon, Andrew. 2010. "Improved Numerical Methods for Distributed Hydrological Models." UWSpace. <http://hdl.handle.net/10012/4963>.

———. 2016. "Upscaling of Coupled Models with Topography-Driven Surface-Water/Groundwater Interactions." UWSpace. <http://hdl.handle.net/10012/10489>.

Sood, Aditya, and Vladimir Smakhtin. 2015. "Global Hydrological Models: A Review." *Hydrological Sciences Journal* 60 (4): 549–65. <https://doi.org/10.1080/02626667.2014.950580>.

Taylor, Karl E., Ronald J. Stouffer, and Gerald A. Meehl. 2012a. “An Overview of CMIP5 and the Experiment Design.” *Bulletin of the American Meteorological Society* 93 (4): 485–98. <https://doi.org/10.1175/BAMS-D-11-00094.1>.

———. 2012b. “An Overview of CMIP5 and the Experiment Design.” *Bulletin of the American Meteorological Society* 93 (4): 485–98. <https://doi.org/10.1175/BAMS-D-11-00094.1>.

Tegegne, Getachew, Dong Kwan Park, and Young-Oh Kim. 2017. “Comparison of Hydrological Models for the Assessment of Water Resources in a Data-Scarce Region, the Upper Blue Nile River Basin.” *Journal of Hydrology: Regional Studies* 14 (December): 49–66. <https://doi.org/10.1016/j.ejrh.2017.10.002>.

Teng, Fei, Wenrui Huang, and Isaac Ginis. 2018. “Hydrological Modeling of Storm Runoff and Snowmelt in Taunton River Basin by Applications of HEC-HMS and PRMS Models.” *Natural Hazards* 91 (1): 179–99. <https://doi.org/10.1007/s11069-017-3121-y>.

Teng, Jin, Jai Vaze, Francis H. S. Chiew, Biao Wang, and Jean-Michel Perraud. 2012. “Estimating the Relative Uncertainties Sourced from GCMs and Hydrological Models in Modeling Climate Change Impact on Runoff.” *Journal of Hydrometeorology* 13 (1): 122–39. <https://doi.org/10.1175/JHM-D-11-058.1>.

Thompson, David W. J., Elizabeth A. Barnes, Clara Deser, William E. Foust, and Adam S. Phillips. 2015. “Quantifying the Role of Internal Climate Variability in Future Climate Trends.” *Journal of Climate* 28 (16): 6443–56. <https://doi.org/10.1175/JCLI-D-14-00830.1>.

Thompson, David W. J., John J. Kennedy, John M. Wallace, and Phil D. Jones. 2008. “A Large Discontinuity in the Mid-Twentieth Century in Observed Global-Mean Surface Temperature.” *Nature* 453 (7195): 646–49. <https://doi.org/10.1038/nature06982>.

Thompson, David W. J., John M. Wallace, Phil D. Jones, and John J. Kennedy. 2009. “Identifying Signatures of Natural Climate Variability in Time Series of Global-Mean Surface Temperature: Methodology and Insights.” *Journal of Climate* 22 (22): 6120–41. <https://doi.org/10.1175/2009JCLI3089.1>.

Ting, Mingfang, Yochanan Kushnir, Richard Seager, and Cuihua Li. 2009. “Forced and Internal Twentieth-Century SST Trends in the North Atlantic\*.” *Journal of Climate* 22 (6): 1469–81. <https://doi.org/10.1175/2008JCLI2561.1>.

Tolson, Bryan A., and Christine A. Shoemaker. 2007. “Dynamically Dimensioned Search Algorithm for Computationally Efficient Watershed Model Calibration.” *Water Resources Research* 43 (1). <https://doi.org/10.1029/2005WR004723>.

———. 2008. “Efficient Prediction Uncertainty Approximation in the Calibration of Environmental Simulation Models.” *Water Resources Research* 44 (4). <https://doi.org/10.1029/2007WR005869>.

Trenberth, Kevin E. 2018. “Climate Change Caused by Human Activities Is Happening and It Already Has Major Consequences.” *Journal of Energy & Natural Resources Law* 36 (4): 463–81. <https://doi.org/10.1080/02646811.2018.1450895>.

Vrugt, Jasper A., Hoshin V. Gupta, Willem Bouten, and Soroosh Sorooshian. 2003. “A Shuffled Complex Evolution Metropolis Algorithm for Optimization and Uncertainty Assessment of Hydrologic Model Parameters.” *Water Resources Research* 39 (8). <https://doi.org/10.1029/2002WR001642>.

Wallace, J. M., Q. Fu, B. V. Smoliak, P. Lin, and C. M. Johanson. 2012. “Simulated versus Observed Patterns of Warming over the Extratropical Northern Hemisphere Continents during the Cold Season.” *Proceedings of the National Academy of Sciences* 109 (36): 14337–42. <https://doi.org/10.1073/pnas.1204875109>.

Wallach, Daniel, Linda O. Mearns, Alex C. Ruane, Reimund P. Rötter, and Senthold Asseng. 2016. “Lessons from Climate Modeling on the Design and Use of Ensembles for Crop Modeling.” *Climatic Change* 139 (3–4): 551–64. <https://doi.org/10.1007/s10584-016-1803-1>.

Wallis, James R. 1965. “Multivariate Statistical Methods in Hydrology-A Comparison Using Data of Known Functional Relationship.” *Water Resources Research* 1 (4): 447–61. <https://doi.org/10.1029/WR001i004p00447>.

Ward, James D., Steve H. Mohr, Baden R. Myers, and Willem P. Nel. 2012. “High Estimates of Supply Constrained Emissions Scenarios for Long-Term Climate Risk Assessment.” *Energy Policy* 51 (December): 598–604. <https://doi.org/10.1016/j.enpol.2012.09.003>.

White, Kati L., and Indrajeet Chaubey. 2005. “Sensitivity Analysis, Calibration, And Validations For A Multisite And Multivariable Swat Model.” *Journal of the American Water Resources Association* 41 (5): 1077–89. <https://doi.org/10.1111/j.1752-1688.2005.tb03786.x>.

Wilks, DS. 1999. “Multisite Downscaling of Daily Precipitation with a Stochastic Weather Generator.” *Climate Research* 11: 125–36. <https://doi.org/10.3354/cr011125>.

Williams, Penny, Mericia Whitfield, Jeremy Biggs, Simon Bray, Gill Fox, Pascale Nicolet, and David Sear. 2004. “Comparative Biodiversity of Rivers, Streams, Ditches and Ponds in an Agricultural Landscape in Southern England.” *Biological Conservation* 115 (2): 329–41. [https://doi.org/10.1016/S0006-3207\(03\)00153-8](https://doi.org/10.1016/S0006-3207(03)00153-8).

Wittig, Rüdiger, Konstantin König, Marco Schmidt, and Jörg Szarzynski. 2007. “A Study of Climate Change and Anthropogenic Impacts in West Africa.” *Environmental Science and Pollution Research - International* 14 (3): 182–89. <https://doi.org/10.1065/espr2007.02.388>.

WMO. 2017. “WMO Statement on the State of the Global Climate in 2017.” <https://doi.org/978-92-63-11212-5>.

Wu, Kangsheng, and Carol A. Johnston. 2008. “Hydrologic Comparison between a Forested and a Wetland/Lake Dominated Watershed Using SWAT.” *Hydrological Processes* 22 (10): 1431–42. <https://doi.org/10.1002/hyp.6695>.

Wu, Zhaohua, Norden E. Huang, John M. Wallace, Brian V. Smoliak, and Xianyao Chen. 2011. “On the Time-Varying Trend in Global-Mean Surface Temperature.” *Climate Dynamics* 37 (3–4): 759–73. <https://doi.org/10.1007/s00382-011-1128-8>.

Xiang, Wei-Ning, and Keith C Clarke. 2003. “The Use of Scenarios in Land-Use Planning.” *Environment and Planning B: Planning and Design* 30 (6): 885–909. <https://doi.org/10.1068/b2945>.



Xu, Yangyang, and Aixue Hu. 2018. “How Would the Twenty-First-Century Warming Influence Pacific Decadal Variability and Its Connection to North American Rainfall: Assessment Based on a Revised Procedure for the IPO/PDO.” *Journal of Climate* 31 (4): 1547–63.

<https://doi.org/10.1175/JCLI-D-17-0319.1>.

Xu, Z. X., Y. N. Chen, and J. Y. Li. 2004. “Impact of Climate Change on Water Resources in the Tarim River Basin.” *Water Resources Management* 18 (5): 439–58.

<https://doi.org/10.1023/B:WARM.0000049142.95583.98>.

Yang, Yun, Shang-Ping Xie, Lixin Wu, Yu Kosaka, Ngar-Cheung Lau, and Gabriel A. Vecchi. 2015. “Seasonality and Predictability of the Indian Ocean Dipole Mode: ENSO Forcing and Internal Variability.” *Journal of Climate* 28 (20): 8021–36. <https://doi.org/10.1175/JCLI-D-15-0078.1>.

Zhang, Ling, Zhuotong Nan, Wenjun Yu, Yanbo Zhao, and Yi Xu. 2018. “Comparison of Baseline Period Choices for Separating Climate and Land Use/Land Cover Change Impacts on Watershed Hydrology Using Distributed Hydrological Models.” *Science of The Total Environment* 622–623 (May): 1016–28. <https://doi.org/10.1016/j.scitotenv.2017.12.055>.

Zhang, Rong, Thomas L. Delworth, Rowan Sutton, Daniel L. R. Hodson, Keith W. Dixon, Isaac M. Held, Yochanan Kushnir, et al. 2013. “Have Aerosols Caused the Observed Atlantic Multidecadal Variability?” *Journal of the Atmospheric Sciences* 70 (4): 1135–44.

<https://doi.org/10.1175/JAS-D-12-0331.1>.

Zhang Y, Najafi MR. Probabilistic Numerical Modeling of Compound Flooding Caused by Tropical Storm Matthew Over a Data-Scarce Coastal Environment. *Water Resources Research*. 2020 Oct;56(10):e2020WR028565.

Zhao, Ming, Isaac M. Held, Shian-Jiann Lin, and Gabriel A. Vecchi. 2009. “Simulations of Global Hurricane Climatology, Interannual Variability, and Response to Global Warming Using a 50-Km Resolution GCM.” *Journal of Climate* 22 (24): 6653–78.

<https://doi.org/10.1175/2009JCLI3049.1>.

## Chapter 3: Hydrological Modelling of the Batchawana Watershed

### 3.1 Introduction

Batchawana in central Ontario is a forested area with three main forest cover types: deciduous, coniferous and mixed of the two types of trees (assumed to be 50% for each tree type). Roots and stems of forest trees affect the infiltration, percolation and snow/water interception processes (Fekedulegn, Hicks, and Colbert 2003; Sun et al. 2002). Therefore, different tree types can affect the hydrological processes differently as they store different amounts of water/energy (Fahey and Jackson 1997; Zhou et al. 2002). Besides, leaf angle and size are the most important factors that affect precipitation interception. The bigger leaves with upper angles have larger precipitation interceptions (Holder and Gibbes 2017; Ginebra-Solanellas et al. 2020). A cone-shaped leaf with a lower angle toward the ground cannot be substantial water storage (Li et al. 2017; Bassette and Bussière 2008). In this study, we assess the effects of the two forest type changes on the regional hydrological processes of the Batchawana watershed.

Satellite imagery of the region shows that the area and types of land covers have changed over the last few decades. Besides, according to the intergovernmental panel on climate change, the fifth assessment (IPCC 2018) global warming is two (at some places, three) times more acute in Canadian lands than the global mean. Therefore, the high risk of temperature increases in Canada requires the analyses of subsequent impacts on regional hydrological characteristics. The land cover and climate change impacts on the hydrology of Batchawana are assessed in this study by setting up and calibrating the Raven hydrological framework (Craig et al. 2020). To verify whether a hydrological model can reliably simulate the hydrologic system, five evaluation criteria are considered. Based on the availability, reliability and quality of the data, the period of 1980 to 2011 is selected for modelling, one year is considered for spin-up, 2/3 of data allocated for calibration and 1/3 is assigned for validation. In this chapter, the study area is introduced and historical hydroclimatic data are discussed to show the trend of temperature, precipitation and streamflow. Then, data and their sources are described. Hydrological model structure, parameters, and other details of the Raven are discussed. Further, algorithms for hydrologic processes are important parts of the modelling and are described next. In the results section of this chapter, the performance of the model is evaluated and visualized.

### 3.2 Study Area

Batchawana is in Central Ontario, Canada, near Lake Superior and is classified under the Algoma forest management (Figure 3-1). Batchawana Bay, near the study area, is one of the tourism targets of Canadians. The reason to select this area is that it includes the Turkey Lake sub-watershed which has been extensively studied to investigate the influence of clear-cut activities etc. on the hydrology/environment of the system. Relevant studies and their results are thoroughly discussed in the literature review and background section. Indigenous tribes living in the area are Batchewana, Garden River, Hornepayne, Michipicoten, Missanabie, Mississauga, Sagamok, Serpent River, Thessalon (<https://batchewana.ca/>). Batchawana watershed (BW) has an area of ~ 1280 km<sup>2</sup> mainly covered by dense forests and encompasses numerous lakes. 11% of the basin is covered by lakes and water bodies. Therefore, in this study, we assess the role of lakes and their impacts on streamflow.

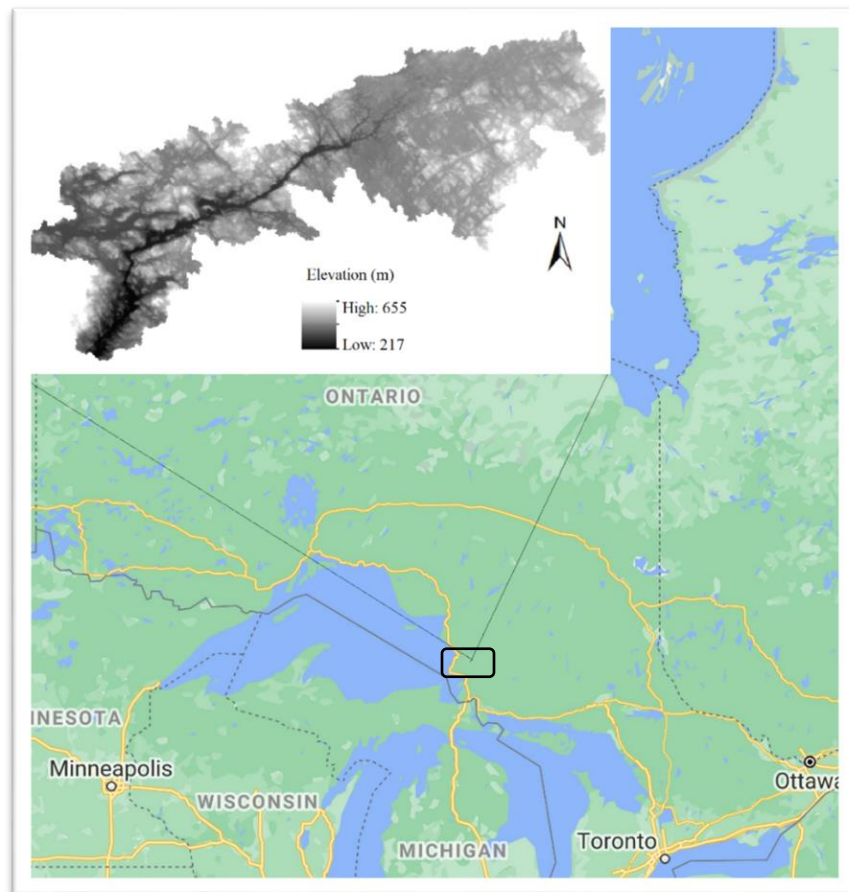


Figure 3- 1: The Batchawana Watershed in Central Ontario.

Based on the land cover image of Batchawana in 2016 (Figure 3-2), there are four considerable land cover types: water/lakes, mixed forests, Deciduous trees and Coniferous trees. Other types/classes cover a relatively negligible area. Coniferous trees are also known as evergreen trees maintain almost a constant leaf area index (LAI) during the year (Seo, Lee, and Choi 2018). LAI is the proportion of a unit area of ground covered by a one-sided green leaf. LAI's unit is  $m^2/m^2$  (it is dimensionless). Leaves of deciduous trees fall during autumn and lose almost all of their leaves reaching zero leaf area index (Hicks and Chabot 1985). The surficial geography of the basin shows that “bedrock” covers most of the area (Ontario Geological Survey, 2003). The elevation varies between 183 m at the watershed outlet and 651 m at the summit of the mountains. Landsat 8 product shows the elevation histogram where the highest frequency ranges between 430 to 470 meters (Figure 3-3).

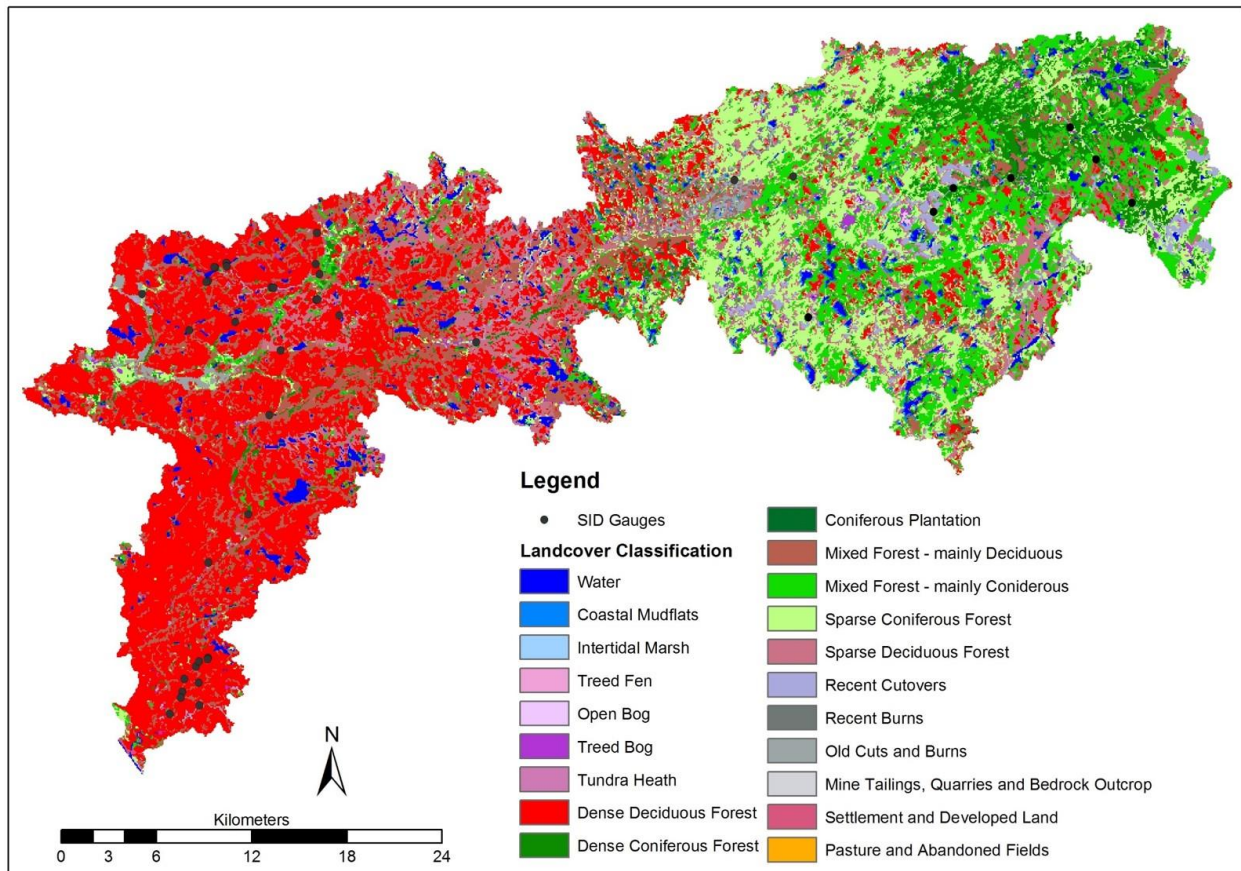


Figure 3- 2: Batchawana land cover map. The Eastern part is covered by mixed and coniferous trees while most of the western part is covered by deciduous trees.

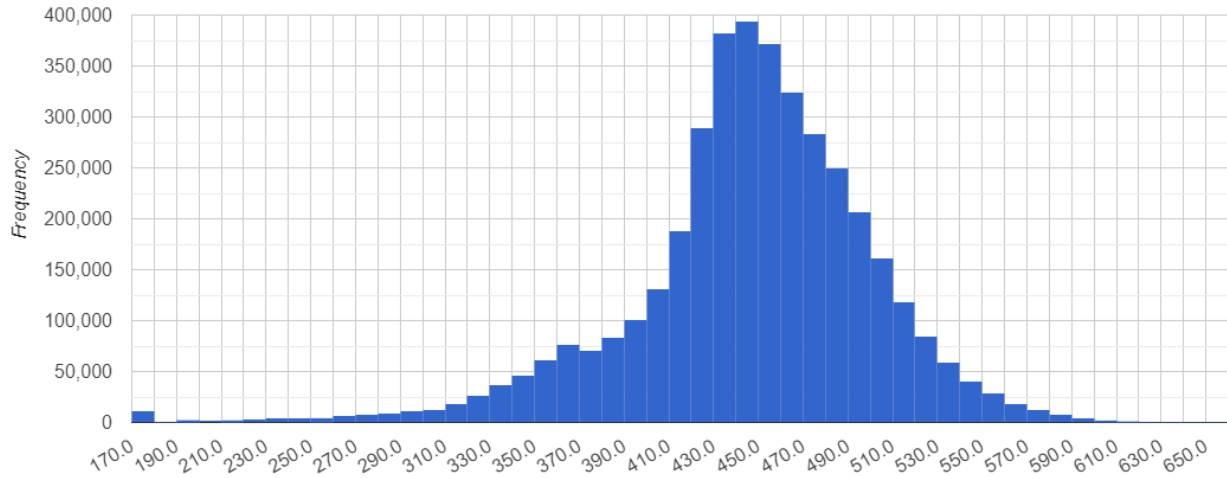


Figure 3- 3: Elevation distribution of the Batchawana watershed.

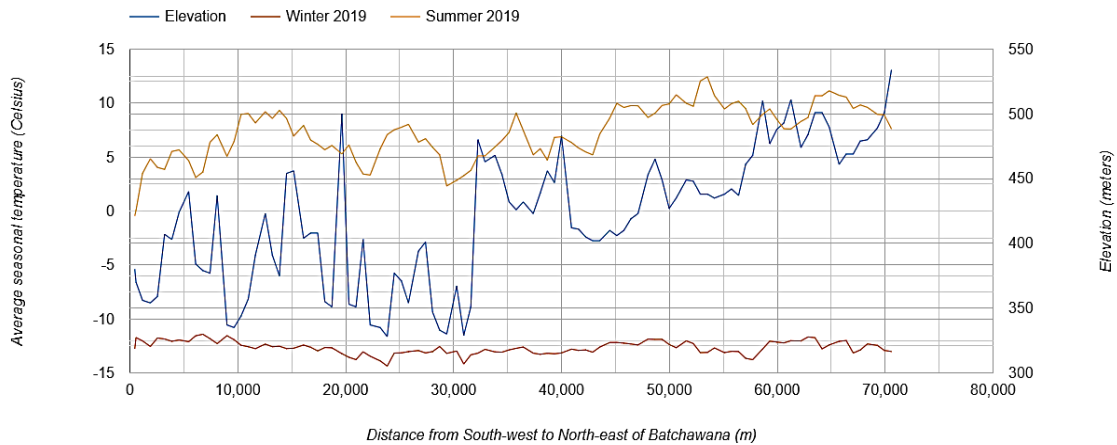


Figure 3- 4: Blue line is a direct line from the most western point to the most eastern point in the basin. The Redline shows the temperature variation of both points during the winter while the orange one shows the temperature of points for summer in a given year (2019)

Data for Batchawana provided by Environment and Climate Change Canada (Semkin et al. 2012) shows that the average annual temperature is  $+4.5^{\circ}\text{C}$  (varying between  $-32.5$  to  $+28.7$ ) from 1980 to 2011 (Figure 3- 5). Based on the annual max and mean temperature of the Batchawana Watershed, the air temperature of the area roughly has increased by  $1^{\circ}\text{C}$  to  $1.5^{\circ}\text{C}$ , respectively (Figure 3- 7). According to the streamflow time series (annual max and annual mean) shown in Figure 3- 6, the annual mean streamflow is decreasing from 1968 to 2011, while there is no trend for annual maximum streamflow. It indicates lower streamflow volumes are available to compare to previous years, while extreme events and floods occur at the same rate.

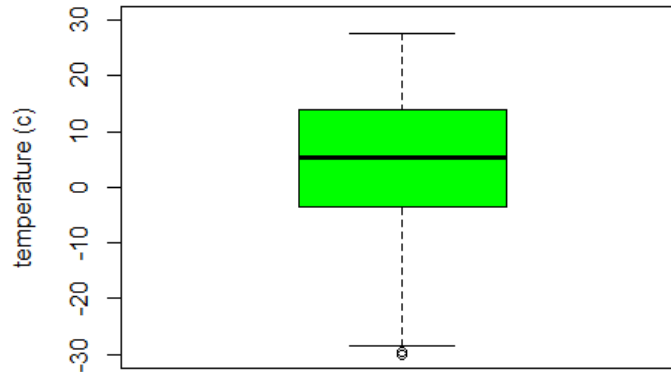


Figure 3- 5: Boxplot of the spatially averaged daily temperature for 1980-2011.

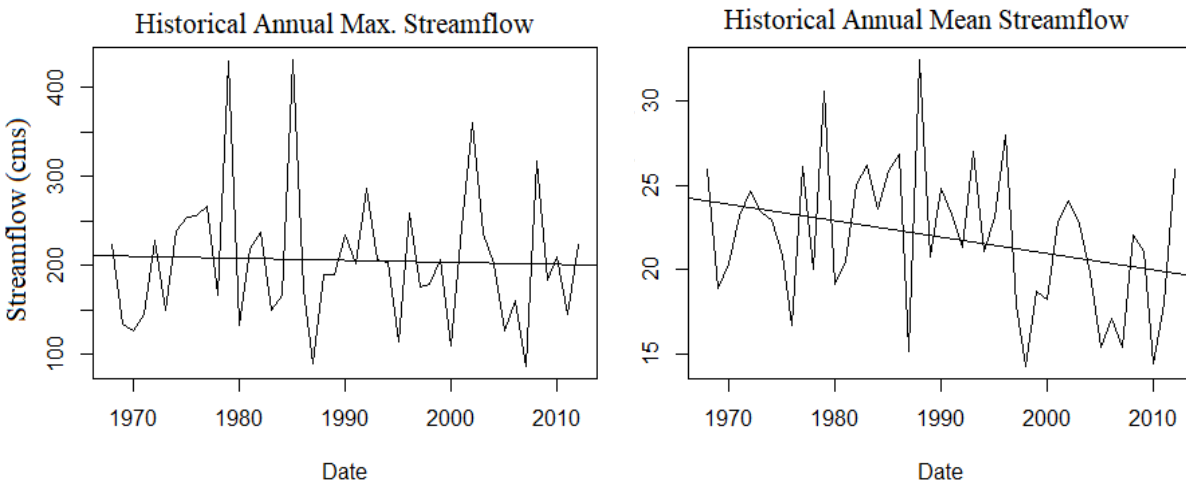


Figure 3- 6: Annual max. and mean streamflow for station # 02FB001 (Batchawana River near Batchawana)

Snow as an important hydrological component, plays a vital role in the Batchawana watershed. Snow falls due to lower atmosphere temperature (usually less than  $0^{\circ}$  C) and it can be stored in different compartments which will be melted and flowed (or stored as water) when the weather temperature increase. During the winter, snow falls and stays and builds snowpacks which start to meltdown at once and make a significant difference in the water quantity of regions. Snowmelt melting in early spring has major contributions to the streamflow. The annual accumulative snow

is shown in Figure 3- 8. The decreasing trend for this period is associated with temperature increases for the same timeframe.

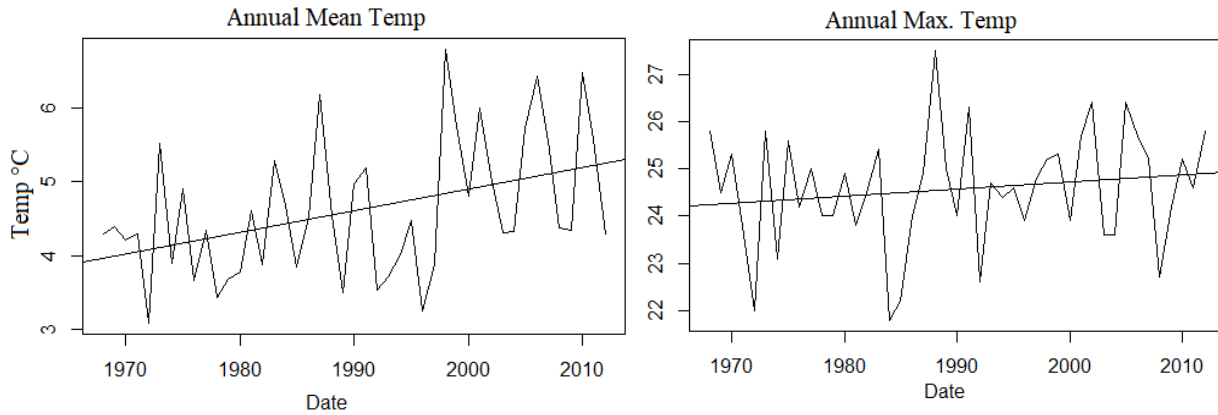


Figure 3- 7: Historical annual max. and mean air temperature

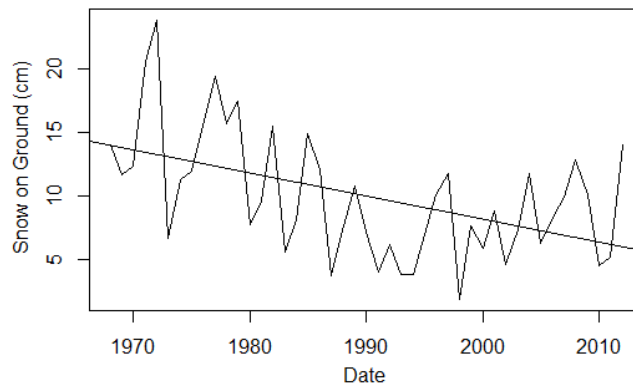


Figure 3- 8: Annual accumulative max snow over the Batchawana watershed

### 3.3 Hydrological Modelling

Raven is a text-based hydrological modelling framework introduced by Craig et al. (2020). Raven provides the flexibility to apply hydrological processes from different hydrological models such as the UBC Watershed Model, Environment Canada’s version of the HBV (HBV-EC), HMETs, MOHYSE and GR4J. The modeller is required to determine the watershed area, sub-basins and HRUs. The parameters corresponding to each class of HRU are then defined (see Table 3-2). For example, the leaf area index is a parameter for vegetation class that is related to the amount of intercepted rain/snow by leaves. Details of input files and assigned value of parameters for the Batchawana Watershed model are provided in the following sections.

### 3.3.1 Model Setup

In this study, the model simulations are performed at a daily time step from the first day of 1980 to the end of 2011. According to Global Soil Data for Earth (GSDE), there is only one soil type available for the region. Three layers of the soil are considered for the model simulations. The hydrologic processes of a model show the water/energy balance through the storages and represent water flows between different storages (Figure 3- 9).

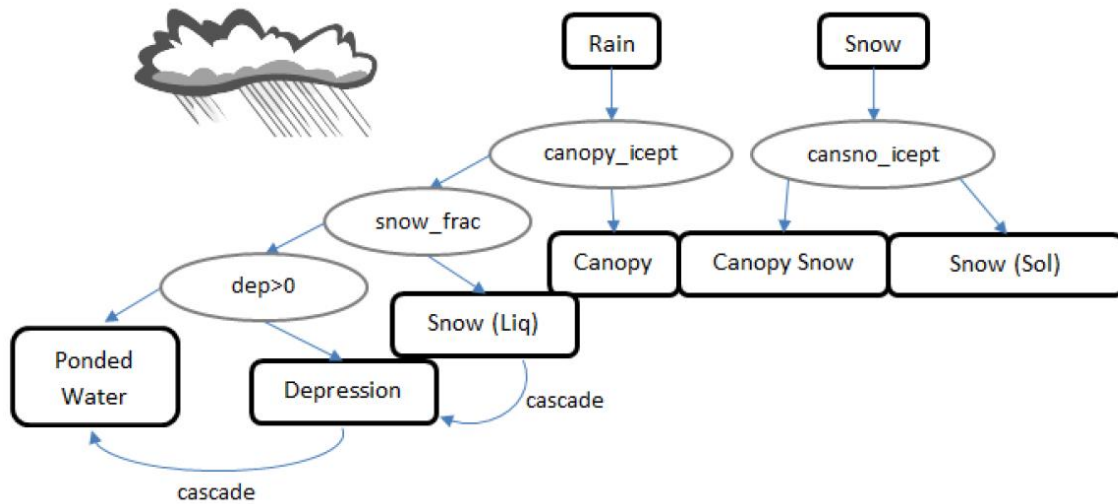


Figure 3- 9: Hydrological processes represented in the Raven hydrological framework.

Precipitation can be stored in soil, canopy, ponds or depressions. Each water storage has a specified capacity and water flows after reaching the maximum capacity

Snow is intercepted by the canopy or falls on the ground. By increases in the temperature above a threshold, it starts to melt and generates flows to fill the storages; i.e. surface water, groundwater. Rain can be intercepted by the canopy or directly fall on lakes or ground. When the precipitation fall in the liquid form it is stored or flows between storages. The representation of the hydrologic processes of the Batchawana watershed is shown in Table 3-1. Soil [0] refers to the surface layer of the soil, soil [1] and soil [2] represent the lower layers of the soil. The algorithms corresponding to the hydrological processes are described in the table.

Table 3-1: Hydrologic processes represented by Raven for the Batchawana watershed.

Hydrologic process	From	To	Algorithm *
--------------------	------	----	-------------



---

Precipitation	Atmosphere	Multiple	Raven's
Infiltration	Surface water/soil[0]	soil[1] and soil[2]	INF_PARTITION
Interflows	soil[0]/soil [1]	soil[1]/soil[2]/surface water	INTERFLOW_PRMS
Baseflow	soil[1] / soil[2]	Surface water	BASE_POWER_LAW
Percolation	soil[0] / soil [1]	soil[1] / soil[2]	PERC_GAWSER
Soil evaporation	soil[0]	Atmosphere	SOILEVAP_ALL
Canopy evaporation	Canopy	Atmosphere	CANEVP_MAXIMUM
Canopy snow evaporation	Canopy snow	Atmosphere	CANEVP_MAXIMUM
Abstraction	Ponded water	Depression	ABST_FILL
Sublimation	Snow	Atmosphere	SUBLIM_KUZMIN
Lake release	Lake storage	Surface water	LAKEREL_LINEAR
Canopy drip	Canopy	ponded water	CANDRIP_RUTTER

---

\*Algorithms are discussed and introduced in the upcoming section.

Multiple algorithms are available within Raven to represent the hydrologic processes, which provides the flexibility to use the most compatible and suitable representation. Table 1 of Craig et al. 2020, gives comprehensive information about all possible algorithms for the hydrological process.

INF\_PARTITION stands for the partition coefficient algorithm for infiltration which is a simple linear relation between participation and infiltration. In Equation 3-1  $M_{inf}$  represents the

infiltration rate (mm/d), R is the rain/snow ratio and P is the partition coefficient value assigned in the land use parameters section.

$$M_{inf} = R \times (1 - P) \quad \text{Equation 3-1}$$

Interflow refers to the lateral subsurface flow of water between the surface soil layers. INTERFLOW\_PRMS stands for precipitation run-off modelling system (PRMS) interflow algorithms (F. Teng et al. 2017). Interflow is a portion of saturated soil moisture that flows between layers and surface water. In Equation 3-2,  $M_{inter}$  is the interflow rate,  $M_{max}$  is the maximum interflow rate of the soil layers, and  $\phi_{soil}$  is the amount of moisture in draining soil and  $\phi_{max}$  and  $\phi_{tens}$  are the maximum tension storage and maximum soil storage [mm], respectively.

$$M_{inter} = M_{max} \times \left( \frac{\phi_{soil} - \phi_{tens}}{\phi_{max} - \phi_{tens}} \right) \quad \text{Equation 3-2}$$

Baseflow occurs between the deeper soil layers or aquifers and surface water due to the head gradient between the saturated soil layer and surface water. Linear and non-linear algorithms are available for baseflow calculations. BASE\_POWER\_LAW in Raven represents a common non-linear approach in the conceptual hydrological model. As Equation 3-3 shows, baseflow is a nonlinear proportion of the storage where  $M_{base}$  [mm/d] is the baseflow rate,  $\phi_{soil}^n$  is the water storage of soil layer/aquifer and n is a specified value for soil parameters known as BASEFLOW\_N. k [1/d] is a specified parameter for the baseflow coefficient.

$$M_{base} = K \phi_{soil}^n \quad \text{Equation 3-3}$$

Percolation is the vertical (downward) movement of water through different layers of the soil. The Guelph All-Weather Sequential-Events Runoff or GAWSER (Meyer, Brouwers, and Martin 2014) method for percolation is considered in BW hydrological model. Equation 3-4 shows the mathematical form for percolation:  $M_{perc}$  is the percolation rate [mm/d] and  $M_{max}$  is the maximum percolation rate [mm/d].  $\phi_{soil}$  is the soil moisture content and  $\phi_{max}$  [mm] and  $\phi_{fc}$  [mm] are the maximum moisture amount in the soil layer and storage capacity of the soil layer at field capacity, respectively.

$$M_{perc} = M_{max} \times \left( \frac{\phi_{soil} - \phi_{fc}}{\phi_{max} - \phi_{fc}} \right) \quad \text{Equation 3-4}$$

Evaporation occurs from the surface layer's storage, i.e. from soil [0], to the atmosphere. Equation 3-5 represents the PET estimation.  $\Delta$  is the slope of the saturation vapour pressure-temperature curve [kPa/ °C],  $\gamma$  is the psychometric constant, and  $S_n$  is the net incoming solar radiation [MJ/m<sup>2</sup>/d]. Raven calculates all parameters for PET estimation based on the temperature data. Further details are discussed in Bormann (2011).

$$PET = 14.57 \left( \frac{\Delta}{\Delta + \gamma} \right) \times \frac{S_n}{58.5} - 0.12 \quad \text{Equation 3-5}$$

Similar to evaporation from the soil, canopy evaporation transforms water (in both snow and rain forms) from canopy storage to the atmosphere. CANEVP\_MAXIMUM is assigned for estimating the canopy evaporation based on Equation 3-6:

$$M_{evap} = PET \cdot F_c \cdot (1 - f_s) \quad \text{Equation 3-6}$$

$M_{evap}$  [mm] is the maximum canopy evaporation, PET is described in the previous equation,  $F_c$  is the forest cover percentage of an HRU and  $f_s$  is the forest sparseness percentage of the same HRU.

In Raven, swales, puddles and ponds are represented by DEPRESSION. Abstraction is the process of moving water from ponded water storage to depression. This process continues until the maximum depression capacity of the HRUs is reached. DEP\_MAX is the maximum depression [mm] capacity of the land use parameters.

Sublimation is the process of directly transforming the snow to vapour skipping the liquid phase. Based on one of the oldest sublimation relationships (Kuzmin 1972, Kuchment and Gelfan 1996) the sublimation rate [mm/d] is estimated by:

$$M_{subl} = (0.18 + 0.098 \cdot v_{ave}) \cdot (P_{sat} - P_{vap}) \quad \text{Equation 3-7}$$

$v_{ave}$  is the wind velocity [m/s] at 10 m elevation,  $P_{sat}$  is the saturated vapour pressure [mb] and  $P_{vap}$  is the vapour pressure [mb].

A considerable proportion of surface runoff is from lake release (Zajac et al. 2017). For the hydrological model of the Batchawana watershed, the presence of lake storage is vital. Lakes' impacts on high and low flows will be discussed thoroughly in Effects of Lake section. In this model, LAKEREL\_LINEAR is selected as the estimation algorithm of lake release to surface water.

In Equation 3-8,  $M_{irel}$  [mm/d] is the lake release,  $K_{irel}$  [1/d] is the linear storage coefficient (which is a land use parameter) and  $\emptyset_{lake}$  [mm] is the lake net storage.

$$M_{irel} = K_{irel} \cdot \emptyset_{lake} \quad \text{Equation 3-8}$$

Canopy drip is the movement of intercepted rain from leaves to ponded water or ground. The dripped water can infiltrate, percolate, generate runoff or depressions after being stored in ponded water storage. Based on the CANDRIP\_RUTTER, water drips from leaves to the ground whenever it fills the maximum storage capacity [mm] of the vegetation type.

### 3.3.2 Data

Required data are obtained from Environment and Climate Change Canada (ECCC), the Ontario government's website and Satellite imagery (i.e. MODIS and Landsat series). ArcGIS 10.3, R, python and Java, Tableau and ArcSWAT are used to process the data. Generally, hydrological models, including Raven, require data for soil characteristics, streamflow records, meteorological data, the morphology of the watershed, vegetation types, land use classes, among others (Silberstein 2006; Bergström 1991).

Daily natural (non-regulated) flow data at Batchawana River near Batchawana (Station #02BF001) are provided by Environment and Climate Change Canada (ECCC) for 1968 to 2019 without missing records. Maximum, minimum and average daily temperature and daily precipitation data are provided by ECCC for Turkey Lake. After removing days with missing data, a dataset from 1980 to 2011 is considered for modelling purposes. Figure 3-4 shows that temperature does not vary dramatically across the region. The Global Soil Data for Earth (GSDE) is considered to represent the BW's soil type (Shangguan et al. 2014).

Digital Elevation Model (DEM) at 30 m vertical spatial resolution is extracted from Ontario GeoHub (2020) for southern Ontario which 30 m is commonly considered a moderate resolution for hydrological modelling (Fonji and Taff 2014). Information about the soil texture, biodiversity, land use and forest management is acquired from Scholars GeoPortal (2020). Using the DEM file and the "raster" and "terrain" R packages (Hijmans & van Etten, 2012) the slope is calculated. The land cover map of the basin is acquired from satellite imagery (Landsat for 2011) and its accuracy is controlled by data from NRCan and OFAT (Ontario Flow Assessment Tool, 2020). In further detail, products of Landsat satellites according to the aimed year is downloaded for days with than

10% cloud cover and no rain/snow incidents during the summer. Then, the ArcGIS land cover map extraction tool is trained and supervised to run the satellite products and produce the land cover maps. Every specific land cover type possesses a specific wavelength wherein ArcGIS by defining and training a few dots for each land cover type, the whole land cover map will be produced. The step by step process is thoroughly explained in ([www.esri.com](http://www.esri.com))

Percentages of the sand, clay, silt and organic contents along with the depth of each layer are quantified by GSDE. Vegetation is divided into three distinct classes: deciduous forest, evergreen forest or coniferous trees, mixed forest. The maximum height [m] of each vegetation class, maximum leaf area index (LAI) and maximum leaf conductance [mm/s] are specified based on the advice from NRCan scientists and the literature review about the watershed. Also, the seasonal LAI of each vegetation class is quantified based on the seasonal changes of each canopy. “Forest” is the only land-use class for this basin. Global parameters are the same for all water storages. The following parameters are required for the hydrological model structure representing the Batchawana watershed (Table 3-2):

Table 3-2: Storages, classes and parameters for Raven’s model for the Batchawana watershed.

Water Storages	soil	Vegetation	Land use	Global parameters
Classes for each storage	Soil[0]	Mixed forest		
	Soil[1]	Deciduous forest	Forest	NA
	Soil[2]	Coniferous forest		
Parameters of each class	Porosity	Extinction coefficient	The fraction of land covered by vegetation canopy	Rain/snow halfway transition temperature
	HBV $\beta$			
	Baseflow coefficient	The ratio of stem area index to height	Maximum snowmelt factor used in degree-day models	Water saturation
	Baseflow N			Fraction of snow
	Max interflow rate	Percentage of snow		Default snow temperature
	Field capacity			

	Hygroscopic minimum saturation	intercepted (maximum)	Degree day reference (freezing) temperature	Avg annual snow as SWE
	Max percolation rate	Percentage of rain intercepted (maximum)	Minimum snowmelt factor used in degree-day models	Range of rain-snow transition zone
	Max Baseflow rate	Maximum canopy storage capacity	Maximum refreeze factor used in degree-day models	
		Maximum canopy snow (as SWE) storage capacity	HBV snowmelt forest correction	
			Partitioning coefficient	
			The fraction of PET to apply to lake evaporation	
			Outflow rate with full depression storage	
			Linear storage Coefficient	

### 3.3.3 Basin Information

To delineate the basin, sub-basins and HRUs, the ArcSWAT tool of ArcMap 10.2 is applied using the land cover (2011), soil, land use and slope maps of the region (<https://swat.tamu.edu/>). Because the only natural gauge (other than the main gauge; 02FB001) covers a small area of 10 km<sup>2</sup>, one sub-basin is considered including 9 HRUs (Table 3-3). Six hydrologic and morphologic features are attributed to the HRUs including area, elevation, land use class, vegetation type, soil class and

slope degree. The areas of the hydrologic response units vary between 40 to 315 km<sup>2</sup>. The mean elevations of HRUs vary between 270 to 560 m. As discussed before, one soil type is considered for the domain, except for the lakes. Similarly, the forest is the constant land-use class for all HRUs other than the lake HRU. Mixed forests, deciduous and coniferous forests are the three mainland cover classes. The average slope of the HRUs varies between 1.4 to 2.5 degrees. The slope for the lake HRU is 0.

Table 3-3: Delineated HRUs based on land cover, DEM, soil and slope maps using ArcSWAT.

HRU #	Area (km <sup>2</sup> )	Elevation (m)	Land use	Vegetation	Soil	Slope (degrees)
1	215	350	forest	Deciduous	Type A	1.5
2	40	300	forest	Deciduous	Type A	2.5
3	315	400	forest	Mixed	Type A	1.4
4	104	370	forest	Mixed	Type A	2.5
5	124	550	forest	Coniferous	Type A	2.0
6	144	560	forest	Coniferous	Type A	2.5
7	98	340	forest	Mixed	Type A	2.0
8	89	270	forest	Mixed	Type A	1.5
9	150	270	NA	NA	Lake	0

### 3.3.4 Calibration and Validation of the Model

Several parameters in the model are not accurately measured and should be calibrated/optimized so that the simulations closely follow the observed data (Refsgaard and Storm 1990). Manual

calibration is inefficient and time-consuming, while automatic calibration uses computational capacities to optimize the selected parameters (Götzinger and Bárdossy 2008).

OSTRICH (Mattot, LS 2017) is applied for automatic calibration of the Raven hydrological model. OSTRICH is a model-independent optimization tool, which supports several calibration algorithms including Gauss-Marquardt-Levenberg (Levenberg 1944), Particle Swarm Optimization (Eberhart and Yuhui Shi, 2001), Binary-coded Genetic Algorithm (Yoon and Shoemaker 2001) and Shuffled Complex Evolution or SCE (Duan, Gupta, and Sorooshian 1993).

The dynamically dimensioned search algorithm (DDS; Tolson and Shoemaker 2007) is selected to calibrate the model and infer 16 parameters. After selecting the ideal model structure within the Raven hydrological framework, a list of necessary parameters regarding the selected algorithms and structures was acquired. A few of the necessary parameters should be calculated based on the available data/map. For instance, forest coverage is calculated by dividing the number of cells containing forest by the total number of cells of the region in the satellite data using the ArcGIS software. A few other parameters are gathered from reliable and earlier cited literature about the target watershed. The rest of the necessary parameters are selected to be calibrated. Also, the manual file of the Raven is introducing the recommended parameters for the calibration.

DDS is found to be a robust optimization algorithm in previous studies (Khedr, Tolson, and Ziemann 2015; Lespinas, Dastoor, and Fortin 2018; Becker et al. 2019; J. H. Lee et al. 2020; Samimi et al. 2020; J. M. Leach and Coulibaly 2020; Dembélé et al. 2020). It has outperformed several other optimization algorithms in several comparative analyses for highly complex problems (Huang et al. 2014; Arsenault et al. 2014; Tolson and Shoemaker 2007). DDS is a stochastic single-solution heuristic algorithm that searches for the global optimum point.

Table 3-4 represents the calibration parameters, their calibration range and the estimated value of each parameter. Parameters are repeated for different classes of storage, for example, rain interception percentage is calibrated for all four different vegetation types. The calibrated values of the vegetation parameters are relatively more varied as their characteristics differ dramatically based on their leaves' types.



Table 3-4: Calibrated parameters of Raven’s hydrological modelling framework for the Batchawana watershed. 16 parameters from different storages are calibrated. Their calibration range and the final estimated values are provided.

Class	Parameter	unit	Range		Calibrated value
			From	To	
Land Use	Imperviousness	[0..1]	0	1	0.03
	Forest sparseness	[0..1]	0	1	0.12
	Forest PET correction	-	0.1	1	0.76
Soil	HBV $\beta$	-	1	7	4.51
	Baseflow N	-	1.0	10.0	2.97
	Max interflow rate	mm/d	100	1000	480.02
	Field capacity	[0..1]	0.0	1.0	0.57
	Sat wilt	[0..1]	0.0	0.9	0.51
	Porosity	[0..1]	0.1	0.6	0.4
Vegetation	Max Baseflow rate	mm/d	0.001	1000	385.69
	Max snow capacity	mm	100	10000	1269.35
	Rain intercept %	-	0.02	0.2	0.09
	Snow intercept %	-	0.02	0.2	0.13
Global	Rain/snow temperature	°C	-1.0	1.0	0.01
	Snow temperature	°C	-2.0	0.0	-1.09
	Rain/snow delta	°C	0	4	2.59

Three distinct time frames are considered for modelling: spin up, calibration and validation. During the spin-up period, also called warm-up, the model reaches an equilibrium between different storages/states. Model output for the spin-up period is often unrealistic and misleading as the initial condition for most models is unknown or zero (Rahman and Lu 2015). Considering BW as a snow-dominated watershed, allocating 365 running steps (1 year) is reasonable (Haghnegahdar et al. 2015; Seck, Welty, and Maxwell 2015). The model is driven from 1980 to the end of 2011, with the first year of the simulations considered as the spin-up period (and removed from model evaluations). The calibration budget is the time frame that is allocated to train the model (Jain and Srinivasulu 2008). Based on literature e.g. (K. Ajami et al. 2004; Haghnegahdar et al. 2015), two-

third of the running period is allocated for calibration, including data from 1 January 1981 to 1 September 2001 equal to 7549 successive days. The period of 2 September 2001 to the end of 2011, 3774 successive days, is considered as the validation period.

### 3.3.5 Modelling Workflow and Evaluation

The input data should be changed to the text format as Raven is a text-based model. The land cover map of 2011 is selected for the calibrated model (base model). Four land cover types are detectable using remote sensing techniques. For land-use data, there is only one type; forest. To discretize the hydrologic response units, ArcSWAT, nested in ArcGIS, is used. DEM, land cover, land use and soil types maps are introduced to ArcSWAT to determine the HRUs of BW (Moriasi et al. 2019; Pignotti et al. 2017; Teshager et al. 2016). All HRUs with their specific information on the landcover type, land use type, soil type, latitude and longitude are included in the model. The meteorological station and flow measuring station's locations are added. In the final step of the model setup, simulated and observed hydrographs are compared to evaluate the model's capability to represent the watershed's characteristics.

## 3.4 Results

The results of Raven for calibration and validation periods are discussed in this section. RavenR package developed by Robert Chlumsky (2020), Raven's visualization tool (<http://raven.uwaterloo.ca/hydroglyph/>), Tableau, and Excel are used to visualize the results. The performance evaluations for calibration and validation periods are shown in Table 3-5. Simulated and observed values at the daily time step for the validation period are represented in Figure 3- 10.

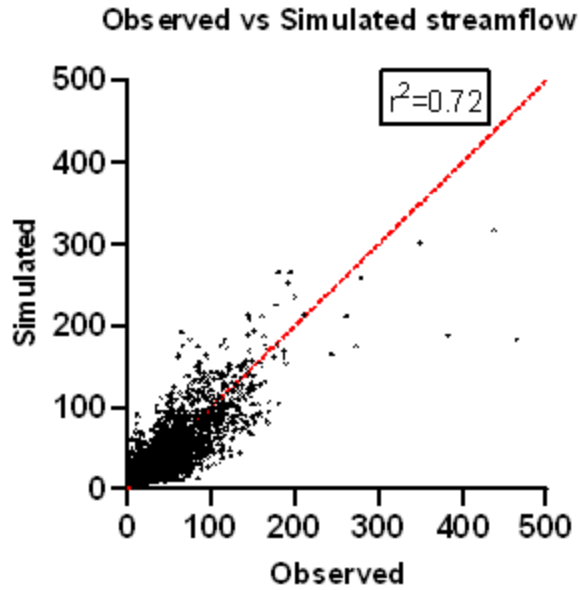


Figure 3- 10: Simulated and observed streamflow during the validation period

Table 3-5: Performance evaluation of the Raven hydrological model simulations at daily time steps for the calibration and validation periods

	KGE	NSE	Log-NSE	PBIAS	R <sup>2</sup>
Calibration	0.81	0.73	0.63	-1.63	0.74
Validation	0.76	0.71	0.58	0.78	0.72

Daily maximum and minimum temperature are represented in Figure 3- 11 wherein most of the places in the northern areas, the temperature starts to increase from March to late July and then a decreasing trend happens from August to late February. March, April and May are defined as the spring season. June, July and August are the summer months. September, October and November are Fall/Autumn and finally December, January and February are winter months.

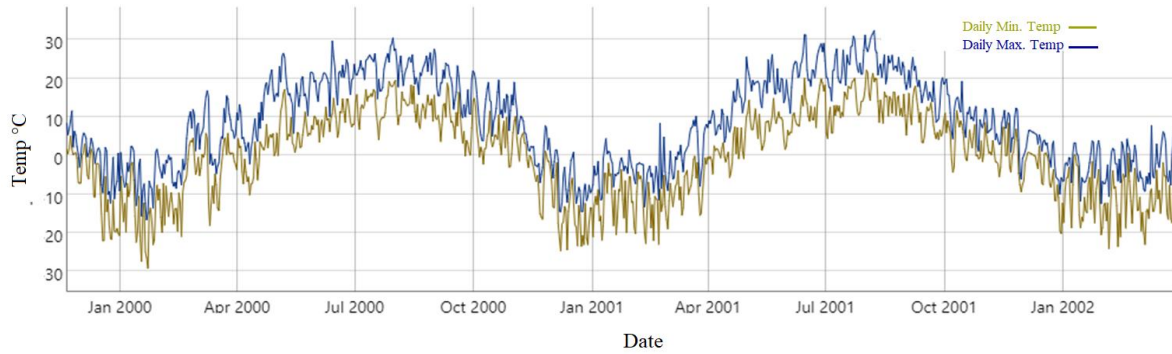


Figure 3- 11: Maximum and minimum daily temperature variations at the Batchawana watershed

Precipitation can fall in snow, rain, or mixed regimes (Bourgouin 2000). Raven considers a temperature threshold to identify the precipitation regime. Figure 3- 12 shows when snowfall and when rainfall is occurring. Blue lines are representing the rainfall events. It can rain any time in a year cycle, but snow usually happens from mid-fall to mid-spring period with a higher frequency during the winter.

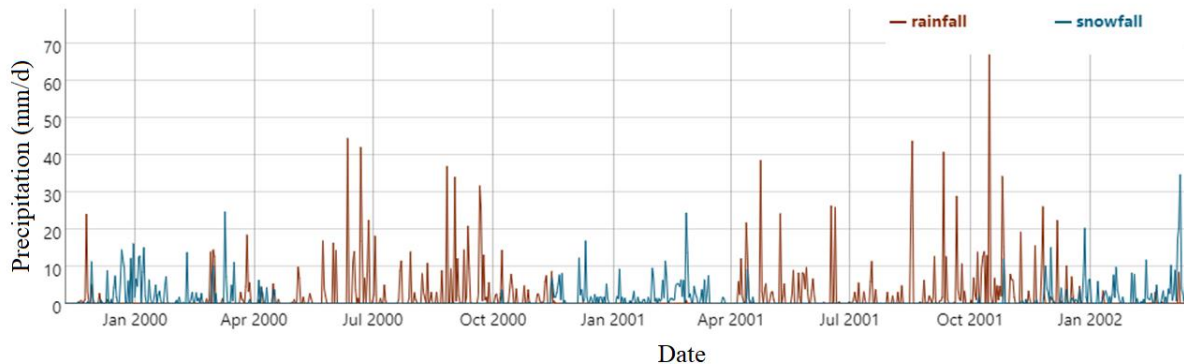


Figure 3- 12: Daily values for rainfall and snow water equivalent (SWE) over the Batchawana watershed

Figure 3- 13 is a two-year random period representing the PET. By increasing the temperature and changing the season to a warmer one, potential evapotranspiration (PET) is increasing accordingly. PET spikes by starting the summer season in June. Potential evapotranspiration is increasing during the warm season and declines during the cold seasons.

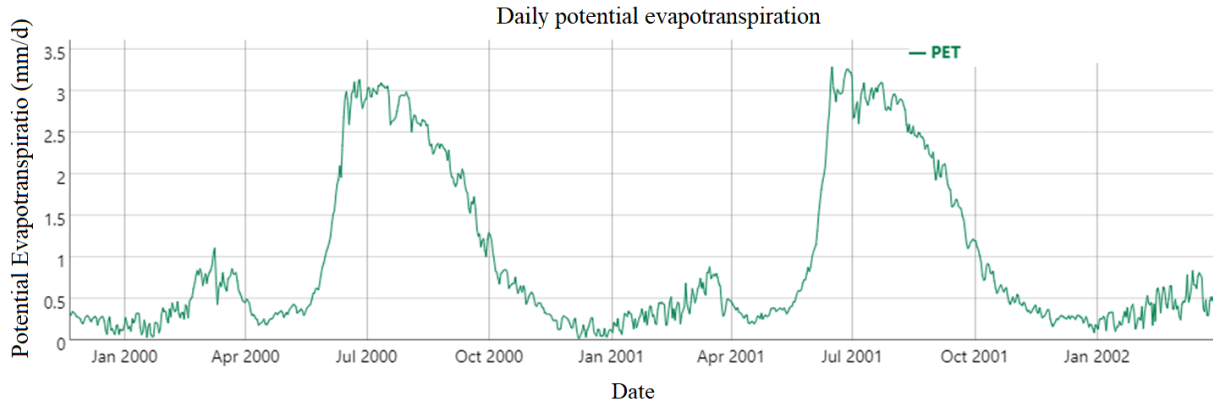


Figure 3- 13: Daily potential evapotranspiration based on daily precipitation and temperature.

The simulated and observed streamflow of the model is illustrated in Figure 3- 14. Both calibration and validation periods are divided by a black vertical line to show the model performance during these periods. It is understandable from the figure and evaluation criteria that model performance is reasonable, and it follows the overall trends of the observed (reality) streamflow.

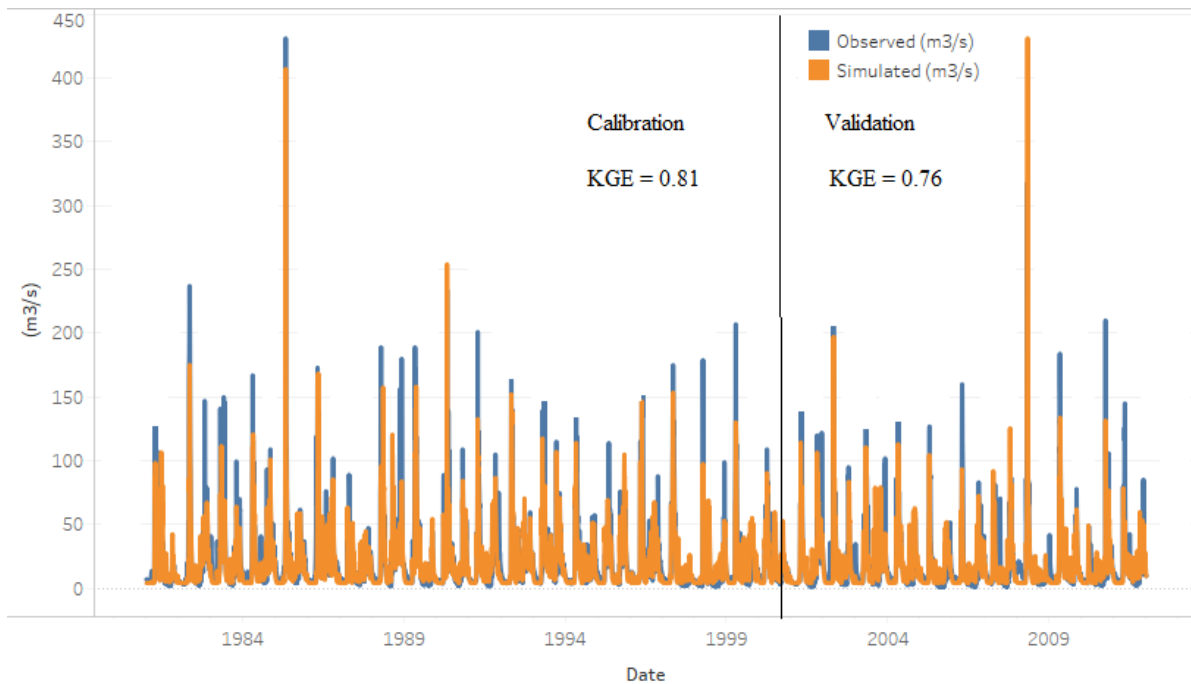


Figure 3- 14: Observed and simulated daily streamflow during the calibration (1981-2001) and validation (2001-2011) periods for Batchawana River Station.

To give detailed with higher resolution information on the model’s performance, a three-year timeframe from 2003 to 2006 (selected randomly) at the daily time step is represented in Figure 3 -15. It can be driven that the darker blue line (simulated streamflow) is following the overall trends

of the lighter line. It means the structure and outcome of the model are logical and it follows the natural hydrological system of the watershed. The timing of the simulation to react to the incidents is almost precise. However, in two high flow incidents model fails to simulate accurately, but in other high flow occurrences model is simulating with a slight difference. Its performance for low flows is also reasonable. Almost the same quality of simulation is happening for other time frames as well. Looking at Figure 3- 15 annual maximum streamflow of every year occurs during the snow melting period. In this region of study, March, April and May (spring) are the snow-melting periods.

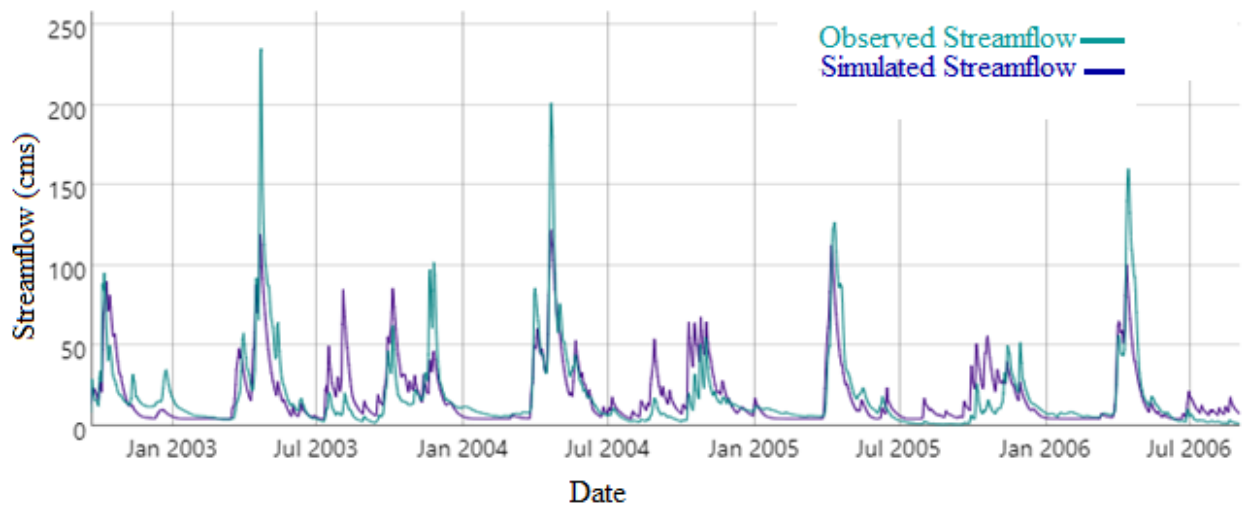


Figure 3- 15: Comparison between daily observed and simulated streamflow at the Batchawana station for three years

Figure 3- 16 shows the monthly average observed and simulated streamflow for calibration and validation periods. The same as Figure 3- 14, this figure also indicates that the model can reasonably follow the ups and downs of the observed data.

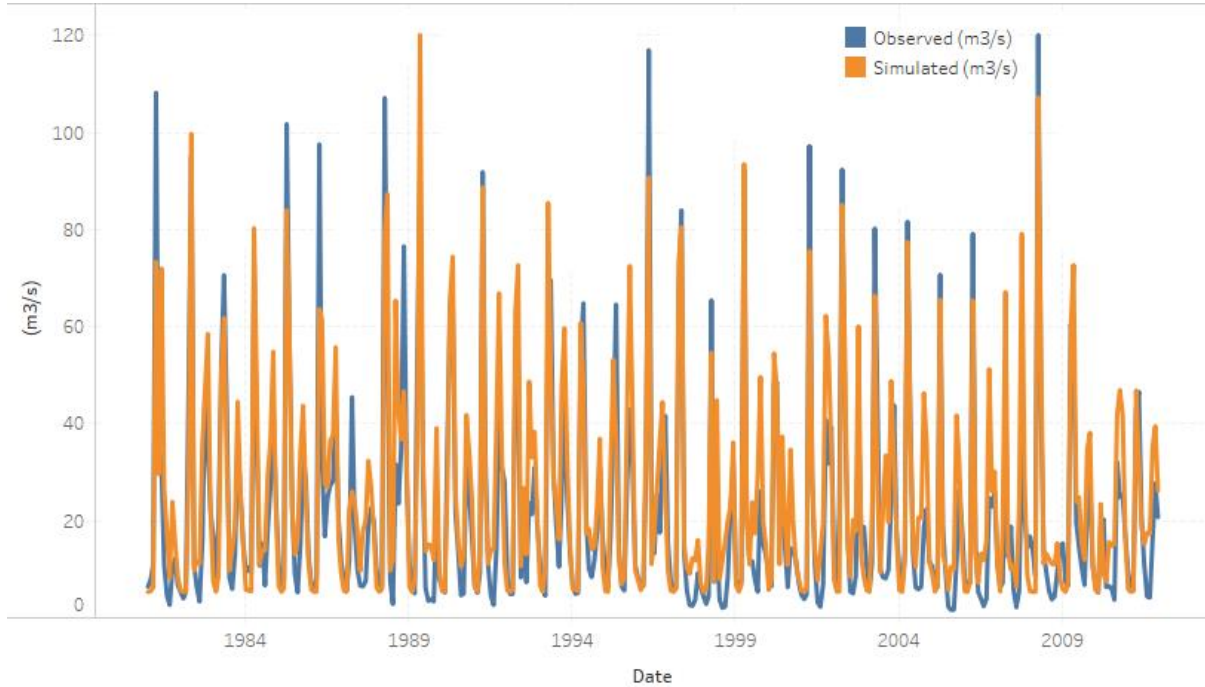


Figure 3- 16: Monthly average observed and simulated streamflow for calibration and validation periods

To zoom out more and show the model's capability in annual timeframes Figure 3- 17 is generated. This figure shows the annual mean (Figure 3-17b) and annual maximum (Figure 3-17a) simulated and observed streamflow, respectively. The model can follow the annual mean streamflow with a slight error for the entire period of the study while capturing the annual maximum streamflow of the region is a drawback of the model. However, it is notable that model efficacy is evaluated under the daily time-steps where the desired results are acquired. During the process of the model set up, it would be possible to set up a model with a better capability in capturing annual maximum, but due to the importance of low flows for this region, it has been decided to set up a model with reasonable ability in both high and low flow simulation.



Figure 3- 17: Annual mean (a) and max (b) of observed and simulated streamflow values for 30 years from 1981 to 2011.

### 3.5 Conclusions

In this chapter, we introduce the Batchawana watershed, data sources and hydrological model setup and calibration. Raven, as a robust and flexible hydrological modelling framework, is selected to simulate the hydrology of the Batchawana watershed for 1981 to 2011 appointing 1 sub-basin and 9 hydrologic response units. The Ostrich optimization tool is applied to calibrate the semi-distributed model based on the Dynamically dimension search (DDS) method. 2/3 of the data (1981 to 2001) used for calibration and the rest was used for the validation process. We assess the performance of the model using Nash-Sutcliff, Kling-Gupta,  $R^2$ , bias percentage and Logarithm of Nash-Sutcliff. Results show that the model performance is satisfactory with KGE = 0.79 (0.78), NSE= 0.73 (0.71), Log-NSE= 0.63 (0.58), PBIAS = -1.63% (0.78%) and  $R^2$ = 0.74 (0.72) for calibration (validation) periods. KGE, NSE and  $R^2$  show that simulated streamflow follows the overall variations of the observations. Log-NSE is an evaluation criterion that shows whether the model can capture the low flows. Results show that low flows are well represented in the calibrated model. There is a low negative bias percentage for both calibration and validation periods. The model simulates the hydrological components of the region well including the representation of snow accumulation and snowmelt timing.

The annual mean of the observed streamflow is well-represented in the model, however annual max flows are under-estimated in some years which might be associated with the representation of lakes. The model performance is better during spring and winter compared to fall and summer.



Overall results illustrate that the developed model can simulate the hydrology of the Batchawana reasonably well. Therefore, the calibrated model is used to assess the effects of land cover and climate change on the hydrological processes of this forested watershed.

### 3.6 References

Arsenault, Richard, Annie Poulin, Pascal Côté, and François Brissette. 2014. “Comparison of Stochastic Optimization Algorithms in Hydrological Model Calibration.” *Journal of Hydrologic Engineering* 19 (7): 1374–84. [https://doi.org/10.1061/\(ASCE\)HE.1943-5584.0000938](https://doi.org/10.1061/(ASCE)HE.1943-5584.0000938).

Becker, Rike, Akash Koppa, Stephan Schulz, Muhammad Usman, Tim aus der Beek, and Christoph Schüth. 2019. “Spatially Distributed Model Calibration of a Highly Managed Hydrological System Using Remote Sensing-Derived ET Data.” *Journal of Hydrology* 577 (October): 123944. <https://doi.org/10.1016/j.jhydrol.2019.123944>.

Bergström, Sten. 1991. “Principles and Confidence in Hydrological Modelling.” *Hydrology Research* 22 (2): 123–36. <https://doi.org/10.2166/nh.1991.0009>.

Biondi, Daniela, Gabriele Freni, Vito Iacobellis, Giuseppe Mascaro, and Alberto Montanari. 2012. “Validation of Hydrological Models: Conceptual Basis, Methodological Approaches and a Proposal for a Code of Practice.” *Physics and Chemistry of the Earth, Parts A/B/C* 42–44 (January): 70–76. <https://doi.org/10.1016/j.pce.2011.07.037>.

Bormann, Helge. 2011. “Sensitivity Analysis of 18 Different Potential Evapotranspiration Models to Observed Climatic Change at German Climate Stations.” *Climatic Change* 104 (3): 729–53. <https://doi.org/10.1007/s10584-010-9869-7>.

Bourgouin, Pierre. 2000. “A Method to Determine Precipitation Types.” *Weather and Forecasting* 15 (5): 583–92. [https://doi.org/10.1175/1520-0434\(2000\)015<0583:AMTDPT>2.0.CO;2](https://doi.org/10.1175/1520-0434(2000)015<0583:AMTDPT>2.0.CO;2).

Chlumsky, Robert. 2020. “RavenR.” <https://github.com/rchlumsk/RavenR>.

Colin Cameron, A., and Frank A.G. Windmeijer. 1997. “An R-Squared Measure of Goodness of Fit for Some Common Nonlinear Regression Models.” *Journal of Econometrics* 77 (2): 329–42. [https://doi.org/10.1016/S0304-4076\(96\)01818-0](https://doi.org/10.1016/S0304-4076(96)01818-0).

Craig, James R. n.d. “Raven Hydrological Model.” Accessed September 15, 2020. <http://raven.uwaterloo.ca/>.

Craig, James R., Genevieve Brown, Robert Chlumsky, R. Wayne Jenkinson, Georg Jost, Konhee Lee, Juliane Mai, et al. 2020. “Flexible Watershed Simulation with the Raven Hydrological Modelling Framework.” *Environmental Modelling & Software* 129 (July): 104728. <https://doi.org/10.1016/j.envsoft.2020.104728>.

D. N. Moriasi, J. G. Arnold, M. W. Van Liew, R. L. Bingner, R. D. Harmel, and T. L. Veith. 2007. “Model Evaluation Guidelines for Systematic Quantification of Accuracy in Watershed Simulations.” *Transactions of the ASABE* 50 (3): 885–900. <https://doi.org/10.13031/2013.23153>.

Dembélé, Moctar, Markus Hrachowitz, Hubert H. G. Savenije, Grégoire Mariéthoz, and Bettina Schaefli. 2020. “Improving the Predictive Skill of a Distributed Hydrological Model by Calibration on Spatial Patterns With Multiple Satellite Data Sets.” *Water Resources Research* 56 (1). <https://doi.org/10.1029/2019WR026085>.

Duan, Q. Y., V. K. Gupta, and S. Sorooshian. 1993. “Shuffled Complex Evolution Approach for Effective and Efficient Global Minimizationfile.” *Journal of Optimization Theory and Applications* 76 (3): 501–21. <https://doi.org/10.1007/BF00939380>.

Eberhart, and Yuhui Shi. n.d. “Particle Swarm Optimization: Developments, Applications and Resources.” In *Proceedings of the 2001 Congress on Evolutionary Computation (IEEE Cat. No.01TH8546)*, 1:81–86. IEEE. <https://doi.org/10.1109/CEC.2001.934374>.

Fonji, Simon Foteck, and Gregory N Taff. 2014. “Using Satellite Data to Monitor Land-Use Land-Cover Change in North-Eastern Latvia.” *SpringerPlus* 3 (1): 61. <https://doi.org/10.1186/2193-1801-3-61>.

Fontaine, T.A., T.S. Cruickshank, J.G. Arnold, and R.H. Hotchkiss. 2002. “Development of a Snowfall–Snowmelt Routine for Mountainous Terrain for the Soil Water Assessment Tool (SWAT).” *Journal of Hydrology* 262 (1–4): 209–23. [https://doi.org/10.1016/S0022-1694\(02\)00029-X](https://doi.org/10.1016/S0022-1694(02)00029-X).

Götzinger, Jens, and András Bárdossy. 2008. “Generic Error Model for Calibration and Uncertainty Estimation of Hydrological Models.” *Water Resources Research* 44 (12). <https://doi.org/10.1029/2007WR006691>.

Gupta, Hoshin V., Harald Kling, Koray K. Yilmaz, and Guillermo F. Martinez. 2009. “Decomposition of the Mean Squared Error and NSE Performance Criteria: Implications for Improving Hydrological Modelling.” *Journal of Hydrology* 377 (1–2): 80–91. <https://doi.org/10.1016/j.jhydrol.2009.08.003>.

Haghnegahdar, Amin, Bryan A. Tolson, James R. Craig, and Karol T. Paya. 2015. “Assessing the Performance of a Semi-Distributed Hydrological Model under Various Watershed Discretization Schemes.” *Hydrological Processes* 29 (18): 4018–31. <https://doi.org/10.1002/hyp.10550>.

Huang, Xiaomin, Weihong Liao, Xiaohui Lei, Yangwen Jia, Yuhui Wang, Xu Wang, Yunzhong Jiang, and Hao Wang. 2014. “Parameter Optimization of Distributed Hydrological Model with a Modified Dynamically Dimensioned Search Algorithm.” *Environmental Modelling & Software* 52 (February): 98–110. <https://doi.org/10.1016/j.envsoft.2013.09.028>.

Jain, A., and S. Srinivasulu. 2008. “Hydrologic Model Calibration Using Evolutionary Optimisation.” In *Practical Hydroinformatics*, 291–301. Berlin, Heidelberg: Springer Berlin Heidelberg. [https://doi.org/10.1007/978-3-540-79881-1\\_21](https://doi.org/10.1007/978-3-540-79881-1_21).

K. Ajami, Newsha, Hoshin Gupta, Thorsten Wagener, and Soroosh Sorooshian. 2004. “Calibration of a Semi-Distributed Hydrologic Model for Streamflow Estimation along a River System.” *Journal of Hydrology* 298 (1–4): 112–35. <https://doi.org/10.1016/j.jhydrol.2004.03.033>.

Khamis, K., J. P. R. Sorensen, C. Bradley, D. M. Hannah, D. J. Lapworth, and R. Stevens. 2015. "In Situ Tryptophan-like Fluorometers: Assessing Turbidity and Temperature Effects for Freshwater Applications." *Environmental Science: Processes & Impacts* 17 (4): 740–52. <https://doi.org/10.1039/C5EM00030K>.

Khedr, Ayman, Bryan Tolson, and Samuel Ziemann. 2015. "Water Distribution System Calibration: Manual versus Optimization-Based Approach." *Procedia Engineering* 119: 725–33. <https://doi.org/10.1016/j.proeng.2015.08.926>.

Kuchment, L.S., and A.N. Gelfan. 1996. "The Determination of the Snowmelt Rate and the Meltwater Outflow from a Snowpack for Modelling River Runoff Generation." *Journal of Hydrology* 179 (1–4): 23–36. [https://doi.org/10.1016/0022-1694\(95\)02878-1](https://doi.org/10.1016/0022-1694(95)02878-1).

Leach, James M., and Paulin Coulibaly. 2020. "Soil Moisture Assimilation in Urban Watersheds: A Method to Identify the Limiting Imperviousness Threshold Based on Watershed Characteristics." *Journal of Hydrology* 587 (August): 124958. <https://doi.org/10.1016/j.jhydrol.2020.124958>.

Lee, Jung Hwan, Gi Moon Yuk, Hyeon Tae Moon, and Young-II Moon. 2020. "Integrated Flood Forecasting and Warning System against Flash Rainfall in the Small-Scaled Urban Stream." *Atmosphere* 11 (9): 971. <https://doi.org/10.3390/atmos11090971>.

Lespinas, Franck, Ashu Dastoor, and Vincent Fortin. 2018. "Performance of the Dynamically Dimensioned Search Algorithm: Influence of Parameter Initialization Strategy When Calibrating a Physically Based Hydrological Model." *Hydrology Research* 49 (4): 971–88. <https://doi.org/10.2166/nh.2017.139>.

Levenberg, Kenneth. 1944. "A Method for the Solution of Certain Non-Linear Problems in Least Squares." *Quarterly of Applied Mathematics* 2 (2): 164–68.

Lu, Jianbiao, Ge Sun, Steven G McNulty, and Devendra M Amatya. 2005. "A Comparison Of Six Potential Evapotranspiration Methods For Regional Use In The Southeastern United States1." *JAWRA Journal of the American Water Resources Association* 41 (3): 621–33. <https://doi.org/10.1111/j.1752-1688.2005.tb03759.x>.

Masson-Delmotte, V., P. Zhai, H.-O. Pörtner, D. Roberts, J. Skea, E. Lonnoy P.R. Shukla, A. Pirani, W. Moufouma-Okia, C. Péan, R. Pidcock, S. Connors, J.B.R. Matthews, Y. Chen, X. Zhou, M.I. Gomis, and T. Waterfield (eds.) T. Maycock, M. Tignor. n.d. “IPCC, 2018: Global Warming of 1.5°C. An IPCC Special Report on the Impacts of Global Warming of 1.5°C above Pre-Industrial Levels and Related Global Greenhouse Gas Emission Pathways, in the Context of Strengthening the Global Response to the Threat of Cli.”

Meyer, Patricia A., Martinus Brouwers, and Paul J. Martin. 2014. “A Three-Dimensional Groundwater Flow Model of the Waterloo Moraine for Water Resource Management.” *Canadian Water Resources Journal / Revue Canadienne Des Ressources Hydriques* 39 (2): 167–80.

<https://doi.org/10.1080/07011784.2014.914800>.

Moriasi, Daniel N., Naresh Pai, Jean L. Steiner, Prasanna H. Gowda, Michael Winchell, Hendrik Rathjens, Patrick J. Starks, and J. Alan Verser. 2019. “SWAT-LUT: A Desktop Graphical User Interface for Updating Land Use in SWAT.” *JAWRA Journal of the American Water Resources Association* 55 (5): 1102–15. <https://doi.org/10.1111/1752-1688.12789>.

Motovilov, Yuri G, Lars Gottschalk, Kolbjørn Engeland, and Allan Rodhe. 1999. “Validation of a Distributed Hydrological Model against Spatial Observations.” *Agricultural and Forest Meteorology* 98–99 (December): 257–77. [https://doi.org/10.1016/S0168-1923\(99\)00102-1](https://doi.org/10.1016/S0168-1923(99)00102-1).

Muhammad, Ameer, Grey R. Evenson, Tricia A. Stadnyk, Alaba Boluwade, Sanjeev Kumar Jha, and Paulin Coulibaly. 2019. “Impact of Model Structure on the Accuracy of Hydrological Modeling of a Canadian Prairie Watershed.” *Journal of Hydrology: Regional Studies* 21 (February): 40–56. <https://doi.org/10.1016/j.ejrh.2018.11.005>.

Nash, J.E., and J.V. Sutcliffe. 1970. “River Flow Forecasting Through Conceptual Models Part I — A Discussion of Principles.” *Journal of Hydrology* 10 (3): 282–90.

[https://doi.org/10.1016/0022-1694\(70\)90255-6](https://doi.org/10.1016/0022-1694(70)90255-6).

Ontario Flow Assessment Tool.” 2020. 2020.

<https://www.gisapplication.lrc.gov.on.ca/OFAT/Index.html?site=OFAT&viewer=OFAT&locale=en-US>.

Ontario GeoHub.” 2020. 2020. <https://geohub.lio.gov.on.ca/>.

Pechlivanidis, I. G., and B. Arheimer. 2015. “Large-Scale Hydrological Modelling by Using Modified PUB Recommendations: The India-HYPE Case.” *Hydrology and Earth System Sciences* 19 (11): 4559–79. <https://doi.org/10.5194/hess-19-4559-2015>.

Pignotti, Garrett, Hendrik Rathjens, Raj Cibin, Indrajeet Chaubey, and Melba Crawford. 2017. “Comparative Analysis of HRU and Grid-Based SWAT Models.” *Water* 9 (4): 272. <https://doi.org/10.3390/w9040272>.

Rahman, Mohammad, and Minjiao Lu. 2015. “Model Spin-Up Behavior for Wet and Dry Basins: A Case Study Using the Xinanjiang Model.” *Water* 7 (12): 4256–73. <https://doi.org/10.3390/w7084256>.

Refsgaard, J. C., and B. Storm. 1990. “Construction, Calibration and Validation of Hydrological Models.” In , 41–54. [https://doi.org/10.1007/978-94-009-0257-2\\_3](https://doi.org/10.1007/978-94-009-0257-2_3).

Refsgaard, Jens Christian. 1997. “Parameterisation, Calibration and Validation of Distributed Hydrological Models.” *Journal of Hydrology* 198 (1–4): 69–97. [https://doi.org/10.1016/S0022-1694\(96\)03329-X](https://doi.org/10.1016/S0022-1694(96)03329-X).

Samimi, Maryam, Ali Mirchi, Daniel Moriasi, Sora Ahn, Sara Alian, Saleh Taghvaeian, and Zhuping Sheng. 2020. “Modeling Arid/Semi-Arid Irrigated Agricultural Watersheds with SWAT: Applications, Challenges, and Solution Strategies.” *Journal of Hydrology*, September, 125418. <https://doi.org/10.1016/j.jhydrol.2020.125418>.

Sanford, S. E., I. F. Creed, C. L. Tague, F. D. Beall, and J. M. Buttle. 2007. “Scale-Dependence of Natural Variability of Flow Regimes in a Forested Landscape.” *Water Resources Research* 43 (8). <https://doi.org/10.1029/2006WR005299>.

“Scholars Geo Portal.” n.d. [http://geo1.scholarsportal.info/#r/details/\\_uri@=2938003198](http://geo1.scholarsportal.info/#r/details/_uri@=2938003198).

Seck, Alimatou, Claire Welty, and Reed M. Maxwell. 2015. “Spin-up Behavior and Effects of Initial Conditions for an Integrated Hydrologic Model.” *Water Resources Research* 51 (4): 2188–2210. <https://doi.org/10.1002/2014WR016371>.

Semkin, R. G., D. S. Jeffries, R. Neureuther, G. Lahaie, M. McAulay, F. Norouzian, and J. Franklyn. 2012. “Summary of Hydrological and Meteorological Measurements in the Turkey Lakes Watershed, Algoma, Ontario.” Burlington, ON.

Shangguan, Wei, Yongjiu Dai, Qingyun Duan, Baoyuan Liu, and Hua Yuan. 2014. “A Global Soil Data Set for Earth System Modeling.” *Journal of Advances in Modeling Earth Systems* 6 (1): 249–63. <https://doi.org/10.1002/2013MS000293>.

Silberstein, R.P. 2006. “Hydrological Models Are so Good, Do We Still Need Data?” *Environmental Modelling & Software* 21 (9): 1340–52. <https://doi.org/10.1016/j.envsoft.2005.04.019>.

“Swat.Tamu.Edu.” <https://swat.tamu.edu/>.

Teng, Fei, Wenrui Huang, Yi Cai, Chunmiao Zheng, and Songbin Zou. 2017. “Application of Hydrological Model PRMS to Simulate Daily Rainfall Runoff in Zamask-Yingluoxia Subbasin of the Heihe River Basin.” *Water* 9 (10): 769. <https://doi.org/10.3390/w9100769>.

Teshager, Awoke Dagne, Philip W Gassman, Silvia Secchi, Justin T Schoof, and Girmaye Misgna. 2016. “Modeling Agricultural Watersheds with the Soil and Water Assessment Tool (SWAT): Calibration and Validation with a Novel Procedure for Spatially Explicit HRUs.” *Environmental Management* 57 (4): 894–911. <https://doi.org/10.1007/s00267-015-0636-4>.

Tolson, Bryan A., and Christine A. Shoemaker. 2007. “Dynamically Dimensioned Search Algorithm for Computationally Efficient Watershed Model Calibration.” *Water Resources Research* 43 (1). <https://doi.org/10.1029/2005WR004723>.

Yoon, Jae-Heung, and Christine A. Shoemaker. 2001. “Improved Real-Coded GA for Groundwater Bioremediation.” *Journal of Computing in Civil Engineering* 15 (3): 224–31. [https://doi.org/10.1061/\(ASCE\)0887-3801\(2001\)15:3\(224\)](https://doi.org/10.1061/(ASCE)0887-3801(2001)15:3(224)).

## Chapter 4: Impacts of Land Cover, External Forcings and Internal Climate Variability

### 4.1 Introduction

In this chapter, we investigate the impacts of possible forest type changes, the influence of lakes, anthropogenic forcings and internal climate variability on the hydrology of the Batchawana Watershed. The techniques applied to extract land covers maps and future scenarios (including changes in forest types and lake shrinkages) are discussed in the following sections. General Circulation Models (GCMs) are discussed in the literature review and the selected climate models are presented in this chapter. Internal climate variability and external forcings are described and their influence on the projected changes in the hydrology of Batchawana is investigated.

### 4.2 Land cover scenarios

Variations in the vegetation types may impact the hydrologic processes in watersheds. Forest land covers can dramatically change due to wildfires, hurricanes, droughts, insects outbreak, forest harvesting, climate change, among others (Célleri and Feyen 2009). As mentioned earlier in chapter 3, three main tree types are covering the Batchawana watershed. The hydrological response of each forest type (vegetation type) can be different. In addition, the leaf area index (LAI) of the vegetation cover can substantially change especially in winter and fall. In the basin of study, deciduous trees start losing leaves by October and leaf out by the end of March. Seasonal relative LAI plays an important role in characterizing the hydrological processes and consequently in modelling accuracy. The highest value for seasonal relative LAI is 1 and the lowest is zero. LAI of 1 occurs when the tree maintains the maximum coverage of leaves which usually happens during the warm seasons and the LAI of 0 represents no leaves on trees. Considering previous studies on LAI variations (Sanford et al. 2007; Lim et al. 2003) we allocated the following relative seasonal LAIs to different forest types;

Deciduous Forest: June to Sept = 1, May and Oct = 0.5, Nov to Apr = 0

Coniferous Forest: Jan to Dec = 1

Mixed Forest: June to Sept = 1, May and Oct = 0.75, Nov to Apr = 0.5

From June to September, deciduous trees hold the maximum LAI, lose half of their leaves during October and regrow them by May. The period of November to April is considered as the cold season when the deciduous trees lose green leaves. The coniferous trees have an LAI value of 1 in



all seasons. Mixed forests include both types of coniferous and deciduous trees (50% each), hence during the cold seasons, the coniferous trees keep the overall LAI value of the mixed forests above 0.5. Like deciduous, mixed forest gain (lose) 25% of their leaves during May (November).

We use the Landsat satellite products and extract land cover images, which show that the land cover of the region has changed over the past few decades. Figure 4 - 1 depicts the types of trees of the Batchawana watershed in 1995, 2000 and 2011, respectively. During the past few decades, deciduous trees have replaced parts of the watershed previously covered by coniferous trees (mostly in the eastern part). Also, mixed forests are growing in the area as well. It appears that coniferous forest has been initially replaced by mixed forest and then by deciduous trees in some areas.

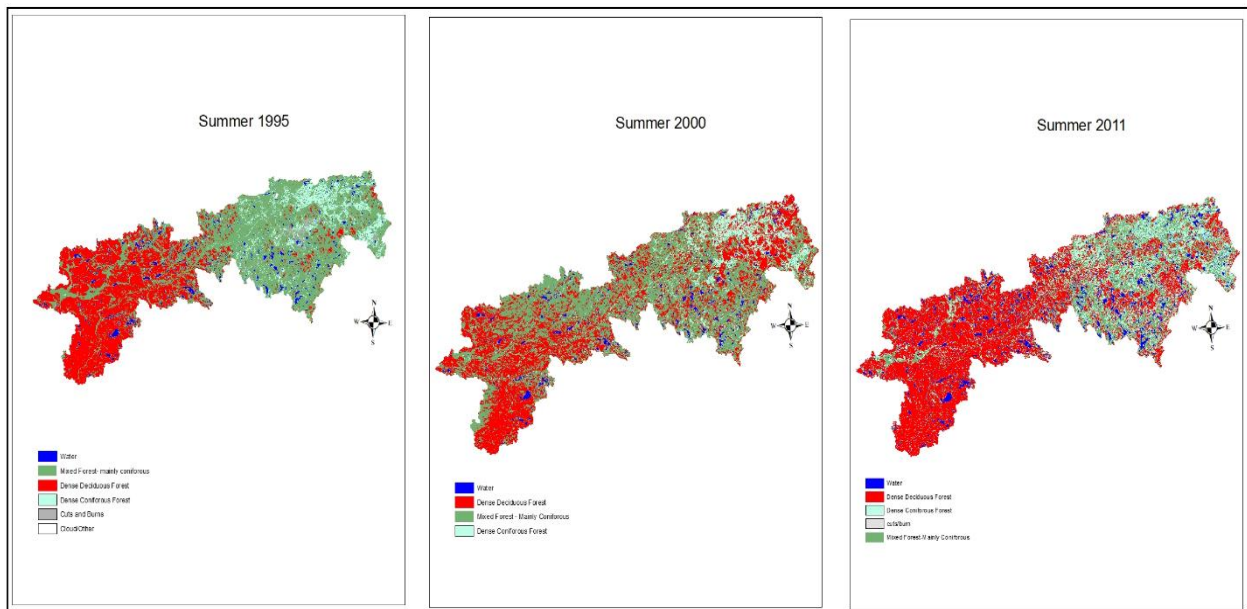


Figure 4 - 1: Satellite Imagery of the Batchawana Watershed. Coniferous or mixed forests have been replaced with deciduous type trees from 1995 to 2011. All satellite products are captured during summer with a cloud cover of less than 10%. Images are produced by processing the Landsat products (<https://www.usgs.gov/core-science-systems/nli/landsat>)

Considering the historical land cover trends, we consider two land cover change scenarios that are more likely to occur over the next few decades:

- a- **Coniferous to Mixed (CTM):** In this scenario, all coniferous trees are replaced by mixed forest. The northeastern part of the region and a majority of coniferous trees are already replaced by

mixed forests. Mixed forest is supposed to include both deciduous and coniferous tree types in an equal proportion.

- b- Coniferous to Deciduous (CTD): In the second scenario the entire coniferous region is replaced with deciduous trees.

Scenarios are not precise predictions and are developed based on historical evidence as well as consultation with experts. Application of the above-mentioned scenarios on the validated hydrological model of the basin would enlighten some aspects of the hydrological characteristics of coniferous, deciduous and mixed forest covers.

#### 4.2.1 Effects of Lakes

In the Batchawana watershed, lakes are substantial factors covering almost 11% of the basin. Satellite imagery of the region from 1980 to 2016 shows a variable extent of water bodies. Figure 4- 2 depicts the histogram of the % area of the basin covered by water bodies. It shows that in 2012, 11% of the region is covered by water bodies (mainly lakes), which is roughly equal to 150 km<sup>2</sup>.

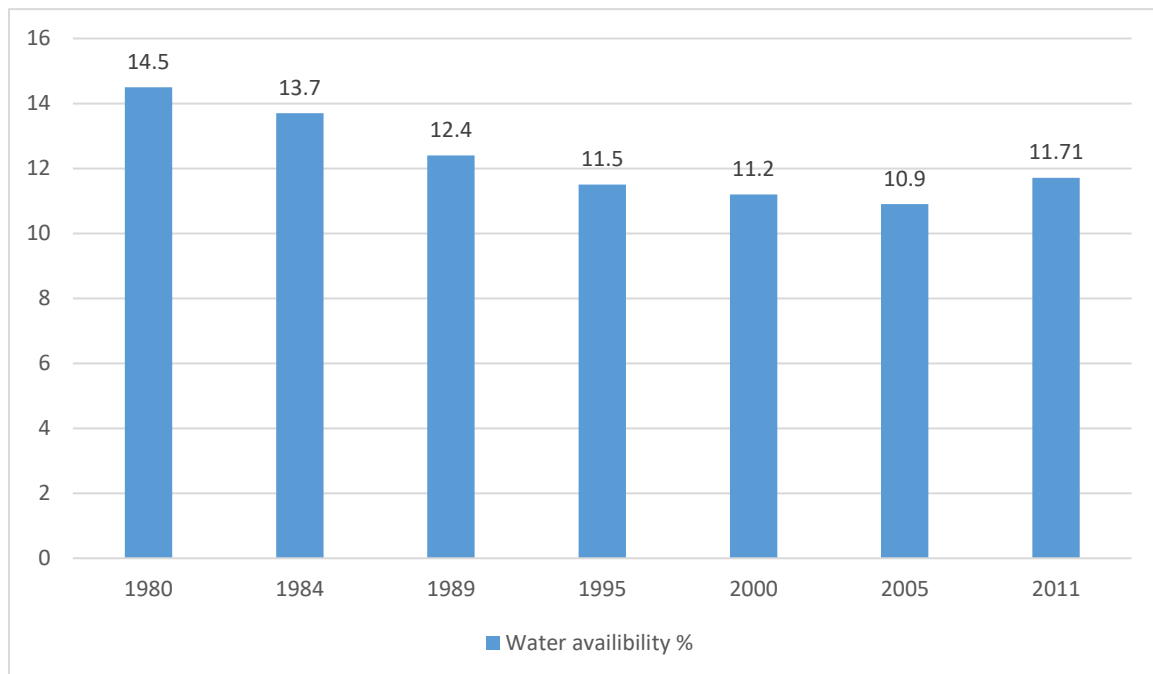


Figure 4-2: Percentage of water bodies in Batchawana. Data are extracted using Landsat products.

Figure 4-2 shows a decreasing trend in the surface water availability in the region from 1980 to the end of 2011. Several filters such as cloud cover percentage, season, humidity, and precipitation are considered for the selection of satellite products with the highest possible quality. The process of selecting the Landsat products is challenging as not all recorded data is useable for land cover extraction. Besides, the quality and resolution (vertical diameter of pixels) of the earlier Landsat satellites (Landsat 1-5) have limited bands each with 60 m resolution while Landsat 8 has 11 bands with 30 m or even 15 m resolution for each band. To minimize the cloud cover-caused error in the land cover map extraction, we select the products only with less than 10% cloud cover (Afrin et al. 2019). All gathered products are in the summer season (preferably around June or early August) to make sure that all vegetation types are detectable. Humidity or wetness of the recorded data has been checked to avoid the selection of satellite records after rainfall incidents. The raw products of the Landsat satellite are downloaded and using the ArcGIS 10.2 software. Using the available land covers from more reliable sources (e.g. OFAT) the software has been supervised and trained to detect and differentiate the land cover classes (<https://developers.arcgis.com/python/sample-notebooks/land-cover-classification-using-sparse-training-data/>).

The water body percentage is calculated by dividing the number of pixels (30 m diameter for each pixel) corresponding to water bodies by the entire number of pixels. With a significant trend ( $p$ -value  $< 0.04$ ) and it shows that water bodies are depleting, therefore lake shrinkage scenarios are investigated to evaluate their corresponding effects on the future hydrology of the Batchawana watershed. The scenarios include 25%, 50%, 75% and 100% reduction in the total areas of the lakes. It is important to note that these scenarios are only to assess the impacts of lakes/water availability on the streamflow characteristics and do not suggest that future lake coverage is projected to decline in this region. This requires further modelling and analysis which is beyond the scope of this study. Besides, the extracted water bodies from satellite data represent rivers and ponds besides lakes.

The lost areas of lakes for each scenario are replaced (assumedly) by mixed forests in the hydrological model. The only available data of lakes is the area of each which was calculated by remote sensing for 2012. The developed model responds to the accumulative areas of lakes regardless of the lakes' depth or other characteristics. Only a few studies have been conducted to assess the lakes in the Batchawana watershed (almost all are focused on the Turkey Lake sub-

watershed). The analysis of the lakes is based on satellite products (focused on the lakes area). Study of other lake's characteristics such as volume was not possible due to data limitations.

### 4.3 Climate Change Scenarios

The following sections discuss the global and regional climate models and the emission scenario (RCP 8.5) considered in this study.

#### 4.3.1 General Circulation Models (GCMs)

Selected GCMs for this study are summarized in Table 4- 1 (Taylor, Stouffer, and Meehl 2012b):

Table 4- 1: Selected global climate models for Batchawana Watershed hydrological modelling.

GCM	Institute	Resolution	Reference
ACCESS1.0	Commonwealth Scientific and Industrial Research Organization	$\sim 1.9^\circ \times 1.25^\circ$	(CSIRO 2016)
BCC-CSM1.1(m)	Beijing Climate Center, China Meteorological Administration	$\sim 1.1^\circ \times \sim 1.1^\circ$	(BCC 2014)
CanESM2	Canadian Centre for Climate Modelling and Analysis	$\sim 2.8^\circ \times \sim 2.8^\circ$	(CCCma 2015)
HadGEM2-ES	Met Office Hadley Centre contributed by Instituto Nacional de Pesquisas Espaciais)	$\sim 1.9^\circ \times 1.25^\circ$	(Liddicoat, Jones, and Hughes 2014)
MIROC-ESM-CHEM	Japan Agency for Marine-Earth Science and Technology, Atmosphere and Ocean Research Institute (The University of Tokyo), and the National Institute for Environmental Studies	$\sim 2.8^\circ \times \sim 2.8^\circ$	(Jamstec, Aori, and Nies 2015)
NorESM1-M	Norwegian Climate Centre	$\sim 2.5^\circ \times \sim 1.9^\circ$	(NCC 2011)

FGOALS-g2	LASG, Institute of Atmospheric Physics, Chinese Academy of Sciences; and CESS, Tsinghua University	$\sim 2.8^\circ \times \sim 2.8^\circ$	(LASG-CESS 2014)
CSIRO-Mk3.6.0	Commonwealth Scientific and Industrial Research Organization in collaboration with the Queensland Climate Change Centre of Excellence	$\sim 1.9^\circ \times \sim 1.9^\circ$	(Jeffrey et al. 2016)

---

\*  $1^\circ \approx 111 \text{ KM}$

GCM resolution is too coarse to conduct regional analyses. Therefore, downscaling is required to translate the climate model outputs at low spatial scales to a fine resolution suitable for regional/local climate change assessments (Peng et al. 2017; Ribalaygua et al. 2013). We use the statistically downscaled data provided by the Pacific Climate Impact Consortium (PCIC) (<https://pacificclimate.org/>). The spatial resolution of the downscaled data is 300 arc-seconds or roughly 10 km and it is available from 1950 to 2100. The downscaling approach is based on bias correction constructed analogues with quantile mapping reordering (BCCAQ; Version 2), which Combines the quantile delta mapping (Cannon, Sobie, and Murdock 2015) and bias correction/constructed analogues (Maurer et al. 2010) downscaling techniques (Hiebert et al. 2018; Fauzi, Kuswanto, and Atok 2020).

#### 4.3.2 Large Ensembles of Regional Climate Models

In addition to the downscaled GCMs, we use three large ensembles of regional climate model simulations to study the uncertainties associated with internal climate variability and distinguish between the influence of external forcings and ICV on the hydrologic projections of the Batchawana watershed. The models include CanRCM4 (50 members) and its two bias-corrected products (i.e. CanLEAD-E and CanLEAD-S). Characteristics of each large ensemble are discussed in the following (Singh et. al, 2021):

- i. The Canadian Regional Climate Model (CanRCM4) Large Ensemble is a 50-member ensemble for the North American region under the RCP 8.5 scenario from 1950 to 2100 (Fyfe et al. 2017; Kirchmeier-Young et al. 2018). The Canadian earth system model

version 2 (CanESM2) (Kirchmeier-Young, Zwiers, and Gillett 2017) is the parent GCM for the novel regional climate model, CanRCM4, developed by the Canadian center for climate modelling and analysis (CCCma) (Scinocca et al. 2016a). The model simulations follow the CMIP5 protocols with each ensemble-driven by a member of the CanESM2 large ensemble (generated based on different initial conditions). Simulations are conducted at 0.22° or ~25 km horizontal grid resolution.

- ii. CanLEAD-S: Canadian Large Ensemble Adjusted Dataset version 1 or CanLEADv1 is the adjusted version of CanRCM4 based on the maximum and minimum daily temperature, and precipitation, relative humidity, surface pressure, wind speed, incoming shortwave radiation and incoming longwave radiation. Bias correction is performed using the Multivariate Bias Correction (MBCn) method developed by Cannon (2015). Data is available at a 0.5-degree rectangular grid size at daily time steps. The adjusted data are referred to as CanLEAD-S when they are bias-corrected based on data from Iizumi et al. 2017.
- iii. CanLEAD-E: Similar to the CanLEAD-S, but bias-corrected based on the data from Lange, 2018. It is available at daily temporal resolution and 0.5-degree rectangular grid spatial resolution.

## 4.4 Methodology

In this, we discuss the global climate model selection procedure and the analysis of the 158 (three large ensembles each with 50 members and 8 GCMs) climate simulations as inputs to the Raven hydrological model.

### 4.4.1 GCM Selection

There are several global climate models available from different climate research institutes (D. Jiang, Sui, and Lang 2016; Taylor, Stouffer, and Meehl 2012b; J. Teng et al. 2012) with 27 downscaled GCMs provided in the PCIC's data portal (<https://pacificclimate.org/>). In this study, 8 GCMs based on RCP 8.5 are selected based on Cannon (2015).

Climate models are verified based on their performance during the historical period, and to analyze the future impacts of climate change, timeframes of 20-30 years are commonly considered to represent the “near future” and “far future” periods (Höglind, Thorsen, and Semenov 2013; Flanner

2009; Höglind, Thorsen, and Semenov 2013; Muhammad et al. 2018; 2020). In 2015 PCC released a special report on the consequences of 1.5 °C global warmings (Jeong, Cannon, and Morris 2020; Masson-Delmotte et al. 2018). In this study, we assess the projected impacts of climate change considering 1.5, 2, 2.5, 3, 3.5 and 4 °C global temperature increase rates compared to the preindustrial (PI) period. For example, CanESM2 projects a 3 °C global warming (compared to the preindustrial era) in 2049. This is based on a 9-year running mean (i.e. 2049 plus and minus 4.5 years). Figure 4-3 and associated data is kindly shared by Jiang et. al, 2016. It shows the period in which each GCM reaches the target temperature. Because different RCPs result in different timeframes for GCMs to reach the target temperature only one scenario (the worst-case scenario) is selected considered.

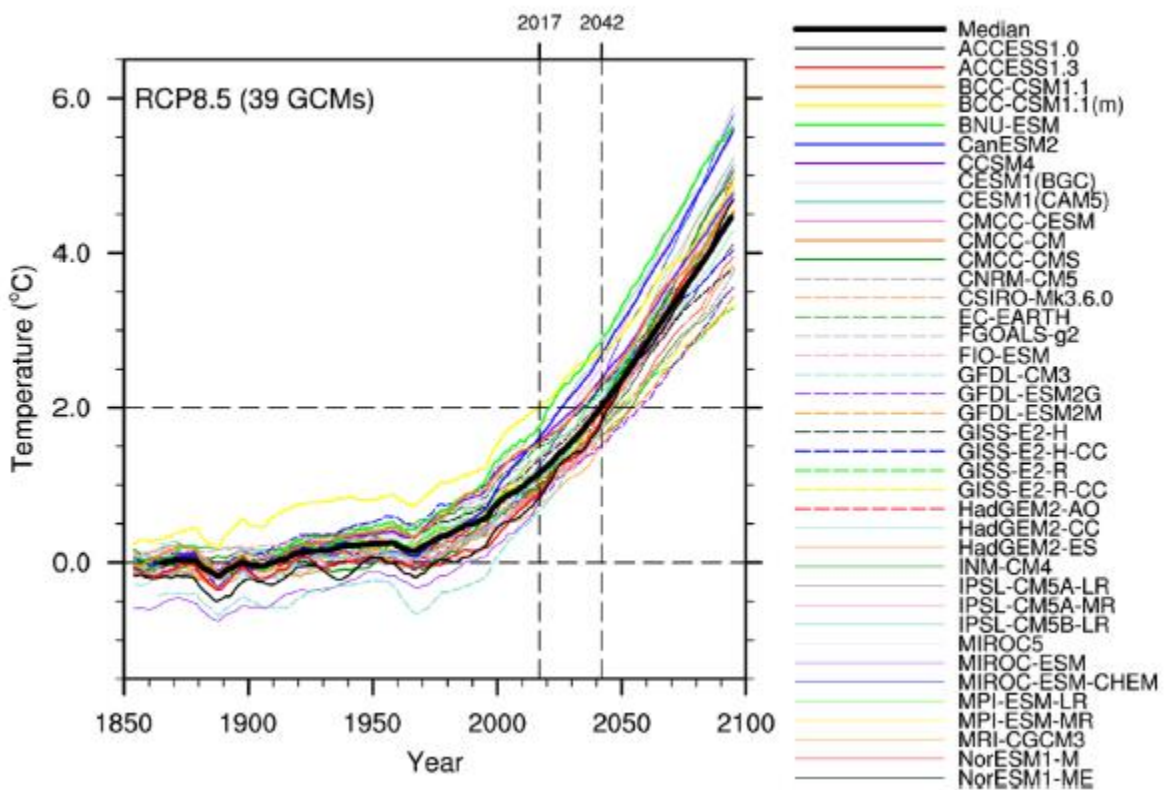


Figure 4-3: Global mean temperature changes for different GCMs under RCP8.5 (Jiang et. al, 2016)

Cannon (2015) conducted a study to select fewer GCMs that represent the variability of all available GCMs for different regions around the world. Based on the regions defined by Giorgi and Francisco, 2000 and extreme climate indices comparison between the observed and globally simulated ones, the most suited GCMs for each region is detected. Among the 12 suggested GCMs

for ENA (Eastern North America) region, 8 GCMs are available in the PCIC's data portal. Concerning Figure 4-3 of GMTCs for GCMs, Table 4- 2 shows the anticipated 9-year time frame when a GCM reaches a target temperature.

Table 4- 2: Anticipated 9-year period for each GCM to reach a specific global mean temperature change. The period represents the average temperature 4.5 years before or after the given year. Data provided by Jiang et. al (2016)

Scenarios/GCM	ACCESS1-0	FGOALS-g2	bcc-csm1-1-m	CanESM2
1.5 °C	2036	2035	1999	2013
2 °C	2045	2051	2017	2026
2.5 °C	2054	2063	2031	2038
3 °C	2067	2077	2052	2049
3.5 °C	2076	2091	2062	2058
4 °C	2085	NA	2077	2068
	NorESM1-M	HadGEM2-ES	CSIRO-Mk3-6-0	MIROC-ESM-CHEM
1.5 °C	2034	2031	2036	2022
2 °C	2050	2040	2046	2035
2.5 °C	2062	2051	2057	2045
3 °C	2073	2058	2066	2052
3.5 °C	2086	2068	2076	2062
4 °C	NA	2076	2083	2070



#### 4.4.2 Assessing the Hydrologic Impacts of Climate Change using Raven

Three simulated outputs from the global/regional climate models are used to drive the Raven hydrological model for climate change impact assessments: precipitation, daily minimum temperature (Tasmin) and daily maximum temperature (Tasmax). In total, there are 8 simulations from the selected statistically downscaled GCMs and  $3 \times 50$  ensemble members from large ensembles of the RCMs for 1950 to 2100. Using the R programming language all ensembles runs (158 forcings) are ingested to the Raven model for hydrologic climate change impact analysis.

#### 4.5 Results and discussion

We first discuss the modelling results of land cover change scenarios. To study the model under different circumstances, the evaluation criteria for all land cover and lake change scenarios are illustrated. Next, climate change scenarios based on GCMs and the large ensembles of RCMs are discussed. Finally, the influence of internal variability on the projected changes of hydrological factors is assessed.

##### 4.5.1 Land cover change scenarios

The monthly average streamflow values corresponding to the CTD and CTM scenarios are shown in Figure 4- 4. The watershed's response to CTM and CTD is almost the same during the spring and summer seasons and slightly varies in winter. There is a considerable difference in the hydrologic response of the watershed to the two scenarios during fall. It shows that both CTD and CTM results yield higher monthly average streamflow compared to the base model's flow. In all months corresponding to fall and winter seasons, CTD has higher average flow rates than CTM flows while they both release higher streamflow compared to the base model. Overall, the hydrologic differences between scenarios are larger in the cold seasons and relatively small in warm seasons, as expected. Notably, there is no month when the average streamflow corresponding to CTM is higher than that of CTD.

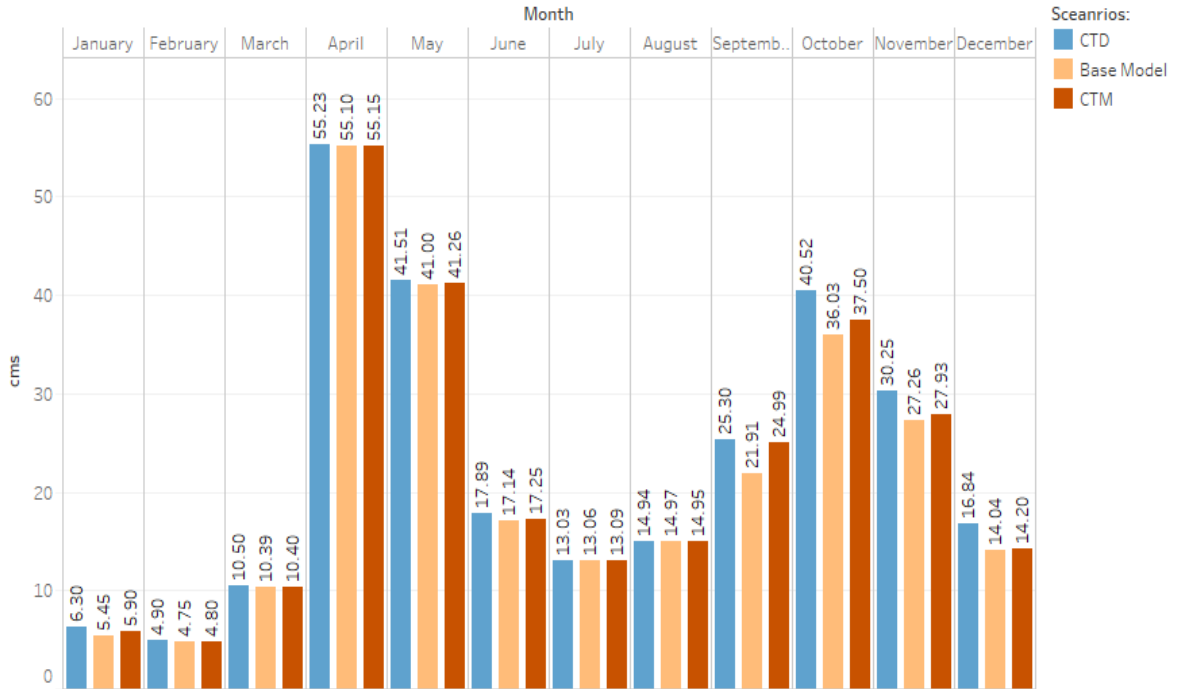


Figure 4- 4: Monthly mean streamflow for land cover change scenarios. Coniferous to deciduous (CTD) and mixed forest scenarios (CTM) result in larger flow rates in the fall compared to the base model.

#### 4.5.2 Lake change scenarios

Figure 4- 5 shows the observed and simulated (No-Lake scenario) flow rates from 1996 to 2001. Daily results corresponding to the No\_Lake scenario show almost zero low flow rates in most years. This highlights the critical role of the lakes in recharging the river system, particularly for low flow periods.

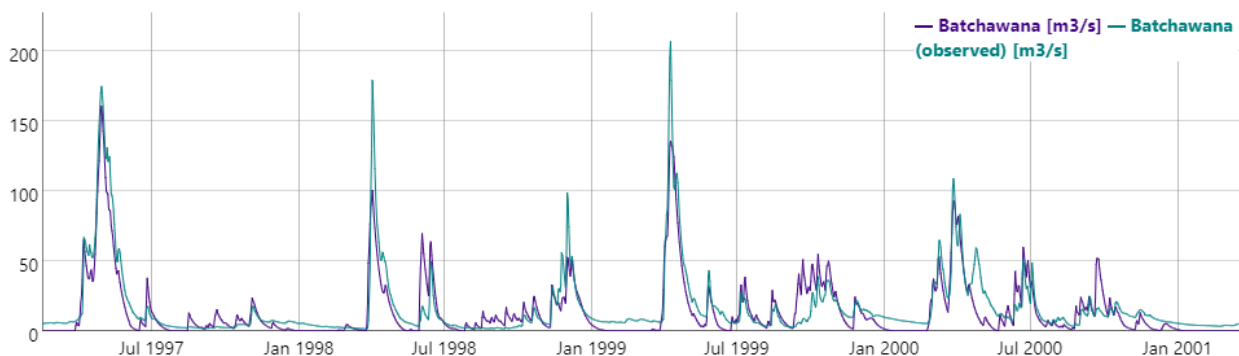


Figure 4- 5: The hydrograph corresponding to the No\_Lake scenario. Simulated values for low flows are almost zero most of the time regardless of the season.

The monthly streamflow rates corresponding to four different lakes area (available water percentage) scenarios are shown in Figure 4- 6. Other lake shrinkage scenarios also show considerable underestimations in flow rates albeit with smaller effects compared to the No-Lake scenario.

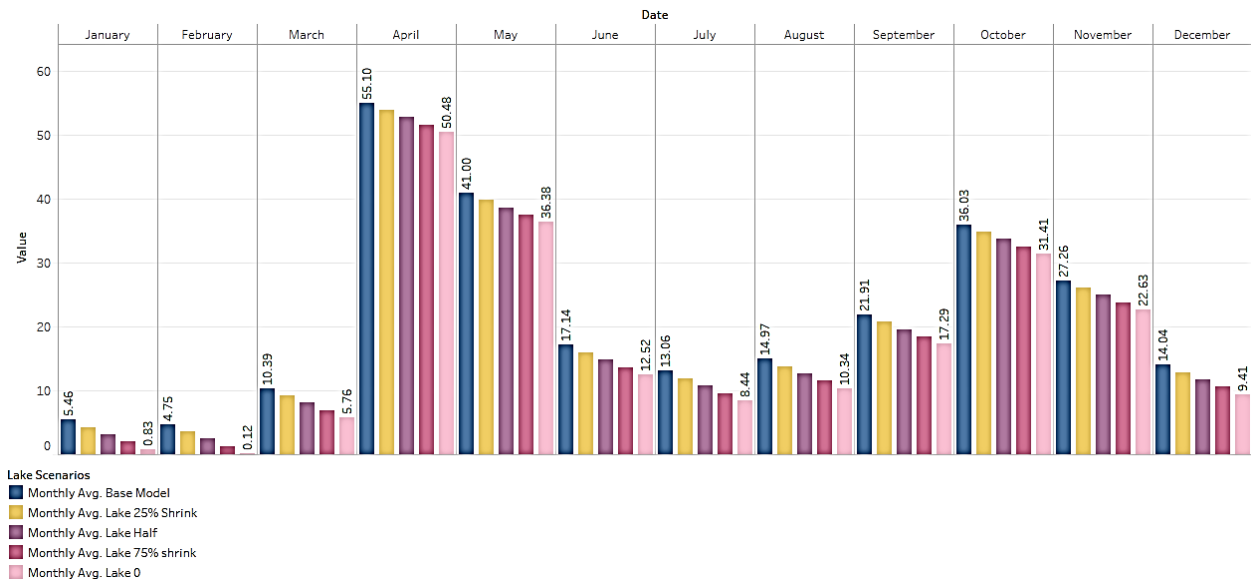


Figure 4- 6: Monthly mean streamflow corresponding to the lake scenarios. Lower lake areas result in lower monthly mean streamflow rates with the No\_Lake scenario showing almost zero values during winter.

All scenarios are following the base model (dark blue) but with lower flow rates in all months. Overall, the monthly average flows decrease with decreases in total lake areas. During the cold season especially in January and February months, the No\_Lake scenario (no available water in the region) yields a negligible amount of streamflow. Even though the overall model performance does not change drastically for different lake scenarios, the model does not represent the watershed response well when the lake effects are not considered accurately.

### 4.5.3 Climate change scenarios

First, the results of the global climate models are presented. The projected impacts of climate change on temperature, precipitation and streamflow are discussed. Then, the results of the large ensembles of regional climate models are elaborated. Finally, the influences of internal variability and external forcings on Batchawana’s streamflow changes are investigated based on the large ensembles.

- GCMs

We assess the projected impacts of climate change on the hydrologic components of Batchawana considering the global mean temperature increases of 1.5, 2, 2.5, 3, 3.5 and 4 degrees Celsius. Table 4- 3 represents the global mean temperature change (from the preindustrial era) for each GCM and also the corresponding mean temperature increase over Batchawana (based on downscaled GCMs). In other words, it shows when the global mean is x °C warmer than PI, what would be the projected temperature increase (than PI) over the watershed.

Table 4- 3: Global mean temperature change (GMTC) for the 8 selected GCMs of the study area.

Global	ACCESS1-0	FGOALS-g2	bcc-csm1-1-m	CanESM2	
1.5	2.4	1.8	0.4	1.2	
2	3.5	2.8	1.7	1.6	
2.5	4.3	4	1.9	3	
3	5.1	5	2.9	3.5	
3.5	6.7	5.9	4	4.2	
4	7	NA	4.6	4.8	
	NorESM1-M	HadGEM2-ES	CSIRO-Mk3-6-0	MIROC-ESM-CHEM	<b>Batchawana</b>
1.5	2.5	2.5	1.4	2.4	<b>1.825</b>
2	3.1	3.1	2.5	3.5	<b>2.725</b>
2.5	4.6	4.3	3.6	5.1	<b>3.85</b>
3	5.1	5	4	5.4	<b>4.525</b>

3.5	6.7	7.1	4.7	6.1	<b>5.675</b>
4	NA	7.5	5.4	7.2	<b>6.08</b>

NA values indicate that the GCM does not reach the 4 degrees Celsius temperature change until 2100. This would happen more if a lower (less pessimistic) RCP scenario were selected. Values for the Batchawana column show the average temperature changes between multiple GCMs. As expected, local temperature from downscaled GCMs follow the trend of global mean temperature changes but the regional values are higher than the global mean. For a lower GMTC, the average of the 8 GCMs (column titled as Batchawana) shows a minor higher value, but as the GMTC increases differences between regional and global mean temperature values start to increase. These results are consistent with the Canadian Climate Change Report (Bush et al. 2019) in which the conducted studies indicated that the Canadian climate is expected to experience a more tangible change compared to other parts of the world. The selected global climate models for the study area project different temperature and precipitation values. The multi-model mean values during the 9-year projected time frames for each GMTC are discussed. The variation of the GCMs projection for temperature being downscaled for Batchawana is shown in Figure 4- 7.

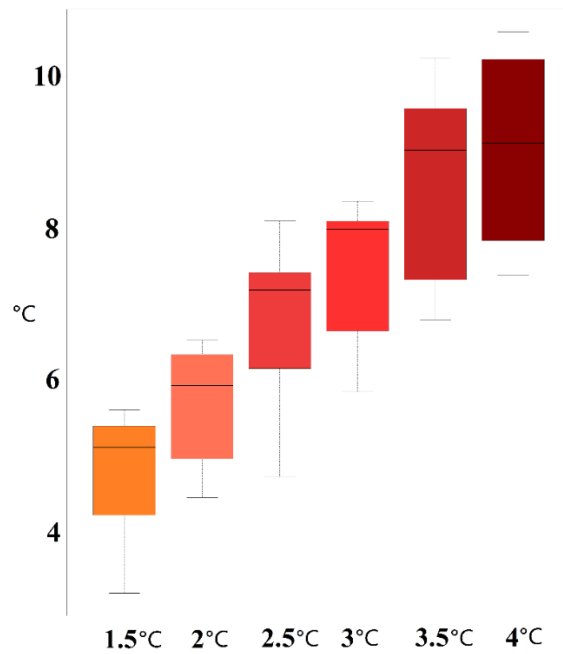


Figure 4- 7: The projected annual mean temperature corresponding to the global mean temperature increases. Darker colours indicate more GMTCs.

Figure 4- 8 shows the future changes in the annual precipitation over the Batchawana watershed. Overall, total precipitation is projected to increase over Batchawana with increases in the global mean temperature. Each boxplot represents GCMs variation range. GMTCs of 4 and 1.5 show relatively higher disagreement.

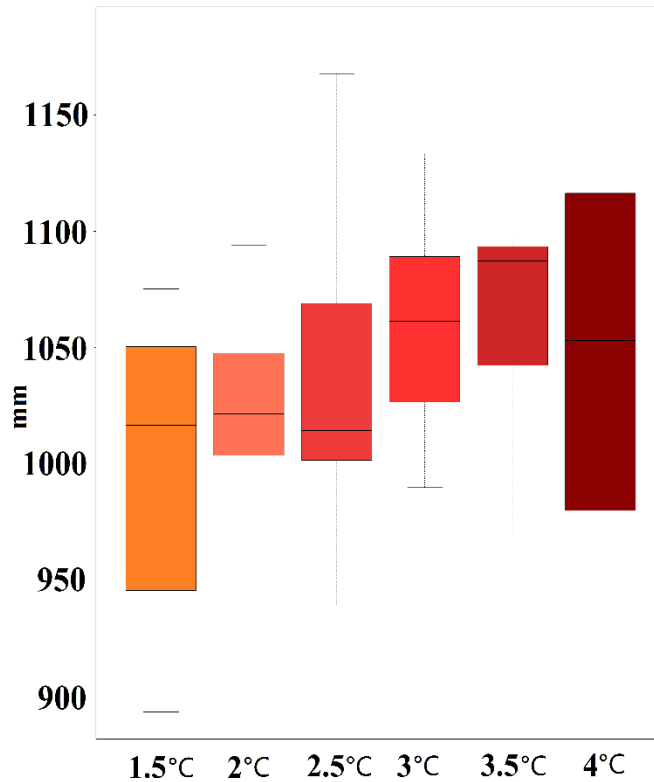


Figure 4- 8: Projected annual precipitation rates corresponding to the global mean temperature increases. The darker colour represents a higher global mean temperature change.

The temperature and precipitation simulations from downscaled GCMs are fed to the validated hydrologic model and the projected annual streamflow values are shown in Figure 4- 9. Darker colours indicate a warmer global mean change scenario. The projected annual mean streamflow is slightly above 14 cms corresponding to GMTC of 1.5 °C, and it drops to below 14 for 2 °C. The projected streamflow increases with higher GMTC rates. Change in the streamflow rate (based on the average GCMs) is relatively sharp from 3°C to 4°C when it reaches 15.6 cms. Overall, the annual streamflow changes are consistent with increases in total precipitation over the study area.

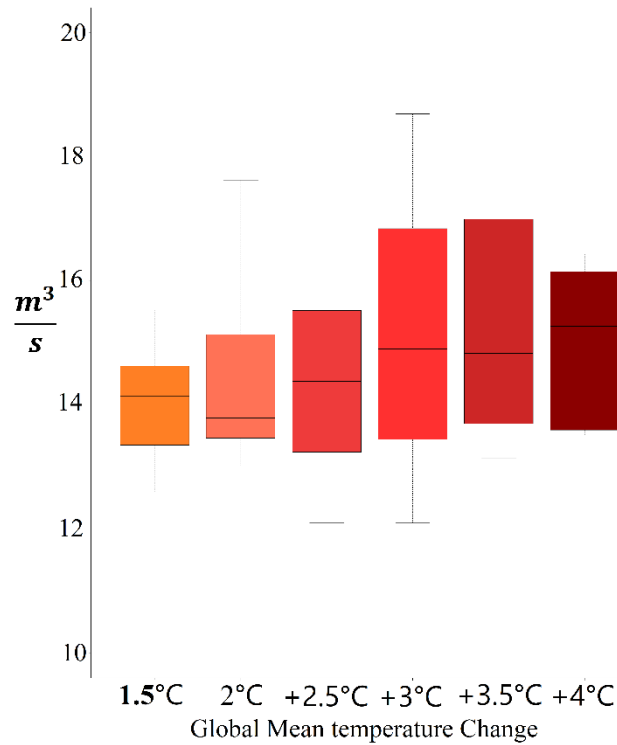


Figure 4- 9: Projected changes in the annual streamflow rates of the Batchawana watershed corresponding to the global mean temperature increases. The boxplots show the variation ranges of projected streamflow by GCMs.

Figure 4- 10 shows the projected annual maximum streamflow for the 6 GMTCs. A decreasing trend is visible in the annual maximum streamflow with increases in the global mean temperature. The annual maximum streamflow is almost similar for the two initial GMTCs but then it drops for GMTC of 2.5 and keeps decreasing for more temperature. With the least variation range for the GMTC of 4, it shows that annual maximum streamflow will deplete.



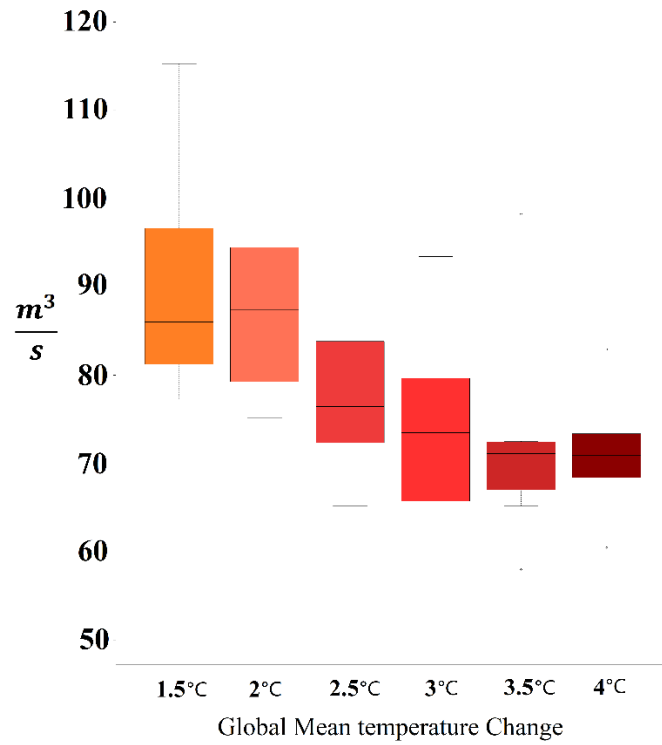


Figure 4- 10: Projected annual maximum streamflow corresponding to the global mean temperature increases. The generated results are showing boxplots which are covering the variation bound of 8 GCMs.

The annual snow projections are shown in Figure 4- 11 where a visible decreasing trend is detectable. For GMTC of 4 snow amounts will be almost three times less than that of GMTC of 1.5. The variation between GCMs is relatively small for the projection of snow projection.

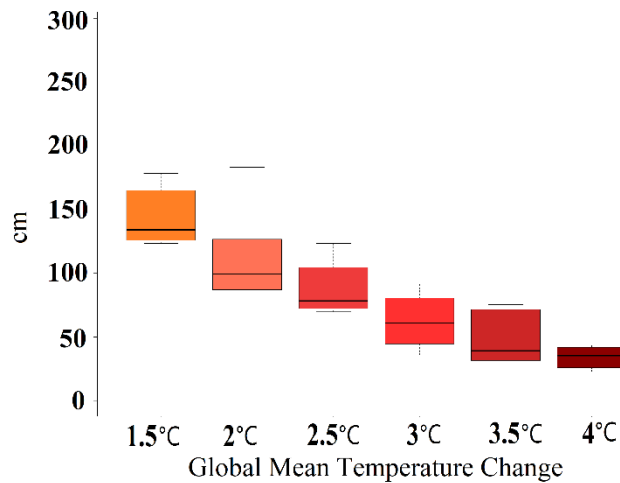


Figure 4- 11: Projected annual snow corresponding to the global mean temperature increases.

- Large Ensembles of RCMs

In addition to the downscaled GCMs, we drive the Raven hydrological model with simulations from three large ensembles of regional climate models for 1950 to 2100 at a daily time scale. The large ensembles are generated by nesting the CanRCM4 model within the CanESM2 GCM. Therefore, the selected large ensembles reach the GMTC targets at the same period as CanESM2 (See Table 4- 2 for the anticipated timeframes for each GCM to reach the target GMTCs).

Figure 4 -12 shows the results of the annual mean temperature for the Batchawana basin. CanRCM4 projects an annual mean temperature much higher than what it is projected based on CanLEAD-S and CanLEAD-E. CanLEAD-E projects a higher annual mean temperature than CanLEAD-S. A comparative study of CanLEAD and CanRCM4 projections for non-stationary compound extreme events in Canada (Singh et. al, 2021) has concluded that CanLEAD products are marginally performing better than the CanRCM4 large ensemble. Therefore, because of a reasonable consistency between CanLEAD and GCMs projections, it would be a possibility that CanRCM4 is not performing desirably for this region.

Figure 4- 13 shows the projected changes in annual precipitation at each GMTC based on the large ensembles. The boxplots represent the large ensemble range (50 members) of the annual precipitation averaged over the 9-year period. CanLEAD-S projects the highest total precipitation for Batchawana Watershed and CanLEAD-E is the second-highest projection. The original

CanRCM4 simulations project considerably lower annual precipitation for the basin of study in the future. Consistent with GCM results, the projected precipitation increases by increasing GMTC i.e. there is a positive association between the GMTC and annual precipitation in the Batchawana basin.

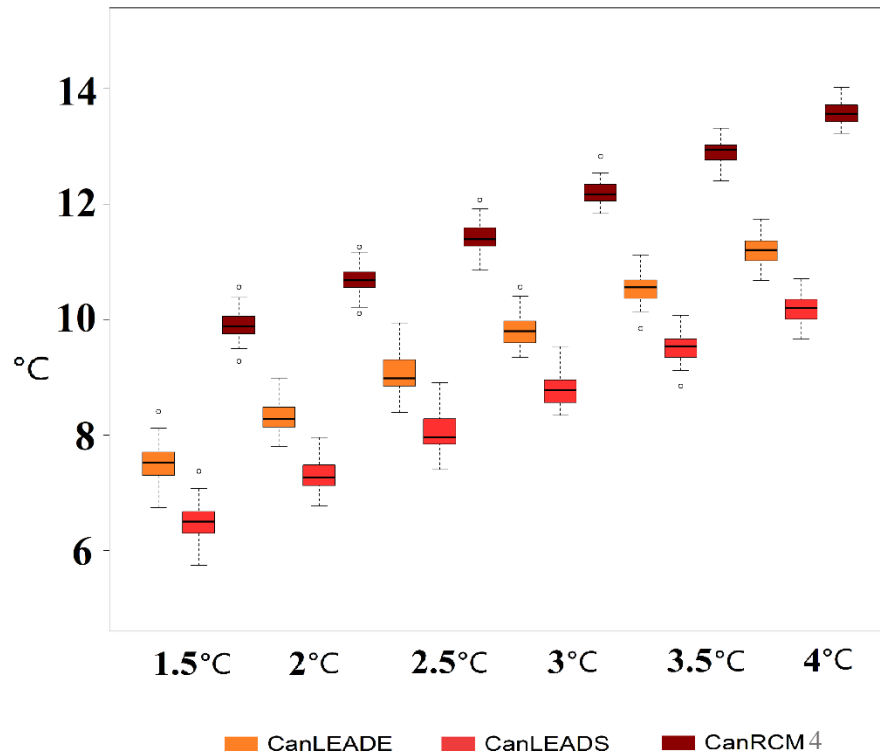


Figure 4- 12: Projected annual mean temperature based on the three large ensembles corresponding to the global mean temperature increases

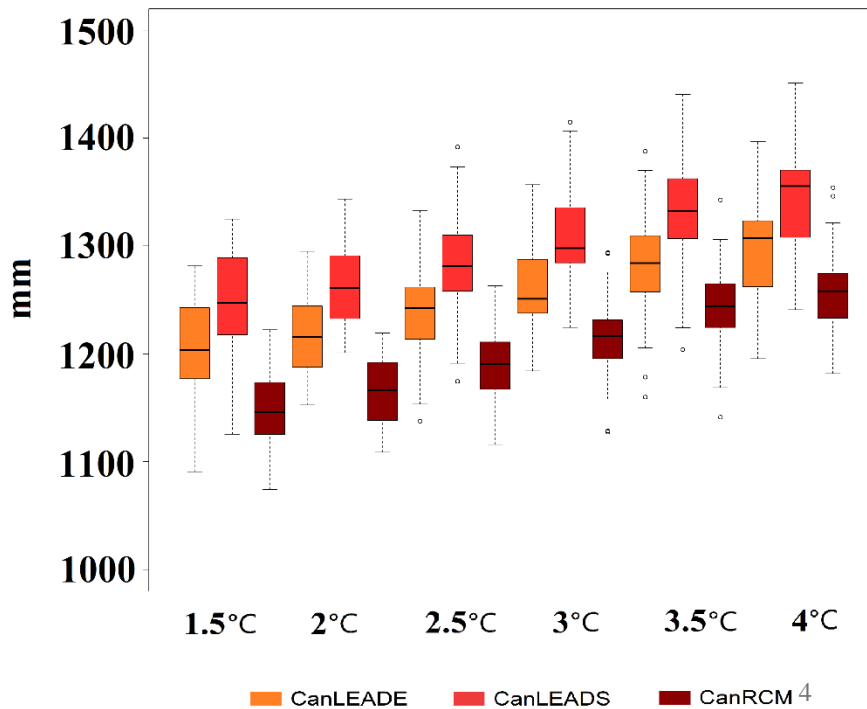


Figure 4- 13: Projected annual precipitation based on the large ensembles corresponding to the global mean temperature increases.

The precipitation and temperature simulations from the large ensembles are used to drive the validated hydrological model to assess the projected streamflow changes in the Batchawana watershed. The model simulations are conducted at a daily time scale. Figure 4- 14 shows the 9-year average of the annual mean streamflow and the boxplots represent the range of large ensemble members (projected streamflow range for each member). CanLEAD-E, CanLEAD-S and CanRCM4 all show an increasing trend with larger annual mean streamflow rates with increases in the global mean temperature. CanLEAD-S projects a higher annual mean streamflow compared to CanLEAD-E and CanRCM4 simulations. While for GMTC rates lower than 3°C CanLEAD-E shows larger annual mean streamflow compared to CanRCM4, for larger temperature increases CanRCM4 results in larger flow rates.

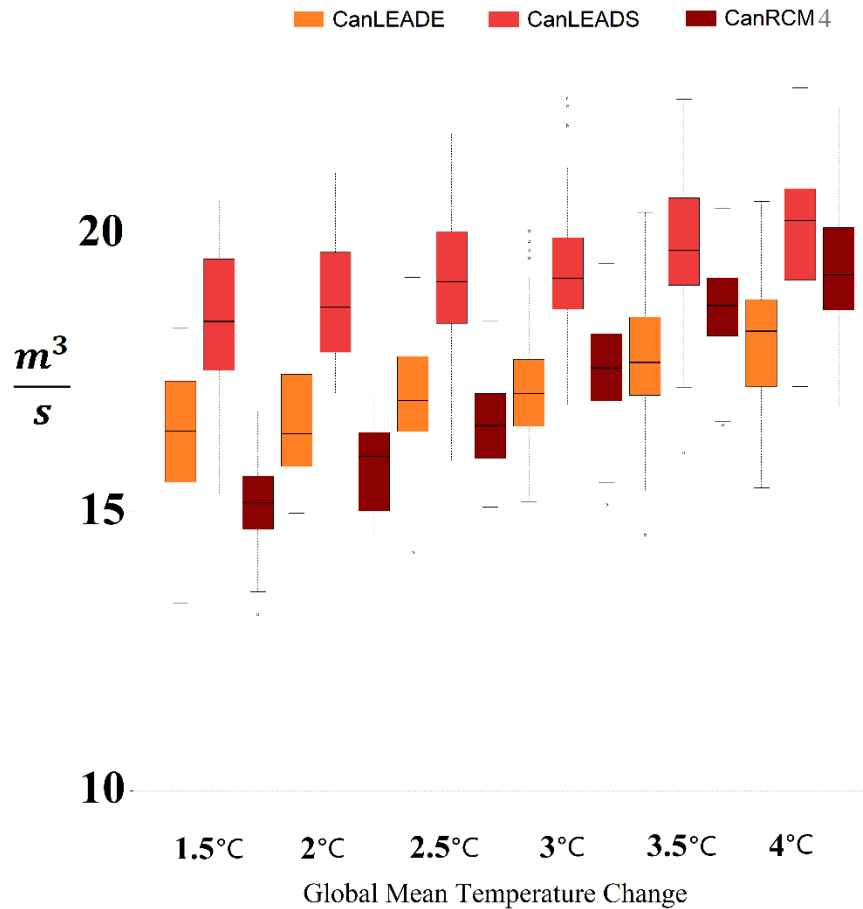


Figure 4- 14: Projected annual mean streamflow for large ensembles corresponding to the global mean temperature increases.

Figure 4- 15 shows the 9-year average of annual maximum streamflow projected by the large ensembles. There are notable differences between CanLEAD and CanRCM4 simulations while CanRCM4 projects a considerably lower annual maximum streamflow compared to the other two large ensembles. CanLEAD-S projects higher annual maximum streamflow compared to CanLEAD-E, a behaviour similar to that of the annual streamflow. However, both CanLEAD-E&S project a decreasing trend with increases in the global mean temperature contrary to

CanRCM4 simulations. Further, the uncertainty ranges in the two CanLEAD products are larger compared to CanRCM4 runs.

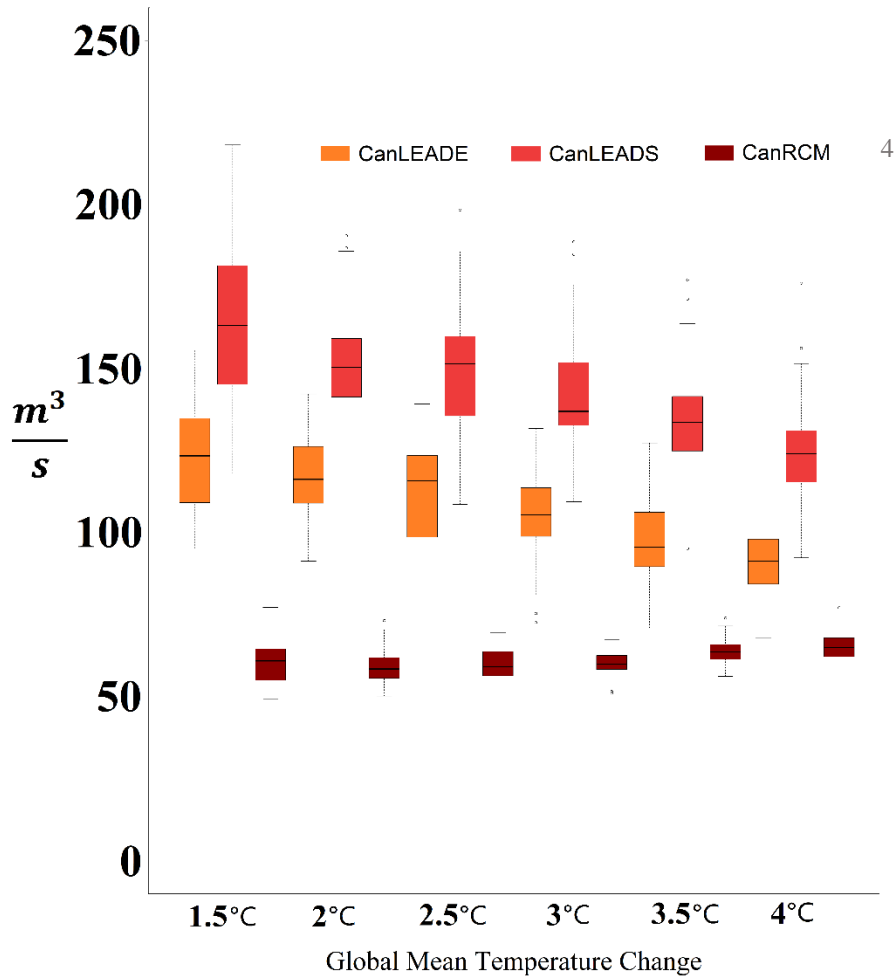


Figure 4- 15: Projected annual maximum streamflow for large ensembles corresponding to the global mean temperature increases.

Figure 4- 16 represents the annual snow for Batchawana based on the RCM simulations. All three large ensembles project a decreasing trend for snow. CanRCM4 simulates relatively less snow for the region of study which reasonably can because of the higher projected temperature by this large ensemble.

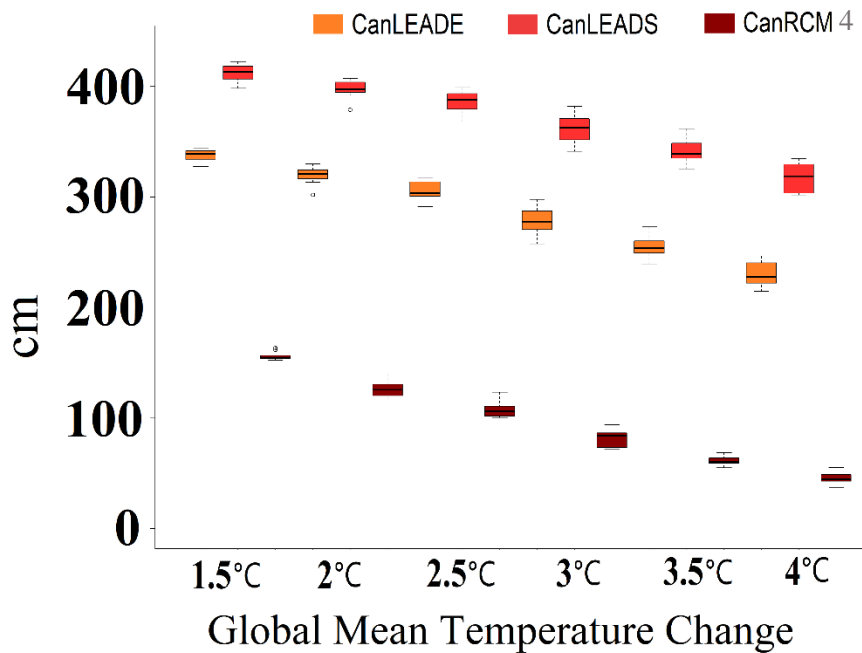


Figure 4- 16: Projected annual snow for three large ensembles corresponding to the global mean temperature increases

#### 4.5.4 The role of internal climate variability & external forcings

To analyze and quantify the influence of internal climate variability and external forcings the mean of the large ensemble members is considered to represent the external forcings, called signal hereafter (Dai and Bloecker 2019). The standard deviation of the residuals is the internal variability, called noise hereafter. The signal is the impact of the external forcing on the trend of the projected hydrologic factor, which is mainly associated with anthropogenic activities (Zwiers and Weaver 2000). Noise is random and natural climate variability. The SNR, signal to noise ratio index is commonly used to assess the relative influence of the external forcings considering the effects of internal climate variability.

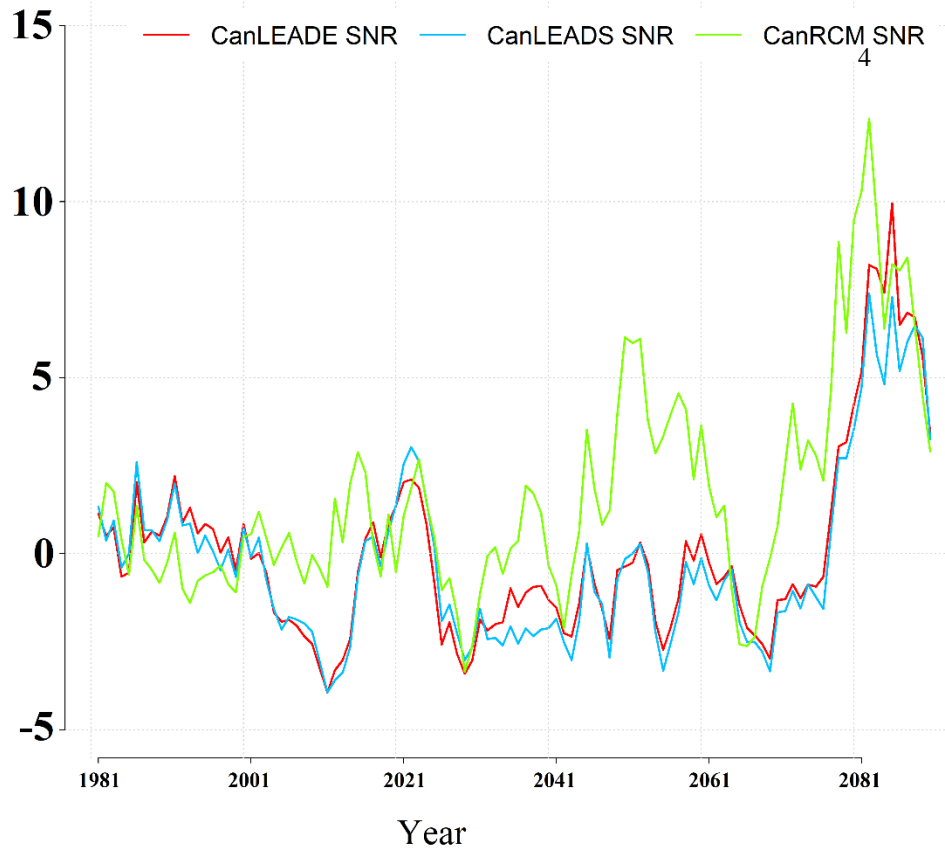


Figure 4- 17: Signal to noise ratio (SNR) anomalies for the large ensembles.

Figure 4- 17 represents the SNR anomalies corresponding to the annual streamflow for the Batchawana basin based on CanRCM4, CanLEAD-E and CanLEAD-S. Anomalies are based on the SNR mean over a 30-year time frame from 1982 to 2011. Analyzing the SNR anomalies shows that CanLEAD-E and CanLEAD-S signifying a decrease in the early 21<sup>st</sup> century and they sharply start to increase for the last third of the 21<sup>st</sup> century. Further, CanRCM4 shows that SNR decreases a decade later than the other two large ensembles, but all three large ensembles perform similarly for the SNR increase. Respecting the overall trends of the SNR anomalies, CanRCM4 shows a higher SNR for the study of the region.



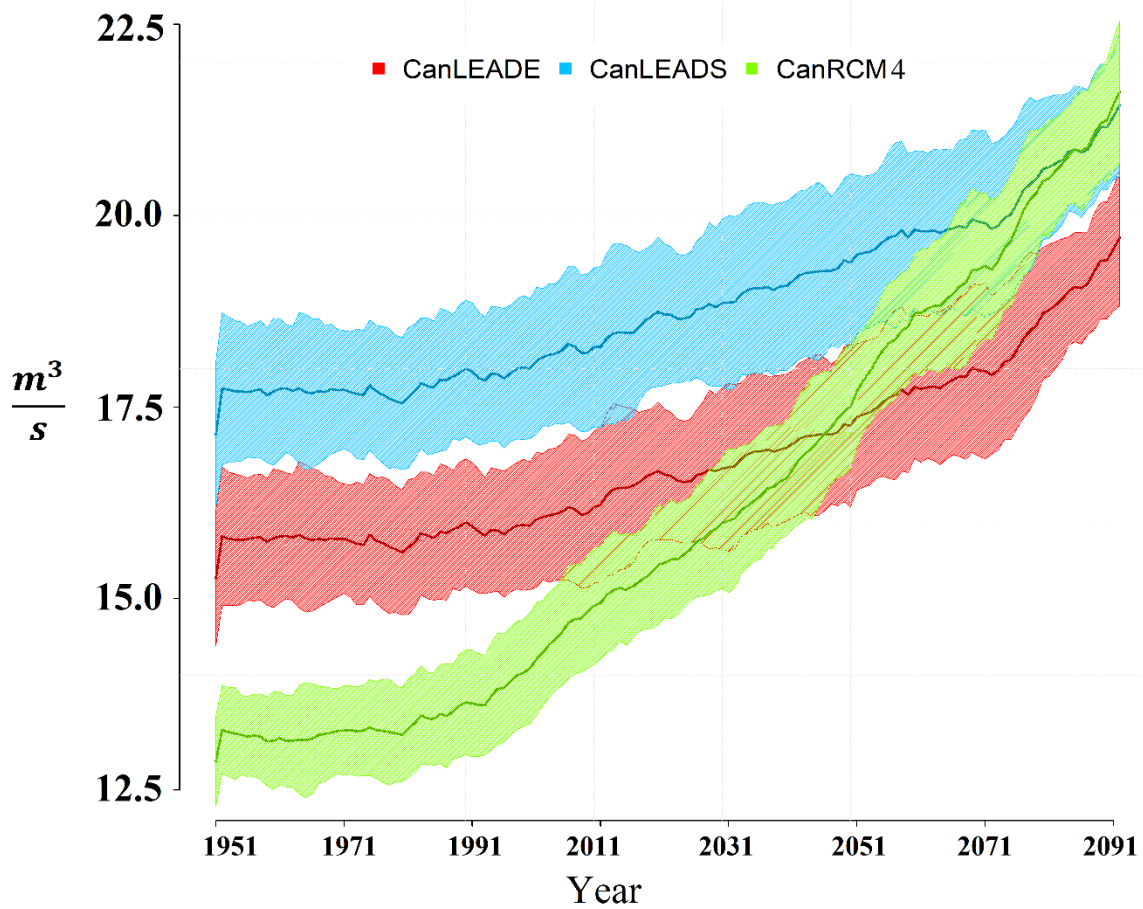


Figure 4- 18: Projected mean and standard deviation of the large ensembles

Figure 4- 18 represents the mean (signal; inner darker line) and the standard deviation of the residuals (noise; surrounding band). CanLEAD-S shows an initial higher annual mean streamflow and CanLEAD-E has a relatively lower value, while CanRCM4 has the lowest annual mean streamflow in the historical period. Both of the CanLEAD products follow a similar increasing trend for the mean (lines) while CanRCM4 shows a spike from the late 20<sup>th</sup> century. In all large ensembles the surrounding bands are narrowing down after the 2070s and they reach the thinnest condition at the of the simulation period.

#### 4.6 Conclusions

Batchawana is a forested watershed where vegetation type plays a critical role in modulating the hydrological processes. Changes in the forest type or forest density can cause extreme hydrological events such as droughts or floods in downstream areas. To observe and analyze the possible

changes in the hydrology of the region, multiple scenarios are investigated. Two forest type (land cover) change scenarios are determined based on historical changes from satellite imagery and foreseen plans for the Batchawana forest management. CTD and CTM are the forest type change scenarios referring to coniferous to deciduous and coniferous to mixed trees, respectively. Available water percentage in the extracted land cover maps using the Landsat satellite products are assumed to be the lakes' area. We assess the sensitivity of the streamflow to changes in lake coverage by considering four shrinkage steps (25% area reduction in each step). These lake scenarios are only for understanding and studying the impacts of lakes on streamflow.

Canada's climate is projected to warm more than global mean temperature changes; hence, it is essential to assess the impacts of climate change especially on forested watersheds, which has significant implications for the environment and industry. Eight statistically downscaled GCM simulations under the RCP8.5 scenario are selected for climate change impact analysis. Further, simulations from three RCM large ensembles are studied (i) CanRCM4 (ii) CanLEAD-E and (iii) CanLEAD-S to assess the role of internal climate variability besides the effects of external forcings.

The Forest type scenarios show changes in the streamflow magnitude in the fall. Comparisons between the monthly mean streamflow rates corresponding to CTD and CTM scenarios and that of the base model suggest that streamflow does not change noticeably in summer, winter and spring seasons. CTD and CTM scenarios both lead to a forest with fewer leaves (less LAI) and less snow/rain interception. Observing no difference in January to late August means that regardless of the vegetation type, and mainly as it is discussed in this thesis, regardless of leaves snowfall happens and stores in the region and it does not change notably if the snow interception capacity has varied. During the summer, deciduous and mixed forests retain the maximum possible LAI (so it is constant). The main difference is during the fall when the precipitation regime is rain-dominated. Monthly mean streamflow (see Figure 4- 4) indicates that during the fall season till early January, CTD yields the highest streamflow compared with CTM and base model. CTM also results in higher streamflow than the base model. The reason is that deciduous forests either in CTM or CTD lose their leaves and consequently, the rain interception rate of the trees drops. Drops of rainfall reach the ground directly (and other storages) without being intercepted by leaves and flow to reach the main channel in the basin.

The presence of lakes can affect the streamflow characteristics (J. A. Leach and Laudon 2019). We consider the available water percentage as lake area and as an indicator of the available lake water supply in the region. Decreases in the lake area (water availability percentage) result in lower streamflow rates at all months, which can dramatically affect the low flow conditions. Lakes could also impact the model setup and calibration. While the model shows satisfactory performance for all lake scenarios based on KGE and NSE ( $\sim 0.85$ ), the Log-NSE metric showed weak performance when the lake areas were not represented in the model well. To assess the model and its capability to simulate the hydrology of the basin, analyzing low flows and high flows are vital steps and using multiple evaluation criteria provides the opportunity to assess the model's capability to capture all features of the streamflow.

To assess the impacts of climate change we consider 9-year periods when each GCM reaches the GMTCC target values: 1.5, 2, 2.5, 3, 3.5 and 4 °C. Overall, the annual mean streamflow is projected to increase in the Batchawana watershed in a warmer climate, consistent with projected increases in total precipitation. Further, the annual maximum streamflow is projected to decrease, and this would potentially due to the warmer environment in the winter season and consequently having lesser snowfalls. The warmer environment slowly depletes the snow storages and during the early spring, when usually the highest flows occur in the base model, there will be lower snow storages to increase the streamflow.

CanRCM4 projects a warmer environment for Batchawana compared to all models. Further, the RCMs project higher precipitation compared to GCM simulations. Overall, CanLEAD-S projects the highest precipitation and the lowest temperature. Higher precipitation results in higher annual mean streamflow. The lower projected temperature by CanLEAD-S also results in lower snowpack depletion and larger spring freshets. This results in the largest annual mean and max streamflow projection based on the product.

CanRCM4 projects a comparatively higher temperature and lower precipitation to the other climate models which is consistent with results from other studies (Scinocca et al. 2016b) where the drawbacks of the CanRCM4 are stated. Also, the annual mean streamflow is projected to be lower than the other two large ensembles for the initial global mean temperature changes. For annual maximum streamflow, the basin in response to CanRCM4 forcings shows an increasing

trend. In other words, unlike the other climate models (regional and global) and also historical data, CanRCM4 assumes that there is not enough snowpack to be melted in April and cause annual max streamflow; The higher temperature causes less snowpack, fewer snowfalls and more evaporation and consequently less annual max streamflow.

Further, we assess the role of internal climate variability using the large ensemble simulations. The signal-to-noise ratio (SNR) is estimated for each ensemble. A higher SNR shows a stronger external forcing signal. Results of the 9- year running average SNR anomalies (Figure 4- 17) for three large ensembles indicates similar trend behaviour in CanLEAD-E and CanLEAD-S. CanRCM4 shows a stronger signal in the future streamflow changes compared to the other two products. All three ensembles consistently show increasing external forcing effects, relative to the internal variability, from ~2010s which dramatically increase from 2070s.

#### 4.7 References

(BCC), Beijing Climate Center. 2014. “Bcc-Csm1-1 Model Output Prepared for CMIP5, Served by ESGF.” World Data Center for Climate (WDCC) at DKRZ. <http://cera-www.dkrz.de/WDCC/CMIP5/Compact.jsp?acronym=BCB1>.

Bonsal, B.R., D.L. Peters, F. Seglenieks, A. Rivera, and Bergm A. n.d. “Changes in Freshwater Availability across Canada; Chapter 6 in Canada’s Changing Climate Report.” Ottawa, Ontario.

Bush, E, N Gillet, E Watson, J Fyfe, F Voge, and N Swart. 2019. “Understanding Observed Global Climate Change, CCCR Chapter 2.” Ottawa, Ontario.

Cannon, Alex J. 2015. “Selecting GCM Scenarios That Span the Range of Changes in a Multimodel Ensemble: Application to CMIP5 Climate Extremes Indices\*.” *Journal of Climate* 28 (3): 1260–67. <https://doi.org/10.1175/JCLI-D-14-00636.1>.

Cannon, Alex J., Stephen R. Sobie, and Trevor Q. Murdock. 2015. “Bias Correction of GCM Precipitation by Quantile Mapping: How Well Do Methods Preserve Changes in Quantiles and Extremes?” *Journal of Climate* 28 (17): 6938–59. <https://doi.org/10.1175/JCLI-D-14-00754.1>.

Célleri, Rolando, and Jan Feyen. 2009. “The Hydrology of Tropical Andean Ecosystems: Importance, Knowledge Status, and Perspectives.” *Mountain Research and Development* 29 (4): 350–55. <https://doi.org/10.1659/mrd.00007>.

Creed, I. F., S. E. Sanford, F. D. Beall, L. A. Molot, and P. J. Dillon. 2003. “Cryptic Wetlands: Integrating Hidden Wetlands in Regression Models of the Export of Dissolved Organic Carbon from Forested Landscapes.” *Hydrological Processes* 17 (18): 3629–48. <https://doi.org/10.1002/hyp.1357>.

CSIRO. 2016. “ACCESS1-0 Model Output Prepared for CMIP5 Historical (Version 2015), Served by ESGF.” 2016. <https://doi.org/10.1594/WDCC/CMIP5.CSA0hiv2015>.

Dai, Aiguo, and Christine E. Bloecker. 2019. “Impacts of Internal Variability on Temperature and Precipitation Trends in Large Ensemble Simulations by Two Climate Models.” *Climate Dynamics* 52 (1–2): 289–306. <https://doi.org/10.1007/s00382-018-4132-4>.

Fauzi, F, H Kuswanto, and R M Atok. 2020. “Bias Correction and Statistical Downscaling of Earth System Models Using Quantile Delta Mapping (QDM) and Bias Correction Constructed Analogues with Quantile Mapping Reordering (BCCAQ).” *Journal of Physics: Conference Series* 1538 (May): 012050. <https://doi.org/10.1088/1742-6596/1538/1/012050>.

Flanner, Mark G. 2009. “Integrating Anthropogenic Heat Flux with Global Climate Models.” *Geophysical Research Letters* 36 (2): n/a-n/a. <https://doi.org/10.1029/2008GL036465>.

for Climate Modelling, Canadian Centre, and Analysis (CCCma). 2015. “CanESM2 Model Output Prepared for CMIP5 EsmFixClim2, Served by ESGF.” World Data Center for Climate (WDCC) at DKRZ. <https://doi.org/10.1594/WDCC/CMIP5.CCE2x2>.

Fyfe, John C., Chris Derksen, Lawrence Mudryk, Gregory M. Flato, Benjamin D. Santer, Neil C. Swart, Noah P. Molotch, et al. 2017. “Large Near-Term Projected Snowpack Loss over the Western United States.” *Nature Communications* 8 (1): 14996. <https://doi.org/10.1038/ncomms14996>.

Gagnon, Alexandre S., and William A. Gough. 2005. "Climate Change Scenarios for the Hudson Bay Region: An Intermodel Comparison." *Climatic Change* 69 (2–3): 269–97.

<https://doi.org/10.1007/s10584-005-1815-8>.

Giorgi, Filippo, and Raquel Francisco. 2000. "Evaluating Uncertainties in the Prediction of Regional Climate Change." *Geophysical Research Letters* 27 (9): 1295–98.

<https://doi.org/10.1029/1999GL011016>.

Hiebert, James, Alex J. Cannon, Trevor Murdock, Stephen Sobie, and Arelia Werner. 2018. "ClimDown: Climate Downscaling in R." *The Journal of Open Source Software* 3 (22): 360.

<https://doi.org/10.21105/joss.00360>.

Höglind, Mats, Stig Morten Thorsen, and Mikhail A. Semenov. 2013. "Assessing Uncertainties in Impact of Climate Change on Grass Production in Northern Europe Using Ensembles of Global Climate Models." *Agricultural and Forest Meteorology* 170 (March): 103–13.

<https://doi.org/10.1016/j.agrformet.2012.02.010>.

Iizumi, Toshichika, Hiroki Takikawa, Yukiko Hirabayashi, Naota Hanasaki, and Motoki Nishimori. 2017. "Contributions of Different Bias-correction Methods and Reference Meteorological Forcing Data Sets to Uncertainty in Projected Temperature and Precipitation Extremes." *Journal of Geophysical Research: Atmospheres* 122 (15): 7800–7819.

<https://doi.org/10.1002/2017JD026613>.

Jamstec, Aori, and Nies. 2015. "MIROC-ESM-CHEM Model Output Prepared for CMIP5 HistoricalGHG, Served by ESGF." World Data Center for Climate (WDCC) at DKRZ.

<https://doi.org/10.1594/WDCC/CMIP5.MIM7hg>.

Jeffrey, Stephen, Leon Rotstajn, Mark Collier, Stacey Dravitzki, Carlo Hamalainen, Chris Moeseneder, Kenneth Wong, and Jozef Syktus. 2016. "CSIRO-Mk3-6-0 Model Output Prepared for CMIP5 Rcp85 (Version 2015), Served by ESGF." World Data Center for Climate (WDCC) at DKRZ.

<https://doi.org/10.1594/WDCC/CMIP5.CQMKr8v2015>.

Jeong, Dae Il, Alex J. Cannon, and Robert J. Morris. 2020. "Projected Changes to Wind Loads Coinciding with Rainfall for Building Design in Canada Based on an Ensemble of Canadian

Regional Climate Model Simulations.” Climatic Change, May. <https://doi.org/10.1007/s10584-020-02745-y>.

Jiang, Dabang, Yue Sui, and Xianmei Lang. 2016. “Timing and Associated Climate Change of a 2 °C Global Warming.” International Journal of Climatology 36 (14): 4512–22. <https://doi.org/10.1002/joc.4647>.

Kirchmeier-Young, Megan C., Francis W. Zwiers, and Nathan P. Gillett. 2017. “Attribution of Extreme Events in Arctic Sea Ice Extent.” Journal of Climate 30 (2): 553–71. <https://doi.org/10.1175/JCLI-D-16-0412.1>.

Kirchmeier-Young, M. C., N. P. Gillett, F. W. Zwiers, A. J. Cannon, and F. S. Anslow. 2018. “Attribution of the Influence of Human-induced Climate Change on an Extreme Fire Season.” Earth’s Future, December, 2018EF001050. <https://doi.org/10.1029/2018EF001050>.

Lange, Stefan. 2018. “Bias Correction of Surface Downwelling Longwave and Shortwave Radiation for the EWEMBI Dataset.” Earth System Dynamics 9 (2): 627–45. <https://doi.org/10.5194/esd-9-627-2018>.

LASG-CESS. 2014. “FGOALS-G2 Model Output Prepared for CMIP5, Served by ESGF.” World Data Center for Climate (WDCC) at DKRZ. <http://cera-www.dkrz.de/WDCC/CMIP5/Compact.jsp?acronym=LSF2>.

Leach, Jason A., and Hjalmar Laudon. 2019. “Headwater Lakes and Their Influence on Downstream Discharge.” Limnology and Oceanography Letters 4 (4): 105–12. <https://doi.org/10.1002/lol2.10110>.

Liddicoat, Spencer, Chris Jones, and John Hughes. 2014. “HadGEM2-ES Model Output Prepared for CMIP5 Esmrcp85, Served by ESGF.” World Data Center for Climate (WDCC) at DKRZ. <https://doi.org/10.1594/WDCC/CMIP5.MOGEE8>.

Lim, Kevin, Paul Treitz, Ken Baldwin, Ian Morrison, and Jim Green. 2003. "Lidar Remote Sensing of Biophysical Properties of Tolerant Northern Hardwood Forests." *Canadian Journal of Remote Sensing* 29 (5): 658–78. <https://doi.org/10.5589/m03-025>.

Masson-Delmotte, V., P. Zhai, H.-O. Pörtner, D. Roberts, J. Skea, P.R. Shukla, A. Pirani, et al. 2018. "Global Warming of 1.5°C. An IPCC Special Report on the Impacts of Global Warming of 1.5°C above Pre-Industrial Levels and Related Global Greenhouse Gas Emission Pathways, in the Context of Strengthening the Global Response to the Threat of Cli." <https://www.ipcc.ch/sr15/>.

Maurer, E. P., H. G. Hidalgo, T. Das, M. D. Dettinger, and D. R. Cayan. 2010. "The Utility of Daily Large-Scale Climate Data in the Assessment of Climate Change Impacts on Daily Streamflow in California." *Hydrology and Earth System Sciences* 14 (6): 1125–38. <https://doi.org/10.5194/hess-14-1125-2010>.

Muhammad, Ameer, Grey R. Evenson, Fisaha Unduche, and Tricia A. Stadnyk. 2020. "Climate Change Impacts on Reservoir Inflow in the Prairie Pothole Region: A Watershed Model Analysis." *Water* 12 (1): 271. <https://doi.org/10.3390/w12010271>.

Muhammad, Ameer, Tricia Stadnyk, Fisaha Unduche, and Paulin Coulibaly. 2018. "Multi-Model Approaches for Improving Seasonal Ensemble Streamflow Prediction Scheme with Various Statistical Post-Processing Techniques in the Canadian Prairie Region." *Water* 10 (11): 1604. <https://doi.org/10.3390/w10111604>.

Nashwan, Mohamed Salem, and Shamsuddin Shahid. 2020. "A Novel Framework for Selecting General Circulation Models Based on the Spatial Patterns of Climate." *International Journal of Climatology* 40 (10): 4422–43. <https://doi.org/10.1002/joc.6465>.

NCC. 2011. "NorESM1-M Model Output Prepared for CMIP5, Served by ESGF." World Data Center for Climate (WDCC) at DKRZ. <http://cera-www.dkrz.de/WDCC/CMIP5/Compact.jsp?acronym=NCCNM>.

PCIC. n.d. "Pacific Climate Impacts Consortium." Accessed May 10, 2020. <https://pacificclimate.org/>.



- Peng, Jian, Alexander Loew, Olivier Merlin, and Niko E. C. Verhoest. 2017. "A Review of Spatial Downscaling of Satellite Remotely Sensed Soil Moisture." *Reviews of Geophysics* 55 (2): 341–66. <https://doi.org/10.1002/2016RG000543>.
- Ribalaygua, J., L. Torres, J. Pórtoles, R. Monjo, E. Gaitán, and M. R. Pino. 2013. "Description and Validation of a Two-Step Analogue/Regression Downscaling Method." *Theoretical and Applied Climatology* 114 (1–2): 253–69. <https://doi.org/10.1007/s00704-013-0836-x>.
- Sanford, S. E., I. F. Creed, C. L. Tague, F. D. Beall, and J. M. Buttle. 2007. "Scale-Dependence of Natural Variability of Flow Regimes in a Forested Landscape." *Water Resources Research* 43 (8). <https://doi.org/10.1029/2006WR005299>.
- Scinocca, J. F., V. V. Kharin, Y. Jiao, M. W. Qian, M. Lazare, L. Solheim, G. M. Flato, S. Biner, M. Desgagne, and B. Dugas. 2016. "Coordinated Global and Regional Climate Modeling\*." *Journal of Climate* 29 (1): 17–35. <https://doi.org/10.1175/JCLI-D-15-0161.1>.
- Stinson, Graham, Gurb Thandi, Darren Aitkin, Chris Bailey, James Boyd, Michelle Colley, Catherine Fraser, et al. 2019. "A New Approach for Mapping Forest Management Areas in Canada." *The Forestry Chronicle* 95 (02): 101–12. <https://doi.org/10.5558/tfc2019-017>.
- Taylor, Karl E., Ronald J. Stouffer, and Gerald A. Meehl. 2012. "An Overview of CMIP5 and the Experiment Design." *Bulletin of the American Meteorological Society* 93 (4): 485–98. <https://doi.org/10.1175/BAMS-D-11-00094.1>.
- Teng, Jin, Jai Vaze, Francis H. S. Chiew, Biao Wang, and Jean-Michel Perraud. 2012. "Estimating the Relative Uncertainties Sourced from GCMs and Hydrological Models in Modeling Climate Change Impact on Runoff." *Journal of Hydrometeorology* 13 (1): 122–39. <https://doi.org/10.1175/JHM-D-11-058.1>.
- Zwiers, F. W., and A. J. Weaver. 2000. "CLIMATE CHANGE: The Causes of 20th Century Warming." *Science* 290 (5499): 2081–83. <https://doi.org/10.1126/science.290.5499.2081>.

## Chapter 5: Concluding Remarks and future works

In this study, we assess the impacts of land cover (forest type and lakes) and climate change on the hydrological processes of a snow-dominated forested watershed, located in central Ontario near Batchawana Bay. Further, we investigate the influence of internal climate variability on future streamflow projections. The analyses are based on the Raven hydrological model framework which is set up and calibrated for the Batchawana watershed with a drainage area of ~1280 km<sup>2</sup>. Snow has a major contribution to the runoff in this watershed resulting in relatively large stream flows during the snowmelt season. Batchawana basin as a forested catchment is an important industrial and economical asset for the government of Canada. The reason to select this area is that it includes the Turkey Lake sub-watershed which has been extensively studied to investigate the influence of clear-cut activities etc. on the hydrology/environment of the system. Several indigenous communities reside in the area (and surrounding regions). Understanding projected changes in hydrological processes of the watershed can help policymakers and stakeholders develop effective adaptation measures. In addition, the procedures and results of this study can contribute to forest management practices in Canada and elsewhere in the world.

This watershed is covered by three major forest types including deciduous, coniferous and mixed trees. Vegetation type differences among the forest types can affect their hydrological response meteorological conditions. Based on the satellite imagery and remote sensing techniques show that during the last few decades coniferous part of the basin on the eastern side has been replaced by deciduous or mixed trees. They also show that the water availability percentage in the land cover maps, which are assumed to be lakes' area' is decreasing during the last few decades. Besides, climate change is expected to impact the hydrological components of the watershed.

The semi-distributed Raven hydrological model is set up and calibrated based on historical ground-based observations. The model is then applied to simulate the hydrologic response of the watershed to land cover (including lake shrinkage) and climate changes. Climate change data include simulations from eight downscaled global climate models and three large ensembles of regional climate models (50 members each).

The calibrated hydrological model shows satisfactory performance during both calibration and validation periods based on KGE, NSE, R<sup>2</sup>, Log NSE and bias evaluation criteria. These metrics

are selected to assess the model performance in representing the overall changes in the observed hydrograph as well as low and high flows. The land cover analyses showed that replacing coniferous with deciduous trees will cause changes in the low flow regime during the Fall season. Deciduous trees lose their leaves (i.e. lower leaf area index) by late September or early October and consequently result in less rain interception. Therefore, larger seasonal streamflow is projected for scenarios in which deciduous and mixed forests replace the coniferous forest. Further, lakes play a major role in characterizing the low flows of the region with considerable differences in the hydrological response of the system with changes in the total lake area. Lake shrinkage results in decreases in the monthly mean streamflow throughout the year. The scenario with no lakes in the region shows almost zero low flows with reductions in the average streamflow rates.

Climate change has significant impacts on the hydroclimate factors of this forested watershed. The regional climate is expected to be at least 1.5 times warmer than the global mean. Along with temperature, precipitation also is projected to be more and make the region a wetter environment. However, there is more consistency among climate models about temperature projections than precipitation projections and this is occurring in most of the future climate modelling researches. Temperature and precipitation are the most important components of a watershed and here in this study, the region of interest is projected to experience a warmer and wetter environment. A warmer and wetter climate can change the hydrologic regime from a nival (snow-dominated) to a rainfall-dominated system by reducing snowpack (due to less snowfall) and snowmelt shift to the earlier time of the year. This can reduce the peak flow during the spring freshet. Analysis of future streamflow changes shows reduced annual maximum streamflow and an increase in the annual mean streamflow, because of increases in total precipitation. In addition, analysis of the signal-to-noise ratios using the large ensembles suggest strong signal from external forcing effects starting in the 2010s with increasing trends in the future with a sharper increase from 2070s.

During this study there were a few limitations;

- The major limitations are related to data availability and uncertainties in measured parameters. Additional meteorological datasets within the watershed can improve the accuracy of the hydrological model (Singh and Najafi, 2020).

- Gauged streamflow data is also limited to only one station in the Batchawana while other gauges (i.e. Turkey Lake Watershed) cover a relatively much smaller area. Because of this limitation developing more sub-basins and HRUs was not practical and useful.
- Several ground-based measurements required for this study were not available including lake area coverage, soil profile, etc. Remote sensing techniques are used to collect some information about lake areas among others.
- The assumption of water availability percentage in the extracted land cover maps from Landsat satellites as lakes' area would cause some uncertainties.

To broaden the scope of the study and enhance its reliability and applicability there are a few recommendations;

- The application of radar or satellite precipitation/temperature data (Moazami and Najafi; 2021; Singh, et al. 2020) can provide more information about the spatial variability of precipitation events. This can increase the efficacy of the model.
- The results of this study can be combined with other process-based and statistical techniques (Mehdipour et al. 2018a; 2019b) to improve the performance of the model.
- Scrutinize the uncertainties associated with hydrological model structure and parameterization in land cover and climate change assessments (Ashrafi et al. 2020; M. R. Najafi et al., 2011).
- Generate land cover scenarios using physically-based vegetation growth models under the effects of climate change
- These analyses can be extended to assess the impacts of climate and land cover change on floods (Najafi et al., 2021). In particular, it is critical to characterize and distinguish between the role of external forcing and internal climate variability in future flood risks.

## 5.1 References

Ashrafi, S. M., H. Gholami, and M. R. Najafi. 2020. "Uncertainties in Runoff Projection and Hydrological Drought Assessment over Ghareesu Basin under CMIP5 RCP Scenarios." *Journal of Water and Climate Change*, September. <https://doi.org/10.2166/wcc.2020.088>.

Mehdipour, V., and M. Memarianfard. 2018. "Ground-Level O<sub>3</sub> Sensitivity Analysis Using Support Vector Machine with Radial Basis Function." *International Journal of Environmental Science and Technology*, May. <https://doi.org/10.1007/s13762-018-1770-3>.

Mehdipour, Vahid. 2017. "Temporal Modeling of Tropospheric Ozone and Analysis of Its Relationship with Photochemical Precursors Considering Meteorological Parameters." <http://dx.doi.org/10.13140/RG.2.2.16522.57288>.

Mehdipour, Vahid, and Mahsa Memarianfard. 2017. "Application of Support Vector Machine and Gene Expression Programming on Tropospheric Ozone Prognosticating for Tehran Metropolitan." *Civil Engineering Journal* 3 (8): 557. <https://doi.org/10.28991/cej-030984>.

Mehdipour, Vahid, David S. Stevenson, Mahsa Memarianfard, and Parveen Sihag. 2018. "Comparing Different Methods for Statistical Modeling of Particulate Matter in Tehran, Iran." *Air Quality, Atmosphere & Health* 11 (10): 1155–65. <https://doi.org/10.1007/s11869-018-0615-z>.

Moazami S, Najafi MR. A comprehensive evaluation of GPM-IMERG V06 and MRMS with hourly ground-based precipitation observations across Canada. *Journal of Hydrology*. 2021 Mar 1;594:125929.

Najafi, M. R., and H. Moradkhani. 2014. "A Hierarchical Bayesian Approach for the Analysis of Climate Change Impact on Runoff Extremes." *Hydrological Processes* 28 (26): 6292–6308. <https://doi.org/10.1002/hyp.10113>.

Najafi, M. R., H. Moradkhani, and I. W. Jung. 2011. "Assessing the Uncertainties of Hydrologic Model Selection in Climate Change Impact Studies." *Hydrological Processes* 25 (18): 2814–26. <https://doi.org/10.1002/hyp.8043>.

Najafi, Mohammad Reza. 2000. "Climate Change Impact on the Spatio-Temporal Variability of Hydro-Climate Extremes." Portland, OR. <https://doi.org/10.15760/etd.1114>.

Najafi, Mohammad Reza, and Hamid Moradkhani. 2015. "Multi-Model Ensemble Analysis of Runoff Extremes for Climate Change Impact Assessments." *Journal of Hydrology* 525 (June): 352–61. <https://doi.org/10.1016/j.jhydrol.2015.03.045>.

Najafi MR, Zhang Y, Martyn N. A flood risk assessment framework for interdependent infrastructure systems in coastal environments. *Sustainable Cities and Society*. 2021 Jan 1;64:102516.

Sihag, P., B. Singh, A. Sepah Vand, and V. Mehdipour. 2018. "Modeling the Infiltration Process with Soft Computing Techniques." *ISH Journal of Hydraulic Engineering*.  
<https://doi.org/10.1080/09715010.2018.1464408>.

Singh, Harsimrenjit, Farshad Jalili Pirani, and Mohammad Reza Najafi. 2020. "Characterizing the Temperature and Precipitation Covariability over Canada." *Theoretical and Applied Climatology* 139 (3–4): 1543–58. <https://doi.org/10.1007/s00704-019-03062-w>.

Singh H, Najafi MR, Cannon AJ. Characterizing non-stationary compound extreme events in a changing climate based on large-ensemble climate simulations. *Climate Dynamics*. 2021 Jan 2:1-7.

Singh H, Najafi MR. Evaluation of gridded climate datasets over Canada using univariate and bivariate approaches: Implications for hydrological modelling. *Journal of hydrology*. 2020 May 1;584:124673.

# Curriculum Vitae

NAME:

**Vahid Mehdipour**

EDUCATION:

- **MSc Civil Engineering – Water Resource Engineering** Jan 2019 – Jan 2021  
Western University, London, Canada
- **MSc Civil Engineering – Environmental Engineering** Sep 2015 – July 2017  
KN Toosi University of Technology, Tehran, Iran
- **Bachelor of Science in Civil Engineering** Sep 2011 – Nov 2015  
Tabriz University, Tabriz, Iran

## SUMMARY OF QUALIFICATIONS

- Highly motivated Water Resources and Environmental Engineer with five years of research and field-based experience in design, management, hydrologic analysis, hydrologic research, coordination, and construction supervision.
- Strong interpersonal, organizational, decision-making, and team working skills. Motivated to learn new subjects.
- Proficient computer skills: Office automation, Hydrological modelling, Geospatial, and statistical analysis, R, AutoCAD, MATLAB, ArcGIS, Remote Sensing and Satellite Imagery (MODIS, Landsat), LiDAR Data, Google Earth Engine, HEC-RAS, HEC-HMS and ArcSWAT.

## PEER-REVIEWED JOURNAL ARTICLES & CONFERENCE PROCEEDINGS (Google Scholar Link)

- **Mehdipour, V**; Najafi, M.R.; Leach, J.A. “Modeling the influence of climate and forest type on the streamflow regime of a historically snow-dominated watershed” AGU Fall meeting 2020 (submitted)
- **Mehdipour, V**; M Memarianfard; and F Homayounfar. “Application of Gene Expression Programming to Water Dissolved Oxygen Concentration Prediction.” Int. J. Hum. Capital Urban Manage 2 (1): 1–10. doi: 10.22034/ijhcum.2017.02.01.004

- **Mehdipour, V**; Stevenson, D.S.; Memarianfard, M.; Sihag, P. “Comparative study on the decision tree, Bayesian network and support vector machine to predict the PM2.5 concentration” *Air Quality, Atm. & Health*. doi: 10.1007/s11869-018-0615-z
- **Mehdipour, V.** and Memarianfard, M. “Ground level O3 sensitivity analysis using support vector machine with radial basis function” *Intl. J. Sci. and Tech.* doi: 10.1007/s13762-018-1770-3
- **Mehdipour, V.** and Memarianfard, M. “Application of support vector machine and gene expression programming on tropospheric ozone prognosticating for Tehran metropolitan” *Civil Engineering Journal*, doi: 10.28991/cej-030984
- Sihag, P., Singh, B., Vand, A. **Mehdipour, V.** “Modeling the Infiltration Process with Soft Computing Techniques” *ISH Journal of Hydraulic Engineering*, doi: 10.1080/09715010.2018.1464408

#### AWARDS AND GRANTS

- Fully funded MSc Position at Western University
- Nominated as the best TA of Engineering faculty at Western University.
- Member of the Elite student researchers in Iran.
- An honoured volunteer member of the United Nations in management and operation.
- Member of the selected students for fully funded Ph.D.at Iranian universities.
- Mahab Araz Ltd. awarded for scrupulous management (\$5000)
- Azar Absheron Ltd. scholarship for BSc degree (\$ 6000/ year)
- Ranked in Top 0.01% in National Universities entrance exam for MSc degree in Iran.
- Ranked in Top 0.01% in National Universities entrance exam for BSc degree in Iran.